Agronomy Research

Established in 2003 by the Faculty of Agronomy, Estonian Agricultural University

Aims and Scope:

Agronomy Research is a peer-reviewed international Journal intended for publication of broad-spectrum original articles, reviews and short communications on actual problems of modern biosystems engineering incl. crop and animal science, genetics, economics, farm- and production engineering, environmental aspects, agro-ecology, renewable energy and bioenergy etc. in the temperate regions of the world.

Copyright:

Agronomy Research online:

Agronomy Research is available online at: http://agronomy.emu.ee/

Acknowledgement to Referees:

The Editors of *Agronomy Research* would like to thank the many scientists who gave so generously of their time and expertise to referee papers submitted to the Journal.

Abstracted and indexed:

SCOPUS, EBSCO, CABI Full Paper and Thompson Scientific database: (Zoological Records, Biological Abstracts and Biosis Previews, AGRIS, ISPI, CAB Abstracts, AGRICOLA (NAL; USA), VINITI, INIST-PASCAL.)

Subscription information:

Institute of Technology, EULS
56 Kreutzwaldi St., 51014 Tartu, ESTONIA
e-mail: timo.kikas@emu.ee

Journal Policies:

Estonian University of Life Sciences, Latvia University of Agriculture, Aleksandras Stulginskis University, Lithuanian Research Centre for Agriculture and Forestry, and Editors of *Agronomy Research* assume no responsibility for views, statements and opinions expressed by contributors. Any reference to a pesticide, fertiliser, cultivar or other commercial or proprietary product does not constitute a recommendation or an endorsement of its use by the author(s), their institution or any person connected with preparation, publication or distribution of this Journal.

ISSN 1406-894X

CONTENTS

Agronomy Research **13**(5), 1165–1192, 2015

Theory of vibration-assisted sugar beet root lifting

V. Bulgakov[1], V. Adamchuk[2], M. Arak[3] and J. Olt[3,*]

[1]National University of Life and Environmental Sciences of Ukraine 15, Heroyiv Oborony Str., UK03041 Kyiv, Ukraine
[2]National Scientific Centre, Institute for Agricultural Engineering and Electrification, 11, Vokzalna Str., Glevakha-1, Vasylkiv District, Kiev Region, UK08631, Ukraine
[3]Estonian University of Life Sciences, Institute of Technology, 56 Kreutzwaldi Str., EE51014 Tartu, Estonia; *Correspondence: jyri.olt@emu.ee

Abstract. The vibration-assisted lifting of sugar beet roots from the soil has been gaining increasingly wide use worldwide and the majority of sugar beet harvesting machinery manufacturers produce beet harvesters equipped with just such kind of lifting units. In such units the priorities are low tractive resistance, the high quality of harvesting in terms of undamaged side surfaces of beet root bodies and intact tail parts as well as the high degree of their initial cleaning from the stuck soil. However, the parameters of the oscillatory processes generated by the vibrational lifting units used on the majority of sugar beet harvesting machinery in the market have rather average values appropriate for relatively favourable harvesting conditions (soft loose soil, beet root sizes close to the average, properly lined up planting rows etc.). But when the harvesting conditions deviate from their favourable values (especially in case of dry and strong soil), the vibrating lifters start performing the digging process with significant damage to the beet roots (breaking and tearing off the tail parts), their power consumption rises excessively sharply, the unit vibration drives prove to be unreliable. The literature source analysis has shown that any sufficiently detailed, comprehensive and dependable theory of direct beet root lifting from the soil is virtually absent. Thus, the aim of this research study has been to work out such a theoretical basis for the process of vibration-assisted beet root lifting, which will allow to calculate, in accordance with the harvesting parameters, the optimal design and kinematic parameters of the process ensuring the high quality of harvesting. A new theory has been developed, which describes the process of direct vibration-assisted beet root lifting performed under the effect of the vertical disturbing force and the pulling force, imparted to the root by the lifting unit. The obtained system of differential equations has made it possible to establish the law of motion of the beet root in the process of its direct vibration-assisted lifting and perform PC-based numerical calculations, which provide the basis for determining optimal kinematic modes of operation and design parameters of vibrational lifting units subject to the condition of maintaining sugar beet roots intact when harvesting them.

Key words: harvesting machinery, sugar beet root, vibration, lifting unit, modelling, elastic medium, differential equations.

INTRODUCTION

The harvesting of sugar beet roots with the use of vibrational lifting units has a number of advantages in comparison with other methods of digging them out (Sarec et. al., 2009; Lammers, 2011; Lammers & Schmittmann, 2013; Gu et al., 2014). For

example, this way of retrieving sugar beet roots from the soil exhibits a lesser extent of root body damage and loss, a relatively low draught resistance and the more intensive clean-up of the root side surfaces from the adhering soil already at the lifting stage.

However, the said advantages of the vibrational method of beet root lifting are observed only under relatively favourable harvesting conditions, when the soil in the beet plantation is medium strong and not dry (especially at the depth of unit running in the soil). In addition, the beet root planting rows need be straight and the root body sizes – close to the average values (Vermeulen & Koolen, 2002).

Hence, the further research into the work process of the vibration-assisted lifting of beet roots from the soil and the development of improved lifting units basing on the results of such research is one of the topical challenges in the sugar beet growing industry (Gruber, 2005).

Problem. Fundamental theoretical research into the vibration-assisted beet root lifting enables the scientific substantiation of the design and kinematic parameters of vibrational lifting units. Such research is needed first of all for the theoretical analysis of the operation of vibrational lifting units specifically in unfavourable harvesting conditions, on heavy, strong and dry soils, when sugar beet harvesting becomes associated with increased power consumption and the reduced durability of beet harvesting machinery.

In its turn, sound theoretical analysis of any work process (including a vibrational one) is possible only after developing appropriate mathematical models representing that process. Moreover, numerical modelling with the use of the developed mathematical models (numerical experiment) allows to reduce significantly the time and resources spent for the experimental study and full-scale testing of new units (Bulgakov, 2005; Bulgakov, 2011).

A fundamental theoretical and experimental study of the vibration-assisted sugar beet root lifting was presented in the work (Vasilenko et al., 1970). In that study the sugar beet root was modelled as a body with elastic properties approximated by a rod with a variable cross-section and one end fixed, which was under the effect of the perturbing force applied in the vertical and transverse plane. But the process of direct sugar beet root lifting from the soil was virtually left aside in that work, it only stated that, using additionally generated kinetostatic equations, it is possible to find out the terms of the complete lifting of a beet root from the soil.

The effectively first monograph on the theory of sugar beet harvesting machinery (Pogorely et el., 1983), regrettably, also does not examine theoretically the direct process of root lifting from the soil with the use of vibrating lifting units.

A significant amount of the results of scientific (mostly experimental) research into the lifting units of beet harvesters has been published for the recent years, but no results has appeared on the vibration-assisted root lifting.

The further development of the theory of vibration-assisted sugar beet root lifting can be found in the works (Bulgakov, 2005; Bulgakov et al., 2005; Bulgakov et al., 2014; Bulgakov et al., 2015a). For example, the paper (Bulgakov, 2005) formulates a new theory of the natural and forced longitudinal oscillations of the beet root body induced by the action of the vertical perturbing force. The said theory was developed in order to assess the effect the mentioned oscillations had on the process of breaking the bonds between the beet root and the soil and find the terms of maintaining the beet root intact during its lifting from the soil.

The same aim was pursued in the works (Bulgakov, 2005), which examined the transverse natural and forced oscillations of the beet root body occurring under the effect of a perturbing force acting along the line of motion of the lifting unit.

The paper (Bulgakov & Ivanovs, 2010) considers the process of lifting the beet root from the soil in the most general case – when the vibrational lifting unit grips the root non-symmetrically. The process is described using kinematic and dynamic Euler equations. The differential equation system obtained in the study characterizes the process of the three-dimensional oscillations of the root fixed in the soil, placed in elastic medium with one fixed point.

Meanwhile, the process of vibration-assisted beet root lifting from the soil is studied in the said work presuming the symmetrical gripping of the root by both vibrational lifting unit shares, since the non-symmetrical gripping of the root by one share goes on only for a short while. As a consequence of the translational movement of the vibrational lifting unit and the tapering of the working passage, the unit will further grip the root on both sides. But if the beet root is located on the vibrational lifting unit's symmetry axis, then the root is gripped on both sides straight from the beginning. And that is just the mode of beet root gripping by the digging shares, which enables the process of direct vibration-assisted lifting of the root from the soil.

The aim of this study is to develop the fundamentals of a theory of the direct vibration-assisted beet root lifting from the soil under the effect of the vertical perturbing force imparted to the root by the vibrational lifting unit and the pulling force generated by the unit's translational movement.

MATERIALS AND METHODS

To make an analytical description of the above-mentioned work process of beet root lifting from the soil it is necessary first to define the equivalent schematic representation and choose the required systems of coordinates (Vasilenko, 1996).

For that purpose, we represent the vibrational lifting unit by two wedges (digging shares or planes): $A_1B_1C_1$ and $A_2B_2C_2$, each of them being inclined at the angles α, β, γ and positioned relative to each other so as to form a working passage tapering rearwards (Fig. 1). The said wedges $A_1B_1C_1$ and $A_2B_2C_2$ oscillate in the longitudinal vertical plane (the digging share oscillation drive mechanism is not shown). The direction of the lifting unit's translational movement is shown by an arrow. The projections of the points B_1 and B_2 on the axis O_1y_1 are designated by the points D_1 and D_2 respectively.

It is assumed that the beet root approximated by a cone-shaped body interacts at the respective points with the surfaces of the wedges $A_1B_1C_1$ and $A_2B_2C_2$ and also the vibrating lifter grips the root on two sides. Further we suppose that the working surface of the wedge $A_1B_1C_1$ makes direct contact with the cone-shaped beet root body at the point K_1 the surface of the wedge $A_2B_2C_2$ – at the point K_2. Following that, the right lines drawn through the beet root contact points K_1 and K_2 and the points B_1 and B_2, when crossing the sides of the wedges A_1C_1 and A_2C_2, generate the corresponding points M_1 and M_2.

Hence, δ is the dihedral angle ($\angle B_1M_1D_1$) between the lower base $A_1D_1C_1$ and the wedge working surface $A_1B_1C_1$ or the same dihedral angle between the lower base $A_2D_2C_2$ and the second wedge working surface $A_2B_2C_2$.

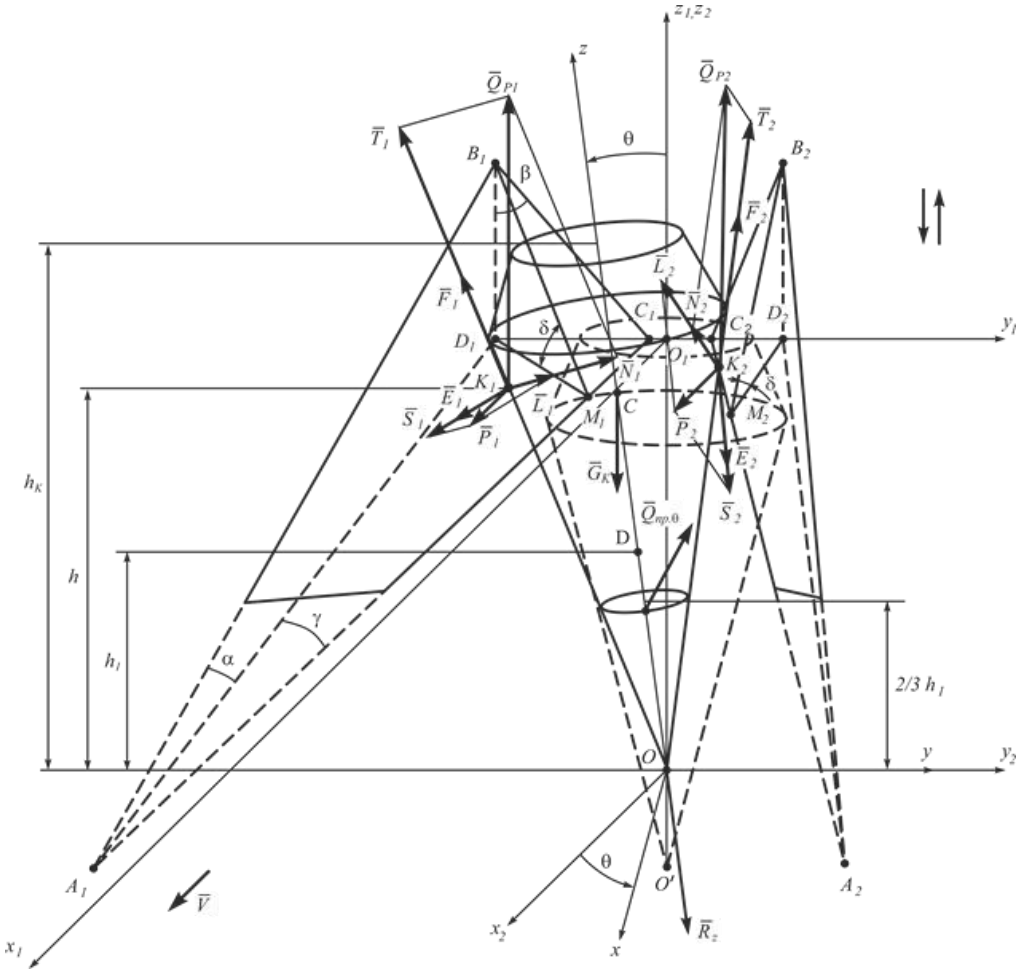

Figure 1. Equivalent schematic model of interaction between vibrational lifting unit and sugar beet root during its lifting from the soil.

Now we are going to associate with the vibrational lifting unit the orthogonal Cartesian coordinate system $x_1O_1y_1z_1$, the centre O_1 of which is placed in the middle of the unit's necked-in passage, the axis O_1x_1 is in line with the direction of the unit's translational movement, the axis O_1z_1 is vertically pointing up, and the axis O_1y_1 is pointing to the right.

Thus, the displacement of the beet root during its direct lifting from the soil shall be viewed with reference to the fixed system of coordinates $x_1O_1y_1z_1$. Further, we introduce the moving system of coordinates $x_cOy_cz_c$ rigidly bound to the beet root, its origin being placed at the root's centre of mass (point C), the axis Cz_c being in line with the beet root symmetry axis, the axes Cx_c and Cy_c lying in the plane that is perpendicular to the axis Cz_c.

Let's examine the process of beet root lifting from the soil with the use of the vibration method in detail from the physical point of view. As the process of oscillation of the beet root itself in the soil as an elastic medium progresses, the bonds between the root and the soil break at a high rate and, accordingly, the restoring forces start sharply decreasing. Following that, the oscillatory process transforms into the process of continuous displacement of the beet root along O_1x_1 and O_1z_1 as well as the continuous angular displacement (turning) of the root around its centre of mass (point C) through some angle θ without the root returning to its initial position.

Accordingly, we arrive to the stage of direct lifting of the beet root from the soil. The process of transition from the beet root oscillatory motion to its continuous displacement in the soil can be described in more detail as follows. Under the effect of the vertical perturbing force the beet root performs translational oscillations together with the surrounding soil, and also the closer the soil is to the beet root, the more these soil oscillations are synchronized with the beet root oscillations. And vice versa – the further the soil is away from the beet root, the less its oscillations copy the beet root oscillations, due to the elastoplastic properties of the soil. Finally, there exists such a distance from the beet root, at which the soil does not oscillate at all, but the limits of the soil area that can oscillate together with the beet root are not outlined quite exactly (all depends on the soil's mechanical-and-physical properties). It is most likely that smooth transition from the soil area oscillating together with the root to the area with no oscillation takes place, and therefore the breaking of the soil at the interface of these areas is unlikely. Supposedly, the most probable scenario is the soil breaking in immediate proximity to the root body surface or even on the beet root body surface itself. This provides the most believable explanation to the fact that during the vibration-assisted sugar beet root lifting a considerably smaller amount of soil remains stuck to the root's sides than in case of the similar lifting with the use of conventional share (or disc) lifting units. As the lifting of the root from the soil can take place, as it was shown earlier, only in case the vibrational lifting unit grips the beet root symmetrically, so, simultaneously with the beet root's translational oscillations, its oscillations through a certain angle about the conditional point of its fixation O take place.

At the first stage of the beet root lifting from the soil, especially during the first oscillations, the restoring force that acts during the angular oscillations and, of course, its moment about the fixation point O are maximal. Therefore, it is most likely that the beet root tilt angle will be insignificant and so full restoration of the root's vertical position or partial restoration of such a position due to the translational movement of the vibrational lifting unit can be expected. But, under the effect of the translational oscillations of the beet root itself together with the surrounding soil the density of the surrounding soil will decrease, so, the restoring force during the angular oscillations will decrease as well. Thus, with each new oscillation the beet root tilt angle will increase, while its restoration to the initial position will decrease. In practice, the beet root will get looser and looser swinging about its conditional fixation point O with the gradual growth of the angle of its tilt forward along the lifting unit's line of motion. This will promote the breaking of bonds between the beet root and the soil along the axis O_1x_1, starting from the upper part of its conical surface situated in unbroken soil and gradually proceeding towards the fixation point O. Thereby, the above-said implies that the breakup of bonds between the beet root and the soil occurs simultaneously in two directions: along the axes O_1x_1 and O_1z_1. In such a case, the forces binding the beet root

with the soil and the elastic forces in the soil will be gradually decreasing until they reach such a minimum level that the oscillatory (vibration) processes will transform into the process of continuous displacement of the beet root upwards along the axis O_1z_1 and forward along the axis O_1x_1 and continuous rotation of the root body around the centre of mass (point C) through certain angle θ up to the complete lifting from the soil. Meanwhile, the elastic forces will just transform into the loosened soil resistance force during the beet root's movement in the working passage of the vibrational lifting unit.

In order to represent the described physical process of the beet root lifting from the soil we show in the equivalent schematic model the forces generated by the interaction between the beet root and the inside surface of the lifting unit working passage.

Now we assume that the vibrational lifting unit exerts, as it was indicated earlier, the vertical perturbing force $\bar{Q}_p$, which varies according to the following harmonic law:

$$Q_p = H\sin(\omega t), \tag{1}$$

where H – amplitude of perturbing force; ω – frequency of perturbing force; t – time.

This force plays the main role in the process of loosening the soil in the vibrational lifting unit working passage area and lifting the beet root from the soil.

The denoted perturbing force $\bar{Q}_p$ is applied to the beet root on both sides of it, therefore, it is represented in the equivalent schematic model by its two components $\bar{Q}_{p1}$ and $\bar{Q}_{p2}$. These forces are applied at the points K_1 and K_2, respectively, at a distance of h from the conditional fixation point O and they are exactly the forces inducing the beet root's oscillations in the longitudinal and vertical plane as well as breaking the bonds between the beet root and the soil and providing the conditions needed for lifting the root completely from the soil.

Since the beet root gripping is symmetrical, obviously, the following relation is going to be observed:

$$Q_{p1} = Q_{p2} = \frac{1}{2} H \sin(\omega t). \tag{2}$$

We resolve these perturbing forces into the normal components $\bar{N}_1$ and $\bar{N}_2$ and tangential components $\bar{T}_1$ and $\bar{T}_2$, as shown in Fig. 1. The compositions of the forces will be as follows:

$$\bar{Q}_{p1} = \bar{N}_1 + \bar{T}_1, \tag{3}$$

$$\bar{Q}_{p2} = \bar{N}_2 + \bar{T}_2. \tag{4}$$

Apparently, the lines of the force vectors $\bar{T}_1$ and $\bar{T}_2$ will be parallel to the right lines B_1M_1 and B_2M_2, respectively.

As the vibrational lifting unit advances linearly along the axis O_1x_1 with respect to the beet root fixed in the soil, so at the moment, when the unit grips the root, there are also moving forces $\overline{P}_1$ and $\overline{P}_2$ acting along the axis O_1x_1. As we did earlier, we resolve the moving forces $\overline{P}_1$ and $\overline{P}_2$ into the normal components $\overline{L}_1$ and $\overline{L}_2$ and tangential components $\overline{S}_1$ and $\overline{S}_2$ with reference to the planes $A_1B_1C_1$ and $A_2B_2C_2$, respectively, i.e.:

$$\overline{P}_1 = \overline{L}_1 + \overline{S}_1, \tag{5}$$

$$\overline{P}_2 = \overline{L}_2 + \overline{S}_2. \tag{6}$$

The force vectors $\overline{S}_1$ and $\overline{S}_2$ act along the vector lines of speed of the shares relative to the root surface during the translational motion of the vibrational lifting unit.

Thus, the lifting wedges $A_1B_1C_1$ and $A_2B_2C_2$ exert on the sugar beet root the following forces at the contact points K_1 and K_2:

$$\overline{N}_{K1} = \overline{N}_1 + \overline{L}_1, \tag{7}$$

$$\overline{N}_{K2} = \overline{N}_2 + \overline{L}_2, \tag{8}$$

which act along the normal to the planes $A_1B_1C_1$ and $A_2B_2C_2$, respectively.

Obviously, the magnitudes of these forces are as follows:

$$N_{K1} = N_1 + L_1, \tag{9}$$

$$N_{K2} = N_2 + L_2. \tag{10}$$

Besides that, at the contact points K_1 and K_2 the friction forces $\overline{F}_{K1}$ and $\overline{F}_{K2}$, respectively, are applied, which counteract the slipping of the beet root body on the working surfaces of the wedges $A_1B_1C_1$ and $A_2B_2C_2$, when the lifting unit grips the root. The vectors of these forces have the directions that are opposite to the directions of the vectors of the relative speed of the beet root slipping on the surfaces of the said wedges.

At the root's centre of gravity (point C), the root weight force $\overline{G}_k$ is applied. The forces of resistance exerted by the loosened soil during the beet root's movement in the working passage of the vibrational lifting unit along the axes O_1x_1 and O_1z_1 are designated $\overline{R}_{x1}$ and $\overline{R}_{z1}$, respectively.

During the direct beet root lifting from the soil, the rotation of the root around its centre of mass C takes place under the effect of the couple of resistance forces exerted by the loosened soil. The moment of the couple of forces will be designated *M*.

Now we are going to find the magnitudes of the forces shown in Fig. 1. The tangential components $\overline{T}_1$ and $\overline{T}_2$ of the perturbing forces $\bar{Q}_{p1}$ and $\bar{Q}_{p2}$, respectively, and the tangential components $\overline{S}_1$ and $\overline{S}_2$ of the moving forces $\overline{P}_1$ and $\overline{P}_2$, respectively, do not have any direct effect on the beet root, they only produce loosening of the soil around the root.

It should be noted, taking into account the symmetry of the beet root gripping by the vibrational lifting unit, that the same name forces generated on the two share working surfaces during their interaction with the beet root will have equal magnitudes and symmetrical lines of action with respect to the symmetry plane $x_1O_1z_1$ (Fig. 1). Accordingly, from the schematic model of forces we derive the formulae for finding the normal components $\overline{N}_1$ and $\overline{N}_2$ and the tangential components $\overline{T}_1$ and $\overline{T}_2$ of the perturbing forces $\overline{Q}_{p1}$ and $\overline{Q}_{p2}$. They have the following values:

$$N_1 = N_2 = Q_{p1}\cos\delta, \tag{11}$$

$$T_1 = T_2 = Q_{p1}\sin\delta. \tag{12}$$

From the same schematic force model the formulae for finding the normal components $\overline{L}_1$ and $\overline{L}_2$ and tangential components $\overline{S}_1$ and $\overline{S}_2$ of the moving forces $\overline{P}_1$ and $\overline{P}_2$, respectively, can be derived:

$$L_1 = L_2 = P_1\sin\gamma, \tag{13}$$

$$S_1 = S_2 = P_1\cos\gamma. \tag{14}$$

The magnitudes of the forces $\overline{N}_{K1}$ and $\overline{N}_{K2}$ are as follows, taking into account the expressions (9), (11) and (13):

$$N_{K1} = N_{K2} = Q_{p1}\cos\delta + P_1\sin\gamma, \tag{15}$$

or, considering the expression (2), we come to the following:

$$N_{K1} = N_{K2} = \frac{1}{2}H\cos\delta\sin(\omega t) + P_1\sin\gamma. \tag{16}$$

Hence, the magnitudes of the friction forces $\overline{F}_{K1}$ and $\overline{F}_{K2}$ are:

$$F_{K1} = F_{K2} = f\,N_{K1} = f\left(Q_{p1}\cos\delta + P_1\sin\gamma\right), \tag{17}$$

or, considering the expression (2), we come to:

$$F_{K1} = F_{K2} = \frac{1}{2}f\,H\cos\delta\sin(\omega t) + f\,P_1\sin\gamma, \tag{18}$$

where f – coefficient of friction.

Apparently, during the immediate contact between the wedges $A_1B_1C_1$ and $A_2B_2C_2$ and the beet root surface, the friction force vectors $\bar{F}_{K1}$ and $\bar{F}_{K2}$ always lie in the wedge planes $A_1B_1C_1$ and $A_2B_2C_2$, respectively. Besides that, due to the soil resistance forces, the slipping of the beet root on the surfaces of the wedges along the lines of action of the forces $\bar{T}_1$, $\bar{T}_2$ (parallel to the lines B_1M_1 and B_2M_2) and in the direction opposite to the forces $\bar{S}_1$ and $\bar{S}_2$ is possible.

Therefore, the vector of the relative speed of the beet root slipping on the surfaces of the wedges can be resolved into components in the above said directions. Thus, the friction force $\bar{F}_{K1}$ can also be resolved into two components: $\bar{F}_1$ – in the direction opposite to the vector $\bar{T}_1$, and $\bar{E}_1$ – in the direction of the vector $\bar{S}_1$, i.e.:

$$\bar{F}_{K1} = \bar{F}_1 + \bar{E}_1 . \tag{19}$$

Similarly, the friction force $\bar{F}_{K2}$ can as well be resolved into two components: $\bar{F}_2$ – in the direction opposite to the vector $\bar{T}_2$, and $\bar{E}_2$ – in the direction of the vector $\bar{S}_2$, i.e.:

$$\bar{F}_{K_2} = \bar{F}_2 + \bar{E}_2 . \tag{20}$$

Obviously, $F_1 = F_2$, $E_1 = E_2$.

Now let's find the magnitudes of the components of the forces $\bar{F}_1$ and $\bar{E}_1$, and consequently $\bar{F}_2$ and $\bar{E}_2$. Basing on the above considerations and expression (16), a deduction can be drawn that in the intervals $[2k\pi, (2k + 1)\pi]$, $k = 0, 1, 2, \ldots$, particularly in the interval $[0, \pi]$, the magnitude of the friction force $\bar{F}_{K1}$ ($\bar{F}_{K2}$) shall be determined in accordance with the formula (18), moreover, in the interval $\left[0, \frac{\pi}{2}\right]$ it rises from its minimum value:

$$F_{K1\min} = F_{K2\min} = f P_1 \sin\gamma , \tag{21}$$

to the maximum value:

$$F_{K1\max} = F_{K2\max} = \frac{1}{2} f H \cos\delta + f P_1 \sin\gamma , \tag{22}$$

While in the interval $\left[\frac{\pi}{2}, \pi\right]$ it decreases from $\bar{F}_{K1\max}$ ($\bar{F}_{K2\max}$) to $\bar{F}_{K1\min}$ ($\bar{F}_{K2\min}$). Besides that, the direction of the friction force vector in the interval $\left[0, \frac{\pi}{2}\right]$ also changes. The vector $\bar{F}_{K1\min}$ ($\bar{F}_{K2\min}$) has the same direction as the friction force vector of a usual share lifter (in the absence of any perturbing force), i.e. parallel to the right lines A_1O_1' (A_2O_2'), while $\angle O_1'A_1M_1 = \angle O_2'A_2M_2 = \gamma$ (Bulgakov, 2005). The vector $\bar{F}_{K1\max}$ ($\bar{F}_{K2\max}$) deflects from the vector $\bar{F}_{K1\min}$ ($\bar{F}_{K2\min}$) through a certain angle $\alpha_{K1max}(\alpha_{K2max})$, while $\alpha_{K1max} = \alpha_{K2max}$.

So, in the interval $\left[0, \frac{\pi}{2}\right]$ the force vector $\bar{F}_{K1}$ ($\bar{F}_{K2}$) changes from the vector $\bar{F}_{K1\min}$ ($\bar{F}_{K2\min}$) to the vector $\bar{F}_{K1\max}$ ($\bar{F}_{K2\max}$), and in the interval $\left[\frac{\pi}{2}, \pi\right]$ – from the vector $\bar{F}_{K1\max}$ ($\bar{F}_{K2\max}$) to the vector $\bar{F}_{K1\min}$ ($\bar{F}_{K2\min}$). Hence, the angle $\alpha_{K1}(\alpha_{K2})$ of the deflection of the vector $\bar{F}_{K1}$ ($\bar{F}_{K2}$) from the vector $\bar{F}_{K1\min}$ ($\bar{F}_{K2\min}$) changes in the interval $[0, \pi]$ under the following law:

$$\alpha_{K2} = \alpha_{K1} = \alpha_{K1\max} \sin(\omega t). \tag{23}$$

Apparently, the value $\alpha_{K1\max}$ ($\alpha_{K2\max}$) depends first of all on the ratio $\frac{H}{P_1}$ $\left(\frac{H}{P_2}\right)$ and the greater the ratio is, the greater the value grows. Therefore, in the interval [0, π] the magnitude of the friction force vector $\bar{F}_{K1}$ ($\bar{F}_{K2}$) changes according to the law (18), while its direction – according to the law (23).

So, in the interval [0, π] we have the following values of the component forces $\bar{F}_1$ ($\bar{F}_2$) and $\bar{E}_1$($\bar{E}_2$):

$$F_1 = F_2 = F_{K1} \sin(\gamma + \alpha_{K1}), \tag{24}$$

$$E_1 = E_2 = F_{K1} \cos(\gamma + \alpha_{K1}), \tag{25}$$

then, taking into account (18) and (23), we obtain:

$$F_1 = F_2 = \left(\frac{1}{2} f H \cos\delta \sin(\omega t) + f P_1 \sin\gamma\right) \sin\left(\gamma + \alpha_{K1\max} \sin(\omega t)\right), \tag{26}$$

$$E_1 = E_2 = \left(\frac{1}{2} f H \cos\delta \sin(\omega t) + f P_1 \sin\gamma\right) \cos\left(\gamma + \alpha_{K1\max} \sin(\omega t)\right). \tag{27}$$

The formulae (26) and (27) are effective in any of the intervals [$2k\pi$, $(2k + 1)\pi$], $k = 0, 1, 2, \ldots$

Obviously, within the intervals [$(2k + 1)\pi$, $2k\pi$], $k = 0, 1, 2, \ldots$, the friction forces $\bar{F}_{K1}$ ($\bar{F}_{K2}$) are as follows:

$$F_{K1} = F_{K2} = F_{K1\min} = f P_1 \sin\gamma. \tag{28}$$

Hence, the following is observed in the denoted intervals:

$$F_1 = F_2 = F_{K1\min} \sin\gamma = f P_1 \sin\gamma \sin\gamma = f P_1 \sin^2\gamma, \tag{29}$$

$$E_1 = E_2 = F_{K1\min} \cos\gamma = f P_1 \sin\gamma \cos\gamma = \frac{1}{2} f P_1 \sin 2\gamma. \tag{30}$$

It can be assumed that the loosened soil resistance forces during the direct beet root lifting from the soil are a function of the speed, with which the beet root travels in the loosened soil. However, as a first approximation, the magnitudes of these forces can be regarded constant. Hence, overall, in order to simplify the mathematical model, we consider the forces $\bar{R}_{x1}$, $\bar{R}_{z1}$ and the moment of couple M to be constant.

THEORY AND MODELLING

Taking into account the equivalent schematic model (model of forces) drawn above, the differential equations of motion of the beet root's centre of mass during its direct lifting from the soil in the vectorial form will be as follows:

$$m_k \bar{a} = \bar{N}_1 + \bar{N}_2 + \bar{L}_1 + \bar{L}_2 + \bar{F}_1 + \bar{F}_2 + \bar{E}_1 + \bar{E}_2 + \bar{G}_k + \bar{R}_{z1} + \bar{R}_{x1}, \quad (31)$$

where m_k is the beet root mass; $\bar{a}$ is the acceleration of the beet root's centre of mass.

Further, we are going to derive the differential equations of motion of the beet root's centre of mass (point C) during its translational movement along the axes O_1x_1 and O_1z_1. As the process of beet root lifting from the soil occurs in case of the lifting unit symmetrically gripping the root body, so the root's movement along the working passage effectively takes place in the longitudinal and vertical plane (plane $x_1O_1z_1$), therefore, the vector equation (31) is reduced to differential equations in the projections on the axes Ox_1 and Oz_1 of the following form:

$$\left.\begin{aligned} m_k \ddot{x}_1 &= N_{1x1} + N_{2x1} + L_{1x1} + L_{2x1} + F_{1x1} + F_{2x1} + E_{1x1} + E_{2x1} - R_{x1}, \\ m_k \ddot{z}_1 &= N_{1z1} + N_{2z1} + L_{1z1} + L_{2z1} - F_{1z1} - F_{2z1} - G_k - R_{z1}. \end{aligned}\right\} \quad (32)$$

Let's determine the values of the force projections on the axes Ox_1 and Oz_1 used in the system of equations (32). Taking into account the formulae derived in (Bulgakov et al., 2015b), the projections of the normal components $\bar{N}_1$ and $\bar{N}_2$ on the axis O_1x_1 are determined as follows:

$$\bar{N}_{1x1} = \bar{N}_{2x1} = \frac{N_1 \tan\gamma}{\sqrt{\tan^2\gamma + 1 + \tan^2\beta}}, \quad (33)$$

or, taking into account the expression (11), we obtain:

$$\bar{N}_{1x1} = \bar{N}_{2x1} = \frac{Q_{p1} \cos\delta \tan\gamma}{\sqrt{\tan^2\gamma + 1 + \tan^2\beta}}. \quad (34)$$

The projections of the normal components $\bar{L}_1$ and $\bar{L}_2$ on the axis O_1x_1 have the following values:

$$L_{1x1} = L_{2x1} = \frac{L_1 \tan\gamma}{\sqrt{\tan^2\gamma + 1 + \tan^2\beta}}, \quad (35)$$

or, taking into account the expression (13), we obtain:

$$L_{1x1} = L_{2x1} = \frac{P_1 \sin\gamma \tan\gamma}{\sqrt{\tan^2\gamma + 1 + \tan^2\beta}}. \quad (36)$$

For the projections of the friction force components $\bar{F}_1$ and $\bar{F}_2$ the following expressions are obtained:

$$F_{1x1} = F_{2x1} = F_1 \cos\delta \sin\gamma, \tag{37}$$

or, taking into account the expression (26), we have:

$$F_{1x1} = F_{2x1} = \left[\frac{1}{2} fH \cos\delta \sin(\omega t) + fP_1 \sin\gamma\right] \times \\ \times \sin[\gamma + \alpha_{K1max} \sin(\omega t)] \cos\delta \sin\gamma, \tag{38}$$

$$\omega t \in [2k\pi, (2k+1)\pi],\ k = 0, 1, 2,...$$

Taking into consideration the formula (29), we come to:

$$F_{1x1} = F_{2x1} = f P_1 \sin^3\gamma \cos\delta, \\ \omega t \in \left[(2k-1)\pi,\ \ 2k\pi\right], \quad k = 1, 2,... \tag{39}$$

The projections of the friction force components $\bar{E}_1$ and $\bar{E}_2$ on the axis O_1x_1 will be as follows:

$$E_{1x1} = E_{2x1} = E_1 \cos\gamma, \tag{40}$$

or, taking into account (27), we have the following expression:

$$E_{1x1} = E_{2x1} = \left[\frac{1}{2} fH \cos\delta \sin(\omega t) + fP_1 \sin\gamma\right] \\ \times \cos[\gamma + \alpha_{K1max} \sin(\omega t)] \cos\gamma, \tag{41}$$

$$\omega t \in [2k\pi, (2k+1)\pi],\ k = 0, 1, 2,...$$

Taking into account the expression (30), we obtain:

$$E_{1x1} = E_{2x1} = \frac{1}{2} f P_1 \sin 2\gamma \cos\gamma, \\ \omega t \in \left[(2k-1)\pi,\ \ 2k\pi\right], \quad k = 1, 2,... \tag{42}$$

The projections of the friction force components $\bar{E}_1$ and $\bar{E}_2$ on the axis O_1z_1 are equal to zero in any interval, i.e. $E_{1z1} = E_{2z1} = 0$.

The projections of the normal components $\bar{N}_1$ and $\bar{N}_2$ on the axis O_1z_1, according to (Bulgakov et al., 2015b), are as follows:

$$N_{1z1} = N_{2z1} = \frac{N_1 \tan\beta}{\sqrt{\tan^2\gamma + 1 + \tan^2\beta}}, \tag{43}$$

or, taking into account the expression (11), we come to:

$$N_{1z1} = N_{2z1} = \frac{Q_{p1} \cos\delta \tan\beta}{\sqrt{\tan^2\gamma + 1 + \tan^2\beta}}. \tag{44}$$

The projections of the normal components $\bar{L}_1$ and $\bar{L}_2$ on the axis O_1z_1 will be equal to:

$$L_{1z1} = L_{2z1} = \frac{L_1 \tan\beta}{\sqrt{\tan^2\gamma + 1 + \tan^2\beta}}, \tag{45}$$

or, taking into account the expression (13), we have:

$$L_{1z1} = L_{2z1} = \frac{P_1 \sin\gamma \tan\beta}{\sqrt{\tan^2\gamma + 1 + \tan^2\beta}}. \tag{46}$$

The projections of the friction force components $\bar{F}_1$ and $\bar{F}_2$ on the axis O_1z_1 will be equal to:

$$F_{1z1} = F_{2z1} = F_1 \sin\delta, \tag{47}$$

or, taking into account the expression (26), we have:

$$\begin{aligned} F_{1z1} = F_{2z1} = &\left[\frac{1}{2} f H \cos\delta \sin(\omega t) + f P_1 \sin\gamma\right] \\ &\times \sin[\gamma + \alpha_{K1max} \sin(\omega t)] \sin\delta, \\ \omega t \in &[2k\pi, (2k+1)\pi], \; k = 0, 1, 2,... \end{aligned} \tag{48}$$

Taking into consideration the formula (29), we obtain:

$$\begin{aligned} &F_{1z1} = F_{2z1} = f P_1 \sin^2\gamma \sin\delta, \\ &\omega t \in \left[(2k-1)\pi, \;\; 2k\pi\right], \qquad k = 1, 2,... \end{aligned} \tag{49}$$

By substituting the expressions (34), (36), (38) or (39), (41) or (42), (44), (46), (48) or (49) into the system of differential equations (32), we obtain the following system of differential equations:

$$
\left.
\begin{aligned}
m_k\ddot{x}_1 = {} & \frac{2Q_{p1}\cos\delta\tan\gamma}{\sqrt{(\tan\gamma)^2+1+(\tan\beta)^2}} + \frac{2P_1\sin\gamma\tan\gamma}{\sqrt{(\tan\gamma)^2+1+(\tan\beta)^2}} \\
& + +2\left[\frac{1}{2}fH\cos\delta\sin(\omega t)\right. \\
& \left. + fP_1\sin\gamma\right]\sin[\gamma+\alpha_{K1max}\sin(\omega t)]\cos\delta\sin\gamma \\
& + 2\left[\frac{1}{2}fH\cos\delta\sin(\omega t)\right. \\
& \left. + fP_1\sin\gamma\right]\cos[\gamma+\alpha_{K1max}\sin(\omega t)]\cos\gamma - R_{x1} \\
m_k\ddot{z}_1 = {} & \frac{2Q_{p1}\cos\delta\tan\beta}{\sqrt{(\tan\gamma)^2+1+(\tan\beta)^2}} + \frac{2P_1\sin\gamma\tan\beta}{\sqrt{(\tan\gamma)^2+1+(\tan\beta)^2}} \\
& - 2\left[\frac{1}{2}fH\cos\delta\sin(\omega t)\right. \\
& \left. + fP_1\sin\gamma\right]\sin[\gamma+\alpha_{K1max}\sin(\omega t)]\sin\delta - G_k - R_{z1}, \\
& \omega t \in [2k\pi,(2k+1)\pi], \qquad k = 1,2,\ldots
\end{aligned}
\right\} \quad (50)
$$

or:

$$
\left.
\begin{aligned}
m_k\ddot{x}_1 = {} & \frac{2P_1\sin\gamma\tan\gamma}{\sqrt{\tan^2\gamma+1+\tan^2\beta}} \\
& + 2fP_1\sin^3\gamma\cos\delta + fP_1\sin 2\gamma\cos\gamma - R_{x1}, \\
m_k\ddot{z}_1 = {} & \frac{2P_1\sin\gamma\tan\beta}{\sqrt{\tan^2\gamma+1+\tan^2\beta}} - 2fP_1\sin^2\gamma\sin\delta - G_k - R_{z1}, \\
& \omega t \in [(2k-1)\pi, 2k\pi],\ k = 1,2,\ldots
\end{aligned}
\right\} \quad (51)
$$

In the systems of equations (50), (51) the magnitudes of the loosened soil resistance forces $\bar{R}_{x1}$ and $\bar{R}_{z1}$ acting during the beet root's movement in the working passage of the vibrational lifting unit are regarded constant.

Now we are going to establish the initial conditions for the differential equations (50), (51). Since the beet root prior to the start of its direct lifting from the soil performs oscillations about the equilibrium position, the following can be taken as the initial conditions for the coordinates of the root's centre of mass (point C):

at $t = 0$:

$$
x_1 = x_{10}, \qquad z_1 = -\frac{1}{3}h_k,
$$

Where x_{10} is the distance from the vertical centreline of the beet root to the origin of coordinates (point O_1) at the time point $t = 0$.

An error, if any, can arise only within the limits of the beet root oscillation amplitude, which is very insignificant as compared with the length of the lifting unit working passage and the running depth in soil, where the root lifting is done. Considering

further that during each oscillation, within the whole period, the instants exist, when the beet root displacement velocity is equal to zero, we take as the initial time point exactly such an instance during the last oscillation followed further by direct beet root lifting from the soil.

Thus, the initial conditions for the systems of differential equations (50), (51) will be as follows:
at t = 0:

$$\dot{x}_1 = 0, \qquad \dot{z}_1 = 0, \qquad x_1 = x_{10}, \qquad z_1 = -\frac{1}{3}h_k. \tag{52}$$

After substituting the expression (2) into the system of equations (50) and making certain transformations, we obtain the following system of differential equations:

$$\left.\begin{aligned}
\ddot{x}_1 = {} & \frac{1}{m_k}\left[\frac{\cos\delta\tan\gamma}{\sqrt{\tan^2\gamma+1+\tan^2\beta}}\right. \\
& + f\cos^2\delta\sin[\gamma+\alpha_{K1max}\sin(\omega t)]\sin\gamma \\
& \left. + f\cos\delta\cos[\gamma+\alpha_{K1max}\sin(\omega t)]\cos\gamma\right] \\
& \times H\sin(\omega t) \\
& + \frac{2}{m_k}\left[\frac{\sin\gamma\tan\gamma}{\sqrt{\tan^2\gamma+1+\tan^2\beta}}\right. \\
& + f\sin^2\gamma\sin[\gamma+\alpha_{K1max}\sin(\omega t)]\cos\delta \\
& \left. + f\sin\gamma\cos\gamma\cos[\gamma+\alpha_{K1max}\sin(\omega t)]\right]P_1 - \frac{R_{x1}}{m_k}, \\
\ddot{z}_1 = {} & \frac{1}{m_k}\left[\frac{\cos\delta\tan\beta}{\sqrt{\tan^2\gamma+1+\tan^2\beta}}\right. \\
& \left. - f\cos\delta\sin[\gamma+\alpha_{K1max}\sin(\omega t)]\sin\delta\right] \\
& \times H\sin(\omega t) + \frac{2}{m_k}\left[\frac{\sin\gamma\tan\beta}{\sqrt{\tan^2\gamma+1+\tan^2\beta}}\right. \\
& \left. - f\sin\gamma\sin[\gamma+\alpha_{K1max}\sin(\omega t)]\sin\delta\right]P_1 - \frac{G_k}{m_k} \\
& - \frac{R_{z1}}{m_k}, \\
& \omega t \in [2k\pi, (2k+1)\pi], \qquad k = 1, 2, \ldots
\end{aligned}\right\} \tag{53}$$

The system of differential equations (53) is nonlinear. It can be integrated only with the use of approximate numerical methods on a PC. First, we are going to make certain assumptions. As a first approximation, we assume that the friction force vectors $\bar{F}_{K1}$ and

$\bar{F}_{K2}$ maintain a constant direction, i.e. the angle between the vectors $\bar{F}_{K1\min}$ and $\bar{F}_{K1}$ is constant and equal to $\frac{\alpha_{K1max}}{2}$, similarly, the angle between the vectors $\bar{F}_{K2\min}$ and $\bar{F}_{K2}$ is also constant and equal to $\frac{\alpha_{K2max}}{2}$, while $\frac{\alpha_{K2max}}{2} = \frac{\alpha_{K1max}}{2}$.

Taking into account these assumptions, the system of differential equations (53) acquires the following form:

$$\left.\begin{aligned}
\ddot{x}_1 = \frac{1}{m_k}\Bigg[&\frac{\cos\delta\tan\gamma}{\sqrt{\tan^2\gamma+1+\tan^2\beta}} \\
&+ f\cos^2\delta\sin\left(\gamma+\frac{\alpha_{K1max}}{2}\right)\sin\gamma \\
&+ f\cos\delta\cos\left(\gamma+\frac{\alpha_{K1max}}{2}\right)\cos\gamma\Bigg] H\sin(\omega t) \\
&+ \frac{2}{m_k}\Bigg[\frac{\sin\gamma\tan\gamma}{\sqrt{\tan^2\gamma+1+\tan^2\beta}} \\
&+ f\sin^2\gamma\sin\left(\gamma+\frac{\alpha_{K1max}}{2}\right)\cos\delta \\
&+ f\sin\gamma\cos\gamma\ \cos\left(\gamma+\frac{\alpha_{K1max}}{2}\right)\Bigg] P_1 - \frac{R_{x1}}{m_k}, \\
\ddot{z}_1 = \frac{1}{m_k}\Bigg[&\frac{\cos\delta\tan\beta}{\sqrt{\tan^2\gamma+1+\tan^2\beta}} - f\cos\delta\sin\left(\gamma+\frac{\alpha_{K1max}}{2}\right)\sin\delta\Bigg] \\
&\times H\sin(\omega t) + \frac{2}{m_k}\Bigg[\frac{\sin\gamma\tan\beta}{\sqrt{\tan^2\gamma+1+\tan^2\beta}} \\
&- f\sin\gamma\sin\left(\gamma+\frac{\alpha_{K1max}}{2}\right)\sin\delta\Bigg] P_1 - \frac{R_{z1}}{m_k} - g\ , \\
&\omega t \in [2k\pi, (2k+1)\pi], \qquad k = 0, 1, 2, \ldots
\end{aligned}\right\} \quad (54)$$

where g – gravitational acceleration.

The system of differential equations (54) is a system of linear second-order differential equations. It can be solved by using the integration method.

To reduce the expression of the system of differential equations (54), we introduce the following designations.

$$\begin{aligned}
\frac{1}{m_k}\Bigg[&\frac{\cos\delta\tan\gamma}{\sqrt{\tan^2\gamma+1+\tan^2\beta}} \\
&+ f\cos^2\delta\sin\left(\gamma+\frac{\alpha_{K1max}}{2}\right)\sin\gamma \\
&+ f\cos\delta\cos\left(\gamma+\frac{\alpha_{K1max}}{2}\right)\cos\gamma\Bigg] = \varphi_1\,,
\end{aligned} \quad (55)$$

$$\left[\frac{\sin\gamma\tan\gamma}{\sqrt{\tan^2\gamma+1+\tan^2\beta}} + f\sin^2\gamma\sin\left(\gamma+\frac{\alpha_{K1max}}{2}\right)\cos\delta + f\sin\gamma\cos\gamma\cos\left(\gamma+\frac{\alpha_{K1max}}{2}\right)\right] = \psi_1\,, \tag{56}$$

$$\frac{1}{m_k}\left[\frac{\cos\delta\tan\beta}{\sqrt{\tan^2\gamma+1+\tan^2\beta}} - f\cos\delta\sin\left(\gamma+\frac{\alpha_{K1max}}{2}\right)\sin\delta\right] = \varphi_2\,, \tag{57}$$

$$\frac{2}{m_k}\left[\frac{\sin\gamma\tan\beta}{\sqrt{\tan^2\gamma+1+\tan^2\beta}} - f\sin\gamma\sin\left(\gamma+\frac{\alpha_{K1max}}{2}\right)\sin\delta\right] = \psi_2 \tag{58}$$

Taking into consideration the expressions (55) – (58), the system of differential equations (54) assumes the following form:

$$\left.\begin{aligned}\ddot{x}_1 &= \varphi_1 H\sin(\omega t) + \psi_1 P_1 - \frac{R_{x1}}{m_k}\,,\\ \ddot{z}_1 &= \varphi_2 H\sin(\omega t) + \psi_2 P_1 - \frac{R_{z1}}{m_k} - g\,.\end{aligned}\right\} \tag{59}$$

Now we are going to integrate the system of differential equations (59). The first integral will be as follows:

$$\left.\begin{aligned}\dot{x}_1 &= -\frac{\varphi_1}{\omega}\cos(\omega t) + \psi_1 P_1 t - \frac{R_{x1}}{m_k}t + C_1\,,\\ \dot{z}_1 &= -\frac{\varphi_2}{\omega}\cos(\omega t) + \psi_2 P_1 t - \frac{R_{z1}}{m_k}t - gt + L_1\,,\end{aligned}\right\} \tag{60}$$

where C_1 and L_1 are arbitrary constants.

The second integral of the system of differential equations (59) will be as follows:

$$\left.\begin{aligned}x_1 &= -\frac{\varphi_1 H}{\omega^2}\sin(\omega t) + \frac{\psi_1 P_1 t^2}{2} - \frac{R_{x1}t^2}{2m_k} + C_1 t + C_2\,,\\ z_1 &= -\frac{\varphi_2 H}{\omega^2}\sin(\omega t) + \frac{\psi_2 P_1 t^2}{2} - \frac{R_{z1}t^2}{2m_k} - \frac{gt^2}{2} + L_1 t + L_2\,,\end{aligned}\right\} \tag{61}$$

where C_2 and L_2 are arbitrary constants.

The arbitrary constants C_1, L_1, C_2 and L_2 are determined by the initial conditions (52). These arbitrary constants are equal to:

$$C_1 = \frac{\varphi_1 H}{\omega}, \qquad L_1 = \frac{\varphi_2 H}{\omega}, \qquad C_2 = x_{10}, \qquad L_2 = -\frac{1}{3} h_k \cdot \tag{62}$$

By substituting the values of the arbitrary constants C_1 and L_1 into the system of differential equations (60), we obtain:

$$\left.\begin{aligned} \dot{x}_1 &= -\frac{\varphi_1 H}{\omega}\cos(\omega t) + \psi_1 P_1 t - \frac{R_{x1} t}{m_k} + \frac{\varphi_1 H}{\omega}, \\ \dot{z}_1 &= -\frac{\varphi_2 H}{\omega}\cos(\omega t) + \psi_2 P_1 t - \frac{R_{z1} t}{m_k} + \frac{\varphi_2 H}{\omega}. \end{aligned}\right\} \tag{63}$$

By substituting the values of the derived arbitrary constants C_1, C_2, L_1 and L_2 into the system of equations (61), we obtain:

$$\left.\begin{aligned} x_1 &= -\frac{\varphi_1 H}{\omega^2}\sin(\omega t) + \frac{\psi_1 P_1 t^2}{2} - \frac{R_{x1} t^2}{2m_k} + \frac{\varphi_1 H t}{\omega} + x_{10}, \\ z_1 &= -\frac{\varphi_2 H}{\omega^2}\sin(\omega t) + \frac{\psi_2 P_1 t^2}{2} - \frac{R_{z1} t^2}{2m_k} - \frac{g t^2}{2} + \frac{\varphi_2 H t}{\omega} - \frac{1}{3} h_k . \end{aligned}\right\} \tag{64}$$

The systems of equations (63) and (64), respectively, characterize the laws of variation of the speed and displacement of the beet root's centre of mass in the process of its direct lifting from the soil. From the second equation of the system (64) the time t_1 of the direct beet root lifting from the soil can be found. For that purpose we have to substitute the value $z_1 = 0$ into the left member of the said equation and solve the resulting equation for t_1. Since the equation is transcendental, it is impossible to derive any analytic expression for finding t_1. However, it can be solved with the use of a PC applying the known methods. The computed value of t_1 can be subsequently used for determining the productivity of the sugar beet root harvesting machine equipped with vibrational lifting units.

Next we are going to give consideration to the system of differential equations (51). To reduce the expression of this system of equations, we again introduce the following designations:

$$\frac{1}{m_k}\left[\frac{2\sin\gamma\tan\gamma}{\sqrt{\tan^2\gamma + 1 + \tan^2\beta}} + 2f\sin^3\gamma\cos\delta + f\sin(2\gamma)\cos\gamma\right] = \psi'_1 \tag{65}$$

$$\frac{1}{m_k}\left[\frac{2\sin\gamma\tan\beta}{\sqrt{\tan^2\gamma + 1 + \tan^2\beta}} - 2f\sin^2\gamma\sin\gamma\sin\delta\right] = \psi'_2 \tag{66}$$

Taking into account the expressions (65), (66), the system of differential equations (51) will take the following form:

$$\begin{aligned} M_{yc}(\bar{F}_1) = M_{yc}(\bar{F}_2) \\ = \left(\frac{1}{2} fH\cos\delta\sin(\omega t) + f\,P_1\sin\gamma\right) \\ \times \sin[\gamma + \alpha_{K1max}\sin(\omega t)]\cos\gamma_k(-h_k + h - z_1)\sin\theta\,, \\ \omega t \in [2k\pi, (2k+1)\pi], \qquad k = 0, 1, 2, \ldots \end{aligned} \tag{67}$$

After the first integration of the system of differential equations (67), we obtain:

$$\left.\begin{aligned} \dot{x}_1 &= \psi_1' P_1 t - \frac{R_{x_1}}{m_k} t + C_1, \\ \dot{z}_1 &= \psi_2' P_1 t - \frac{G_k}{m_k} t - \frac{R_{z_1}}{m_k} t + L_1, \end{aligned}\right\} \tag{68}$$

where C_1 and L_1 are arbitrary constants,

$\omega t \in \left[(2k-1)\pi, \quad 2k\pi\right],\ k = 1, 2, \ldots$

After the second integration of the system of differential equations (67), we obtain:

$$\left.\begin{aligned} x_1 &= \psi_1' P_1 \frac{t^2}{2} - \frac{R_{x_1} t^2}{2m_k} + C_1 t + C_2, \\ z_1 &= \psi_2' P_1 \frac{t^2}{2} - \frac{G_k t^2}{2m_k} - \frac{R_{z_1} t^2}{2m_k} + L_1 t + L_2, \end{aligned}\right\} \tag{69}$$

where C_2 and L_2 are arbitrary constants,

$\omega t \in \left[(2k-1)\pi, \quad 2k\pi\right],\ k = 1, 2, \ldots$

The arbitrary constants C_1, L_1, C_2 and L_2 are determined by the initial conditions (52). These arbitrary constants are equal to:

$$C_1 = 0, \qquad L_1 = 0, \qquad C_2 = x_{10}, \qquad L_2 = -\frac{1}{3} h_k\,. \tag{70}$$

By substituting the values of the arbitrary constants C_1 and L_1 into the system of equations (68), we obtain:

$$\left.\begin{aligned}
&\dot{x}_1 = \psi_1' P_1 t - \frac{R_{x_1}}{m_k} t, \\
&\dot{z}_1 = \psi_2' P_1 t - \frac{G_k}{m_k} t - \frac{R_{z_1}}{m_k} t, \\
&\omega t \in \left[(2k-1)\pi, \quad 2k\pi \right], \; k = 1, 2, ...
\end{aligned}\right\} \tag{71}$$

By substituting the values of the arbitrary constants C_1, L_1, C_2 and L_2 into the system of equations (69), we obtain:

$$\left.\begin{aligned}
&x_1 = \psi_1' P_1 \frac{t^2}{2} - \frac{R_{x_1} t^2}{2m_k} + x_{10}, \\
&z_1 = \psi_2' P_1 \frac{t^2}{2} - \frac{G_k t^2}{2m_k} - \frac{R_{z_1} t^2}{2m_k} - \frac{1}{3} h_k, \\
&\omega t \in \left[(2k-1)\pi, \quad 2k\pi, \right], \; k = 1, 2, ...
\end{aligned}\right\} \tag{72}$$

The systems of equations (71) and (72), respectively, characterize the laws of variation of the speed and displacement of the beet root's centre of mass in the process of its direct lifting from the soil in the absence of the perturbing force action.

Now we are going to derive the differential equation of the beet root's rotation around its centre of mass (around the axis Cy, which passes through the beet root's centre of mass (point C) parallel to the axis O_1y_1). According to (Dreizler & Lüdde, 2010), the said equation will have the following form:

$$I_{yc} \frac{d^2\theta}{dt^2} = M_{yc}^e, \tag{73}$$

where θ is the angular displacement of the beet root around the axis Cy_c; I_{yc} is the root's moment of inertia with reference to the axis Cy_c; M_{yc}^e is the moment of rotation around the axis Cy_c (total moment of all external forces applied to the beet root with reference to the axis Cy_c).

Further, let's find the moments of all external forces with reference to the axis Cy_c in accordance with the schematic model of forces presented in Fig. 1. As the movement of the beet root's centre of mass is considered with reference to the coordinate system $x_1O_1y_1z_1$, so we will determine the positions of K_1 and K_2 – the points of contact between the root and the lifting shares' working surfaces $A_1B_1C_1$ and $A_2B_2C_2$ with reference to the same coordinate system. As we can see in the schematic model in Fig. 1, the ordinate of the contact points K_1 and K_2 in the assumed coordinate system will be equal to:

$$z_{K1} = z_{K2} = -h_k + h,$$

where h is the distance from the conditional fixation point O to the plane that extends through the contact points and is perpendicular to the beet root symmetry axis.

Since the movement of the vibrational lifting unit shares takes place at a certain depth, the value *h* for the specific beet root can vary only within the share oscillation amplitude, which is considerably smaller in comparison with the value *h*. Therefore, the value *h* for any specific beet root can be regarded constant. The ordinate of the beet root's centre of mass (point C) at a random instant will be:

$$z_c = z_1,$$

where z_1 is determined by the second equation of the system (64).

Thus, the ordinate of the points K_1 and K_2 varies from the ordinate of the point C by the value:

$$-h_k + h - z_1.$$

So, for example, from the very beginning of the direct lifting $\left(z_1 = -\frac{h_k}{3}\right)$ we have:

$$-h_k + h + \frac{h_k}{3} = h - \frac{2h_k}{3}.$$

Then the moments of all external forces applied to the beet root at a random instant will be equal to:

$$M_{yc}(\bar{Q}_{p1}) = M_{yc}(\bar{Q}_{p2}) = -Q_{p1}(-h_k + h - z_1)\sin\theta \tag{74}$$

since the force vectors $\overline{Q}_{p1}$ and $\overline{Q}_{p2}$ are parallel to the plane $x_1O_1z_1$.

$$M_{yc}(\bar{P}_1) = M_{yc}(\bar{P}_2) = -P_1(-h_k + h - z_1)\cos\theta, \tag{75}$$

since the force vectors $\overline{P}_1$ and $\overline{P}_2$ are parallel to the plane $x_1O_1z_1$.

$$M_{yc}(\bar{F}_1) = M_{yc}(\bar{F}_2) = F_1\cos\gamma_k\,(-h_k + h - z_1)\sin\theta\,, \tag{76}$$

or, taking into account the expression (26), we have:

$$\begin{aligned} M_{yc}(\bar{F}_1) = M_{yc}(\bar{F}_2) &= \Big(\frac{1}{2}fH\cos\delta\sin(\omega t) \\ &+ fP_1\sin\gamma\Big)\sin[\gamma + \alpha_{K1max}\sin(\omega t)]\cos\gamma_k\,(-h_k + h \\ &- z_1)\sin\theta\,, \\ \omega t \in [2k\pi, (2k+1)\pi], &\qquad k = 0, 1, 2, \ldots \end{aligned} \tag{77}$$

Then, taking into consideration the expression (29), we obtain:

$$\begin{aligned} M_{yc}(\bar{F}_1) = M_{yc}(\bar{F}_2) = fP_1\sin^2\gamma\cos\gamma_k\,(-h_k + h - z_1)\sin\theta\,, \\ \omega t \in [(2k-1)\pi, 2k\pi], \qquad k = 1, 2, \ldots \end{aligned} \tag{78}$$

$$M_{yc}(\bar{E}_1) = M_{yc}(\bar{E}_2) = E_1\cos\gamma\,(-h_k + h - z_1)\cos\theta\,. \tag{79}$$

Considering the expression (27), we obtain:

$$\begin{aligned} M_{yc}(\bar{E}_1) = M_{yc}(\bar{E}_2) \\ &= \left(\frac{1}{2} fH\cos\delta\sin(\omega t) + f\,P_1\sin\gamma\right) \\ &\times \cos[\gamma + \alpha_{K1max}\sin(\omega t)]\cos\gamma_k(-h_k + h - z_1)\cos\theta\,, \\ &\omega t \in [2k\pi, (2k+1)\pi], \qquad k = 0, 1, 2, \ldots \end{aligned} \tag{80}$$

And after using the expression (30), we will come to:

$$\begin{aligned} M_{yc}(\bar{E}_1) = M_{yc}(\bar{E}_2) = \frac{1}{2} fP_1\sin 2\gamma\cos\gamma\,(-h_k + h - z_1)\cos\theta\,, \\ \omega t \in [(2k-1)\pi, 2k\pi,], \qquad k = 1, 2, \ldots \end{aligned} \tag{81}$$

For the remaining forces:

$$M_{yc}(\bar{G}_k) = 0\,, \tag{82}$$

$$M_{yc}(\bar{R}_{x1}) = 0\,, \tag{83}$$

$$M_{yc}(\bar{R}_{z1}) = 0\,, \tag{84}$$

since the vectors $\overline{\boldsymbol{G}_k}$, $\overline{\boldsymbol{R}_{x1}}$ and $\overline{R}_{z1}$ intersect the axis Cy$_c$.

Hence, basing on the expressions (74), (75), (77) or (78), (80) or (81), (82), (83), (84) and the moment M of the couple of forces of the loosened soil's resistance to the rotation of the beet root, we find the value of the rotation moment $M^e_{y_c}$ of all external forces with reference to the axis Cy as follows:

$$\begin{aligned} M^e_{yc} = -2Q_{p1}(-h_k + h - z_1)\sin\theta + 2P_1\cos\theta\,(-h_k + h - z_1) \\ + (fH\cos\delta\sin(\omega t) + 2f\,P_1\sin\gamma) \\ \times \sin[\gamma + \alpha_{K1max}\,sin(\omega t)] \\ \times \cos[\gamma + \alpha_{K1max}\sin(\omega t)]\cos\gamma_k(-h_k + h - z_1)\cos\theta\,, \end{aligned} \tag{85}$$

or, after some transformations:

$$\begin{aligned} M^e_{yc} = 2P_1\cos\theta\,(-h_k + h - z_1) \\ + 2fP_1\sin^2\gamma\cos\gamma_k\,(-h_k + h - z_1)\sin\theta \\ + fP_1\sin 2\gamma\cos\gamma\,(-h_k + h - z_1)\cos\theta - M\,, \\ \omega t \in [(2k-1)\pi, 2k\pi], \qquad k = 1, 2, \ldots \end{aligned} \tag{86}$$

The moment of inertia I_{yc} of the beet root with reference to the axis Cy$_c$ is determined with the use of the expression stated in (Bulgakov, 2011):

$$I_{yc} = \left(0.038 + 0.15\tan^2\gamma_k\right). \tag{87}$$

By substituting the expressions (2), (87), (85) or (86) into the differential equation (73) we obtain the differential equation of the beet root's rotation around the axis Cy_c during its direct lifting from the soil, which has the following form:

$$\begin{aligned}(0.038 + 0.25\tan^2\gamma_k)m_k h_k^2 \frac{d^2\theta}{dt^2} &= -H(-h_k + h - z_1)\sin\theta\sin(\omega t) \\ &+ 2P_1\cos\theta\,(-h_k + h - z_1) \\ &+ (fH\cos\delta\sin(\omega t) \\ &+ 2fP_1\sin\gamma)\sin[\gamma + \alpha_{K1max}\sin(\omega t)]\cos\gamma_k\,(-h_k \\ &+ h - z_1)\sin\theta + (fH\cos\delta\sin(\omega t) \\ &+ 2fP_1\sin\gamma)\cos[\gamma + \alpha_{K1max}\sin(\omega t)]\cos\gamma\,(-h_k + h \\ &- z_1)\cos\theta - M\,, \\ \omega t \in [2k\pi, (2k+1)\pi], &\qquad k = 0, 1, 2, \ldots\end{aligned} \tag{88}$$

or:

$$\begin{aligned}(0.038 + 0.15\tan^2\gamma_k)m_k h_k^2 \frac{d^2\theta}{dt^2} &= 2P_1\cos\theta\,(-h_k + h - z_1) + 2fP_1\sin^2\gamma\cos\gamma_k\,(-h_k \\ &+ h \\ &- z_1)\sin\theta \\ &+ fP_1\sin(2\gamma)\cos\gamma\,(-h_k + h - z_1)\cos\theta - M\,, \\ \omega t \in [(2k-1)\pi, 2k\pi], &\qquad k = 1, 2, \ldots\end{aligned} \tag{89}$$

The initial conditions for the obtained differential equation (89) are established basing on the same considerations as for the differential equation (52) and they will have the following form:

At $t = 0$:

$$\theta = 0, \quad \dot{\theta} = 0\,. \tag{90}$$

The differential equation (88) is nonlinear. It can be solved only with the use of numerical techniques and a PC. With this approach, the value z_1 for each cycle of using the numerical algorithm has to be obtained from the second equation of the system (64) for the respective instant t_k.

The differential equation (89) is also nonlinear, since it includes the value z_1, which is a variable, and for any instant t_k this value z_1 has to be obtained from the second equation of the system (72).

Thus, the obtained analytic expressions, essentially, constitute the theory of direct sugar beet root lifting from the soil with the use of vibrational lifting units. The reached analytic expressions make it possible to define the kinematic modes of vibration-assisted beet root lifting basing on the requirement of keeping the roots intact and the design parameters of the vibrational lifting unit.

RESULTS AND DISCUSSION

Now, let's apply the achieved results of the developed theory and construct an algorithm for computing the kinematic parameters of the work process under consideration. Here are its main provisions:

1. First we specify the required initial data for the calculation.
2. Then we find the values φ_1, ψ_1, φ_2, ψ_2 in accordance with the expressions (55), (56), (57) and (58), respectively.
3. Next, we find the sugar beet root motion law during its direct lifting from the soil, according to the expression (64).
4. Now we move to drawing the diagrams for various values of the initial parameters, from those diagrams we find the time of duration of the direct beet root lifting from the soil.
5. In order to carry out the numerical calculations, we have to specify the required parameters. Thus, according to Pogorely & Tatyanko, (2004) and Bulgakov, (2011), the specified parameters have the following values:

- (average) mass of a sugar beet root: m_k = 0.9 kg;
- (average) length of a sugar beet root: h_k = 0.25 m;
- angles of the vibrational lifting unit's trihedral wedges: $\gamma = 14^\circ$, $\beta = 52^\circ$;
- friction coefficient of steel on the sugar beet root surface: f = 0.45;
- resistance force exerted by the soil, when a sugar beet root moves in it: R_x = 100 N, R_z = 100 N;
- amplitude of perturbing force: H = 500 N;
- transverse moving force: P_1 = 400 N;
- angle of deflection of the friction force vector from the vector of its minimal value: $\alpha_{K1\max} = 30°$;
- initial position of the sugar beet root's centre of mass on the axis O_1x_1: x_{10} = 0.2 m.

The dihedral angle δ between the wedge's working surface and the lower base of the lifting share can be derived from the expression stated in (Bulgakov, 2011): $\delta = arctg \dfrac{\cos\beta}{\sin\delta\cos\gamma}$.

Calculations have been carried out for several values of the vibrational lifting unit oscillation frequency.

Basing on the obtained law of motion of the beet root's centre of mass (64) in the system of coordinates $x_1O_1z_1$, we draw the graphs $x_1 = x_1(t)$, $z_1 = z_1(t)$ in the MathCAD environment (Fig. 2) in order to determine the lifting time.

As may be inferred from the graphs, the duration of the beet root lifting from the soil ($z_1 = 0$) reaches only 0.032 s.

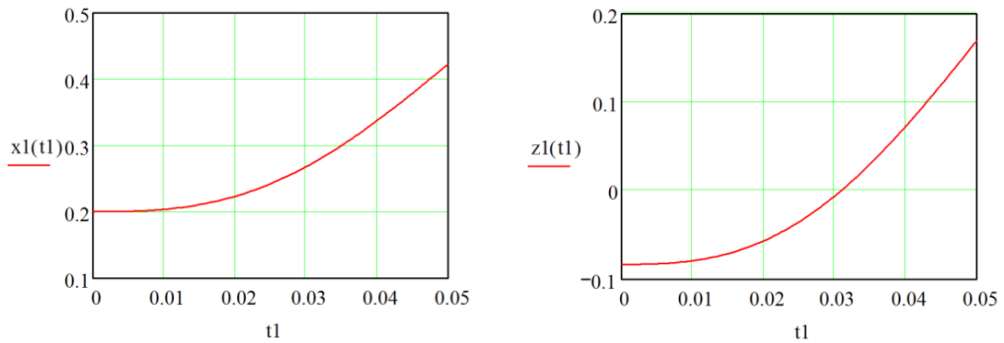

Figure 2. Graphs of the root's centre of mass displacement along the axes O_1x_1 (a) and O_1z_1 (b) as a function of time during the direct beet root lifting from the soil (H = 500 N; P_1 = 400 N; R_x = 100 N; R_z = 100 N; v = 10 Hz).

In Fig. 3, the motion trajectory of the beet root's centre of mass during the direct beet root lifting from the soil is shown.

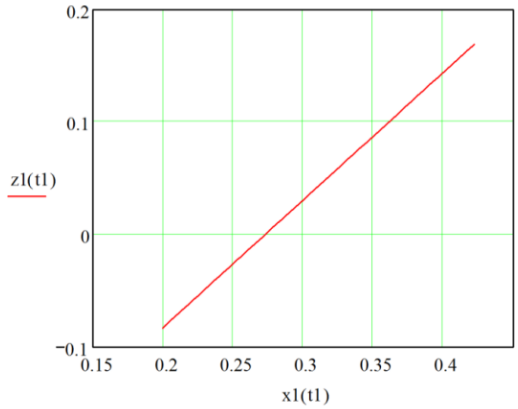

Figure 3. Beet root motion trajectory in the coordinate system $x_1O_1z_1$ during the direct lifting of the root from the soil: (H = 500 N, P_1 = 400 N, R_x = 100 N, R_z = 100 N, v = 10 Hz).

It becomes evident from the presented graph that within the interval of lifting the beet root from the soil ($-0.083 \le z_1 \le 0$) its centre of mass moves effectively on a straight line.

Obviously, this motion trajectory represents the actual trajectory of motion of the beet root's centre of mass only as a certain approximation, since the soil resistance forces during the beet root displacement R_{x1} and R_{z1} are assumed to have constant magnitudes.

Also, calculations have been carried out for the displacement of the beet root's centre of mass along the axis O_1z_1 until its complete lifting from the soil as a function of the changing perturbing force amplitude and $z_1 = z_1(H,t)$ at P_1 = const and $z_1 = z_1(P,t)$ at P = const have been obtained.

In Fig. 4, the surface and profile graph of $z_1 = z_1(H,t)$ subject to the perturbing force amplitude variation within a range of H = 100…700 N (for a transverse moving force value of P_1 = 400 N and an oscillation frequency value of v = 10 Hz) are presented.

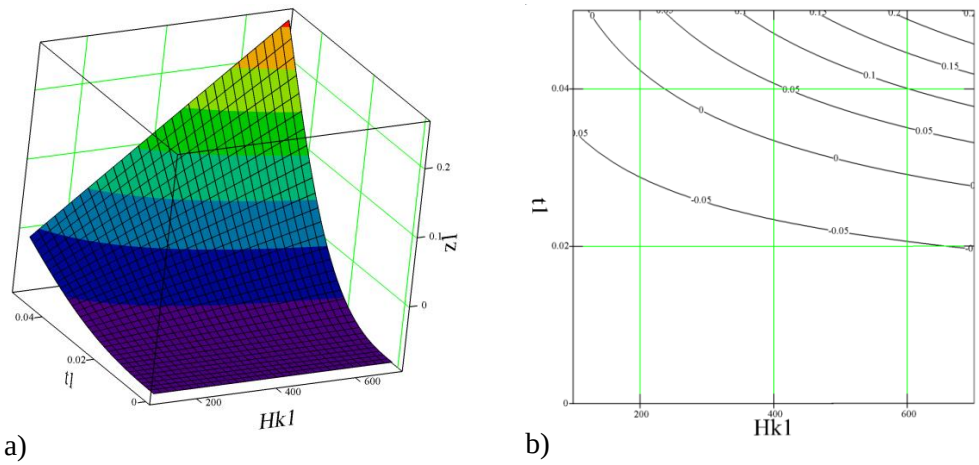

a) b)

Figure 4. Surface (a) and profile graph (b) of function $z_1 = z_1(H,t)$ for the perturbing force amplitude's variation within a range of H = 100…700 N (P_1 = 400 N, v = 10 Hz).

As one may see in the shown graph, when the perturbing force amplitude changes within a range of 100…700 N, the time of beet root lifting from the soil changes within an interval of 0.053…0.028 s.

In Fig. 5, the surface and profile graph of the function $z_1 = z_1(P_1,t)$ subject to the transverse moving force variation within a range of P_1 = 100…700 N (for a perturbing force amplitude value of H = 500 N and an oscillation frequency value of v = 10 Hz) are presented.

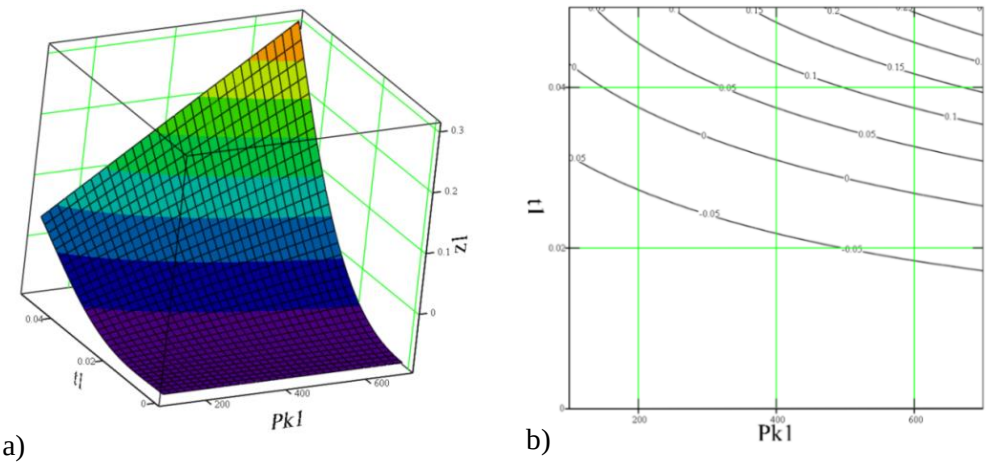

a) b)

Figure 5. Surface (a) and profile graph (b) of function $z_1 = z_1(P_1,t)$ for the transverse moving force variation within a range of P_1 = 100…700 N (H = 500 N, v = 10 Hz).

As may be inferred from the shown graph, when the transverse moving force changes within a range of 100…700 N, the time of beet root lifting from the soil changes within a range of 0.043…0.026 s.

CONCLUSIONS

A new theory of lifting sugar beet roots from the soil with vibrational lifting units has been worked out. This includes the analytic description of the work process at all stages of lifting, starting from the instant, when the vibrational lifting unit grips the root, and up to the complete lifting of the root out of soil.

The system of differential equations for the motions of the root during its direct lifting from the soil has been obtained. Solving the obtained differential equation system allows to find the law of motion of the sugar beet root's centre of mass in the analytical form.

The calculations in the MathCAD environment performed on a PC have made it possible to find the duration of direct beet root lifting from the soil and analyse the effect that the vibrational lifting unit design parameters and the kinematic modes of performing the work process have on the lifting time.

Thus, at a perturbing force amplitude of H = 500 N, a transverse moving force of P_1 = 400 N, soil resistance forces: along the axis Ox_1 – R_x = 100 N and along the axis Oz_1 – 100 N, a perturbing force frequency of v = 10 Hz the time of root lifting from the soil is 0.032 s. When the perturbing force amplitude varies within a range of 100…700 N (at a transverse moving force of P_1 = 400 N and a perturbing force frequency of v = 10 Hz), the time of beet root lifting from the soil varies within a range of 0.053…0.028 s.

When the transverse moving force varies within a range of P_1 = 100…700 N (at a perturbing force amplitude of H = 500 N and a perturbing force frequency of 10 Hz) the time of beet root lifting from the soil varies within a range of 0.043…0.026 s.

The achieved results of the theoretical research provide a possibility to determine the optimal kinematic modes of operation and vibrational lifting unit design parameters, proceeding from the requirement of keeping sugar beet roots intact when harvesting them.

REFERENCES

Bulgakov, V.M. 2005. Theory of beet harvesting machines. Kiev: Publishing Centre of the National Agrarian University, 352 pp. (in Russian).

Bulgakov, V.M. 2011. Sugar beet harvesting machines. Kiev: Agricultural Science, 351 pp.

Bulgakov, V., Adamchuk, V., Kaletnik, G., Arak, M., Olt, J. 2014. Mathematical model of vibration digging up of root crops from soil. *Agronomy Research* **12**(1), 41–58.

Bulgakov, V., Adamchuk, V., Olt, J., Orszaghova, D. 2015a. Use of Euler equations in research into three-dimensional oscillations of sugar beet root during its vibration-assisted lifting. *Agronomy Research* **13**(1), 33–45.

Bulgakov, V., Adamchuk, V., Beloev, H., Borissov, B., Nozdrovicky, L. 2015b. Theory of the sequential oscillations of the sugar beet root during its vibrating digging from soil. In: Agricultural Machinery. Proc. III Int. Sci. and Tech. Congress. 22–25.06.2015, Varna, Bulgaria, pp. 16–20.

Bulgakov, V., Golovats, I., Špokas, L. & Voitjuk, D. 2005. Theoretical investigation of a root crop cross oscillations at vibratinal digging up. *Research papers of IAg Eng LUA & LU of Ag*. **37**(1), 19–35. (in Russian).

Bulgakov, V., Ivanovs, S. 2010. Mathematical simulation of beet vibration extraction. In: Engineering for Rural Development. pp. 25–31.

Dreizler, R.M., Lüdde, C.S. 2010. Theoretical Mechanics. Springer, 402 pp.

Gruber, W. 2005. Trends in sugar beet harvesting. *Landtechnik* **60**(6), 320–321.

Gu, F., Hu, Z., Wu, H., Peng, B., Gao, X., Wang, S. 2014. Development and experiment of 4LT-A staggered-dig sugar beet combine. *Nongye Gongcheng Xuebao/Transactions of the Chinese Society of Agricultural Engineering* **30**(23), 1–9.

Lammers, P.S. 2011. Harvest and loading machines for sugar beet – new trends. *International Sugar Journal* **113(**1348), 253–256.

Lammers, P.S., Schmittmann, O., 2013. Testing of sugar beet harvesters in Germany 2012. *International Sugar Journal*, 115(1370): 100–106.

Pogorely, L.V., Tatyanko, N.V., & Bray, V.V. 1983. *Beet-harvesting machines (designing and calculation)*. Under general editorship of Pogorely, L. V. Tehnika, Kyiv, 232 pp.

Pogorely, L.V., & Tatyanko, N.V. 2004. *Beet-harvesting machines: History, Construction, Theory, Prognosis*, Feniks, Kyiv, 232 pp. (in Ukrainian).

Sarec, P., Sarec, O., Przybyl, J., & Srb, K. 2009. Comparison of sugar beet harvesters. *Listy cukrovarnicke a reparske* **125**(7–8), 212–216. (in Czech).

Vasilenko, P.M. 1996. Introduction in agricultural mechanics. Selhošobrazovanije, 252 p.

Vasilenko, P.M., Pogorely, L.V., & Brey, V.V. 1970. Vibrational Method of Harvesting Root Plants. *Mechanisation and Electrification of the Socialist Agriculture* **2**, 9–13 (in Russian).

Vermeulen, G.D., Koolen, A.J. 2002. Soil dynamics of the origination of soil tare during sugar beet lifting. *Soil & Tillage Research* **65**, 169–184.

Agronomy Research **13**(5), 1193–1201, 2015

The effect of pre-planting thermal treatment of seed tubers on the yield and quality of potato

V. Eremeev*, B. Tein, P. Lääniste, E. Mäeorg and J. Kuht

Estonian University of Life Sciences, Kreutzwaldi 1, EE51014 Tartu, Estonia
*Correspondence: vyacheslav.eremeev@emu.ee

Abstract. Field trials with the potato cultivars 'Ants' (medium late) and 'Laura' (medium early) were carried out on the experimental fields of the Department of Field Crops and Grassland Husbandry located at Eerika (58°22′ N, 26°40′ E), Estonian University of Life Sciences in 2010 and 2011. The yield of tubers and starch, marketable yield of potato, number of tubers per plant and tuber weight were studied. We used the following treatments: untreated control (T_o): seed tubers were planted directly from storage house (storage temperature 4°C); thermal shock (T_S): seed tubers were kept before planting 5 days in a room with temperature of 30°C and 2 days with temperature of 12°C; pre-sprouting (P_S): before planting the seed tubers were kept 26 days in a room with temperature of 15°C and 10 days with temperature of 12°C. The results are presented as the averages of studied years.

According to the average results of two experimental years, the pre-planting treatment with thermal shock increased the number of tubers per plant of cultivar 'Ants' by 30.6%, compared to control treatment. None of the treatments had any effect on the number of tubers of cultivar 'Laura'. The thermal treatment increased the average weight of tubers of cultivar 'Laura' compared to the control treatment (thermal shock by 14.7%, pre-sprouting by 20.7%), but for cultivar 'Ants' the weight of tubers was decreased by 16.7% (thermal shock treatment). The thermal shock treatment increased the tuber yield of cultivar 'Ants' by 10.7% and the pre-sprouting increased the total tuber yield of cultivar 'Laura' by 9.9%. The thermal shock increased significantly the starch content of cultivar 'Ants' and decreased that of cultivar 'Laura'.

Key words: number of tubers per plant, tuber weight, tuber yield, starch yield, starch content.

INTRODUCTION

One of the main components for stable, economically sustainable potato yield is healthy, biologically active high-yielding seed tubers that are being pre-treated according to the end of use (Struik, 2006). In Estonia the growing area and total yield of potato has steadily decreased while the yield has increased (Statistics Estonia Database, 2013). In order to maintain the high yield potential of potato it is important to apply all the necessary measures for it.

Potato cultivars, which are able to provide high quality yields as early as possible in order to be market competitive are vital. Accumulated temperature, precipitation and radiation during the vegetation period favour the growth of early cultivars rather than late cultivars. One such measure is the pre-sprouting of seed tubers. The pre-sprouting of seed tubers of early as well as late potato cultivars is, among the yield-increasing pre-planting measures, widely used in the Netherlands (Struik & Wiersema, 1999). Late

cultivars are beneficial because of their higher yield potential and also their ability to maintain nutritional quality during storage (Struik, 2006). Another technique also used for obtaining earlier yield, besides pre-sprouting, is thermal treatment (otherwise known as thermal shock), which increases the physiological age of seed tubers and shortens the chronological time needed for the formation of harvestable tubers (Struik & Wiersema, 1999; Struik, 2007).

Increase the physiological age of seed tubers is a suitable alternative option for increasing the yield, stimulating earlier formation of tubers and enhancing their quality (Möller & Reents, 2007). The physiological age of seed tubers is defined as the physiological status of tubers that will have an impact on its productivity. A physiologically young seed tuber has preconditions to develop better and stronger roots as well as all above-ground parts of the plant, and the largest assimilation surface possible, leading to formation of a high tuber yield (Eremeev et al., 2008a; b; Hagman, 2012a; b). The drawback is that the late sprouting and canopy closure decreases the ability of potato plants to compete with weeds. The delayed development of the assimilation surface puts much of the assimilation potential past the time of maximum photosynthetically active radiation (Boyd et al., 2002), thus the maturation of tubers is delayed.

The seed tubers may be treated before planting in various ways. There are methods where tubers are heated for a short period but at higher temperatures like when using thermal shock and also where heating period is longer but the temperatures used are lower like when using pre-sprouting. Temperatures higher than 30–35°C are rarely used in thermal shock, even for a short time, as the albumins curdle at 40°C (Kulaeva, 1997). While thermal shock is recognized as a good alternative to pre-sprouting there is scant in-depth information regarding the treatment in the literature (Essah & Honeycutt, 2004).

Relatively few studies have addressed the complex research on the effects of different methods of pre-planting treatments on some aspects of the development of different parts of potato plant and finally on the tuber yield.

Previous pre-planting treatment methods need some modifications to prevent the mechanical damaging of sprouts. The effectiveness of different pre-sprouting methods is depending also on the particular climate conditions.

The objective of our experiment was to study the effect of pre-planting thermal treatments (thermal shock and pre-sprouting) on the tuber total and marketable yields, and on the starch content and yield of cultivars ‘Ants’ and ‘Laura’. The longer thermal shock period (5 days at 30°C) is a novel approach that has not been studied before.

MATERIALS AND METHODS

Field trials were carried out on the experimental fields of the Department of Field Crops and Grassland Husbandry located at Eerika (58°22′ N, 26°40′ E), Estonian University of Life Sciences in 2010 and 2011. In the field trials potato cultivars ‘Ants’ (medium late) and ‘Laura’ (medium early) were used. A randomized complete block in 4 replications was used (Hills & Little, 1972). The area of a plot was 16.8 m^2, the distance between rows was 70 cm and between seed tubers planted 27 cm. Seed tubers with a diameter of 35–55 mm were used in the experiment. Potato was planted at the beginning of May and harvested in August-September. The total and marketable yield was determined right before the harvest by collecting tubers from 15 consecutive plants. The

soil of the experimental field – *Stagnic Luvisol* (*LVj*) according to the World Reference Base classification (FAO, 2006), and the texture of the soil is sandy loam with a humus layer of 20–30 cm (Reintam & Köster, 2006). The agrotechnical measures used were specific to potato cultivation.

We used the following treatments: 1) T_o – untreated (control): 2 days before planting the seed tubers were brought from storage house (storage temperature of 4°C) in order to raise their temperature to the level of soil temperature; 2) T_S – thermal shock: the seed tubers were kept before planting 5 days at 30°C and were left to cool to soil temperature for 2 days; 3) P_S – pre-sprouting: before planting the seed tubers were kept 26 days at 15°C and 10 days at 12°C. After that the tubers were left to cool in order to reach the temperature similar to soil conditions. The light and moisture conditions of the treatment rooms were in accordance to the physiological needs of the seed tubers.

The pre-crop was wheat. Composted manure (40 t ha^{-1}) before autumn ploughing was used as organic fertilizer. On average, the composted cattle manure contained 9.7 g kg^{-1} total N, 4.6 g kg^{-1} total P, 8.6 g kg^{-1} total K, 138 g kg^{-1} total C and 44.8% dry matter. Mineral fertilizers were applied locally at the same time with planting of potatoes in spring. The mineral fertilizer was applied in spring during planting at a rate of 275 kg ha^{-1} (Yara 11-11-21). The potato was planted on the 13th of May each year.

In present article, the yield results of 2010 (samples collected on the 26th of August, 106 days after planting) and 2011 (samples collected on the 30th of August, 110 days after planting) are used. According article authors the cultivars are at different vegetation period: potato cultivars 'Ants' (medium late) and 'Laura' (medium early) Do both cultivars where harvested at the same time and than tubers where analyzed?

From each plot 15 consecutive plants were collected for structural analysis. The marketable yield was determined as the round tubers with diameter of 35 mm and higher for cultivar 'Ants' and oval tubers with diameter of 30 mm and higher for cultivar 'Laura'. After the potato was harvested, tubers were taken from each replication to measure starch concentrations. Tuber starch concentrations were found through tuber specific gravity for what Parov's weight was used (Viileberg, 1986). The starch yield was calculated based on the starch content and tuber yield.

The weather during the experiment period was monitored with a Metos Compact (Pessl Instruments) electronic weather station, which automatically calculates the average daily temperatures and the sum of precipitation. To obtain the decade average of daily average temperatures at the weather station, the daily temperatures were averaged over each decade. The precipitation in 2010 and 2011 differed considerably from the long-term average (1969–2011) as follows: 2011 was arid with 74.5 mm less rainfall than the long-term average; and 2010 was unusually wet with 461.2 mm of rainfall. Average temperatures showed the expected progression from low in May to high in August with a decrease in September. For the month of May the temperatures were lowest in 2011 and highest in 2010. Over the entire season, 2010 was generally the warmest (Tein et al., 2014).

The results were analyzed with Statistica 11, using ANOVA and Fisher LSD test. Statistically significant differences ($p < 0.05$) between variants are denoted with letters. The strength of correlative relationship (coefficient *R*): if the correlation coefficient is denoted as ***, the relationship is significant with the probability of 99.9%. Note '**' means the probability of 99% and '*' the probability of 95%. The results are presented as averages of two years (2010–2011).

RESULTS AND DISCUSSION

The thermal treatment of seed tubers of cultivar 'Ants'

The number of tuber set by a plant is determined by stem density, spatial arrangement, cultivar and season (Wurr et al., 2001). The best way of manipulating tuber number is by manipulating seed rate, size of the seed tubers and their physiological age. Storage conditions and pre-sprouting treatments strongly influence the number of tubers per plant (Johansen & Nilsen, 2004; Johansen & Molteberg, 2012). Wurr (1979) suggested that tuber number for different genotypes do not result from a difference in number of potential tuber sites, but from some control over tuber initiation. Struik et al. (1990) claimed that tuber set, rather than tuber initiation, determined total tuber number. After the tubers have been set, the growth into various size grades is the result of competition among the tuber settings and growth rate of the individual tubers (Struik et al., 1990; 1991). Our results indicated that the pre-planting thermal shock treatment significantly increased the number of tubers per plant compared to control by 3.7 tubers (30.6%) and to pre-sprouting by 2.6 tubers (19.7%, $p < 0.05$). The average weight of a tuber of cultivar 'Ants' was treated by thermal shock was significantly smaller compared to the other variants (T_o and P_S), 6.8 g (16.9%) and 5.1 g (12.7%, $p < 0.05$) respectively (Table 1).

Table 1. The number of tubers per plant and the average weight of a tuber average results of 2010 and 2011

Cultivar	Variant	Number of tubers per plant	Weight of a tuber, g
Ants			
	Untreated	12.1a ± 0.4*	47.1b ± 1.6
	Thermal shock	15.8b ± 0.4	40.3a ± 1.2
	Pre-sprouting	13.2a ± 0.4	45.4b ± 1.4
Laura			
	Untreated	16.8a ± 0.5	36.7a ± 1.1
	Thermal shock	15.3a ± 0.6	42.1b ± 1.4
	Pre-sprouting	15.5a ± 0.5	44.3b ± 1.4

Note. Within the same column, values with different letters are significantly different (ANOVA, Fisher LSD test); * – ± denote the standard deviation.

Pre-planting thermal shock treatment increased significantly the tuber yield compared to control by 10.7% (3.2 t ha^{-1}, $p < 0.05$) (Table 2). The tuber yield of cultivar 'Ants' had the strongest correlation with the number of tubers in untreated control variant (R = 0.69***) (Fig. 1) and somewhat weaker correlation with thermal treatment – correlation coefficients in case of pre-spouting was R = 0.58** and in case of thermal shock R = 0.43*.

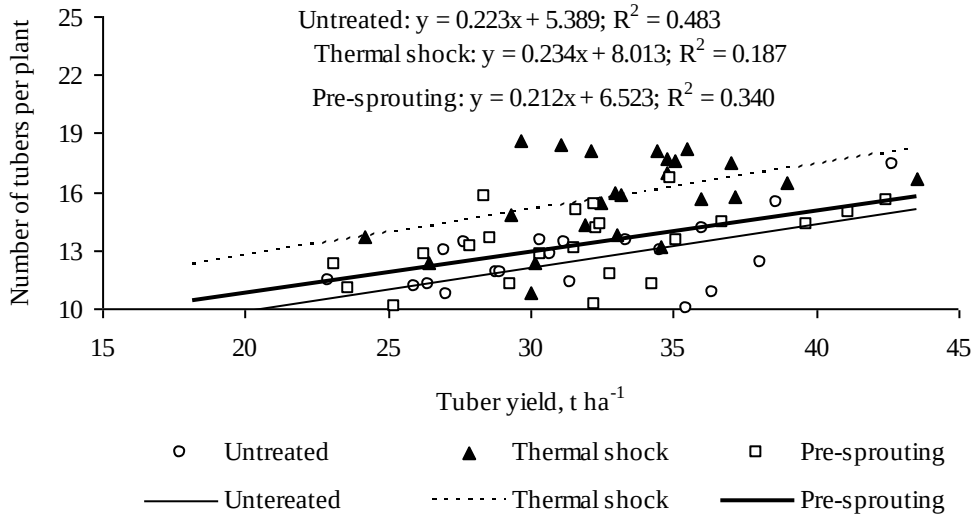

Figure 1. The relationship between the tuber yield and the number of tubers per plant of cultivar 'Ants', due to the effect of pre-planting thermal treatment, average results of 2010 and 2011 (n = 24).

The significant relationship between tuber yield and the weight of tubers of cultivar 'Ants' was observed only in untreated and pre-sprouted treatments (*R* values were 0.62** and 0.55**, respectively) (Fig. 2).

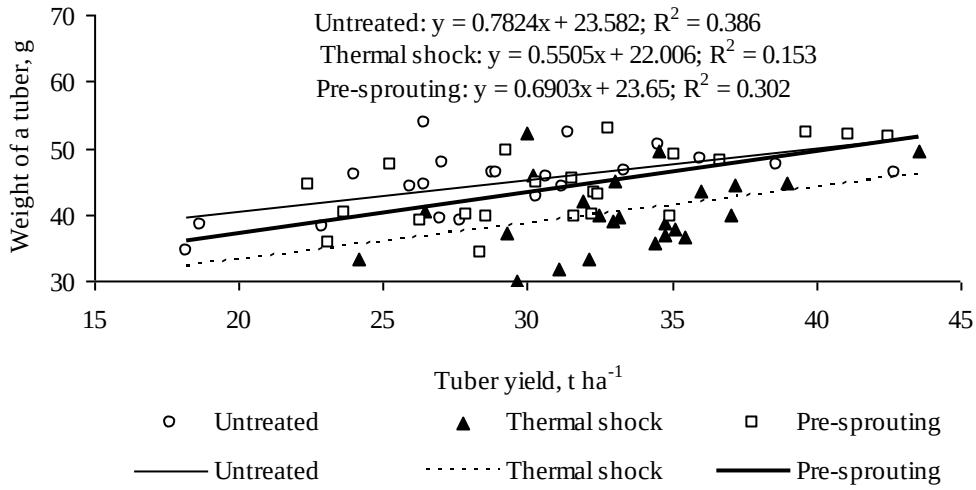

Figure 2. The relationship between the tuber yield and the weight of a tuber of cultivar 'Ants', due to the effect of pre-planting thermal treatment, average results of 2010 and 2011 (n = 24).

In the pre-sprouted treatment the tuber yield did not vary statistically from the control treatment. Also none of the thermal treatments had any effect on the tuber yield (Table 2).

Table 2. The yield of tubers and marketable tubers, due to the effect of pre-planting thermal treatment, average results of 2010 and 2011

Cultivar	Variant	Tuber yield, t ha^{-1}	Marketable yield, t ha^{-1}
Ants			
	Untreated	30.0a ± 1.3*	26.7a ± 1.2
	Thermal shock	33.2b ± 0.8	28.4a ± 0.9
	Pre-sprouting	31.4ab ± 1.1	28.1a ± 1.1
Laura			
	Untreated	32.3a ± 1.0	28.8a ± 1.0
	Thermal shock	33.3ab ± 0.9	30.4ab ± 0.9
	Pre-sprouting	35.5b ± 0.9	32.6b ± 0.8

Note. Within the same column, values with different letters are significantly different (ANOVA, Fisher LSD test); * – ± denote the standard deviation.

Due to the effect of thermal treatment (thermal shock and pre-sprouting) the starch content of cultivar 'Ants' were increased by 1% on average compared to the control ($p < 0.05$) and thermal shock also increased significantly the starch yield by 0.7 t ha^{-1} (16.5%, $p < 0.05$) compared to the control treatment (Table 3), that was directly related to higher total yield (Table 2). The average potato yield in Estonia is 17.5 t ha^{-1} (includes yields from organic farming) and it has been increasing over the past ten years 4.0 t ha^{-1} (Statistics Estonia Database, 2013). The average yield results in this experiment are much higher than Estonian average yields (Table 2). Physiological age is very important for the development of the tuber yield (Struik & Wiersema, 1999). A physiologically older seed accelerates the growth rhythm of potatoes, due to which the yield develops earlier, while the yield formation ability decreases (Caldiz et al., 2001; Johansen et al., 2008). The results also show that the earlier cultivar, the greater the effect of treatment and that the yield develops evenly during the vegetation period in cultivars with longer growth period. Thus, both pre-sprouting and thermal shock increase the physiological age of tubers to some extent.

Table 3. The content and yield of starch, due to the effect of pre-planting thermal treatment, average results of 2010 and 2011

Cultivar	Variant	Starch content, %	Starch yield, t ha^{-1}
Ants			
	Untreated	14.2a ± 0.2*	4.3a ± 0.2
	Thermal shock	15.2b ± 0.1	5.0b ± 0.1
	Pre-sprouting	15.1b ± 0.1	4.7ab ± 0.2
Laura			
	Untreated	14.1b ± 0.1	4.6a ± 0.1
	Thermal shock	13.7a ± 0.1	4.6ab ± 0.1
	Pre-sprouting	14.0ab ± 0.1	5.0b ± 0.1

Note. Within the same column, values with different letters are significantly different (ANOVA, Fisher LSD test); * – ± denote the standard deviation.

The thermal treatment of tubers of cultivar 'Laura'

The average weight of the tubers of a plant depends mostly on the cultivar (Eremeev et al., 2008c). The higher the number of tubers per plant, the lower the average weight of tubers (Eremeev et al., 2008b; Margus et al., 2014). In our experiment the thermal treatment increased the average weight of the tubers of cultivar 'Laura' by 5.4 g (14.7%) in case of thermal shock and by 7.6 g (20.7%) in case of pre-sprouting compared to the control treatment ($p < 0.05$) (Table 1). The number of tubers per plant was not significantly affected by thermal treatments (T_S, P_S). The pre-sprouting increased significantly the total tuber yield by 3.2 t ha^{-1} (9.9%) and the yield of marketable tubers by 3.8 t ha^{-1} (13.2%) ($p < 0.05$) compared to the control (Table 2). As for the cultivar 'Ants' the tuber yield of cultivar 'Laura' depended also on the number of tubers per plant (Fig. 3). Although the relationship was not affected by the thermal treatments used – the correlation between the yield and the number of tubers was strong ($R = 0.52^{**} – 0.54^{**}$). The starch content and the quality of tubers is influenced by several factors: properties of the cultivar, agroecological and climatic conditions, agrotechnical measures, fertilization and storage conditions of tubers (Ierna, 2010). Due to the thermal shock the starch content of the tubers was significantly reduced by 0.4% (6.8% increase compared to the control treatment), but the pre-sprouting increased the starch content by 0.41 t ha^{-1} (20.7%, $p < 0.05$) (Table 3). The use of pre-sprouted tubers provides good basis for higher yield that has also been related to the increase in starch content.

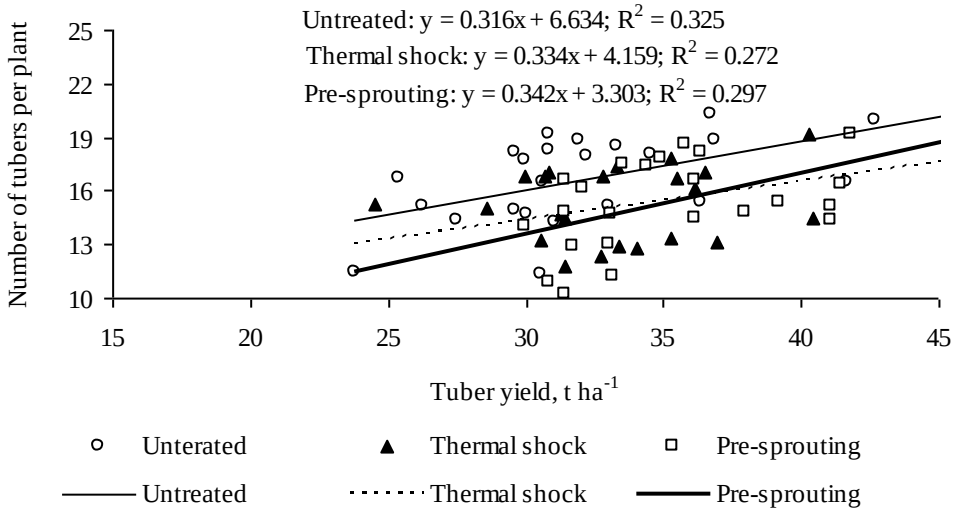

Figure 3. The relationship between the tuber yield and the number of tubers per plant of cultivar 'Laura', due to the effect of pre-planting thermal treatment, average results of 2010 and 2011 (n = 24).

The thermal treatment of tubers did not have any significant impact on the nitrate content of the cultivars studied (71.2–78.2 mg kg^{-1} for cultivar 'Ants' and 21.2–28.9 mg kg^{-1} for cultivar 'Laura'). The values measured were dependent on the properties of the cultivars.

CONCLUSIONS

1. The pre-planting thermal shock treatment of tubers of cultivar 'Ants' increased the number of tubers per plant compared to the control treatment by 30.6%, but no changes were observed in the pre-sprouted treatment.

2. In case of cultivar 'Laura', the pre-planting thermal treatment of tubers did not have any significant effect on the number of tubers per plant, but increased the average weight of tubers compared to the control variant (by 14.7% with thermal shock and by 20.7% with pre-sprouting).

3. The weight of the tubers of cultivar 'Ants' was reduced (by 16.9%) with the use of thermal shock treatment compared to the control treatment.

4. The treatment with thermal shock increased significantly the tuber yield of cultivar 'Ants', by 10.7% compared to the control and pre-sprouting increased the total tuber yield of cultivar 'Laura' by 9.9%.

5. Due to the thermal shock the starch content of cultivar 'Ants' was increased and that of cultivar 'Laura' was decreased.

ACKNOWLEDGMENTS. The experiment was supported by the Estonian Foundation, grant No. 8495.

REFERENCES

Boyd, N.S., Gordon, R. & Martin, R.C. 2002. Relationship between leaf area index and ground cover in potato under different management conditions. *Potato Research* **45**, 117–129.

Caldiz, D.O., Fernandez, L.V. & Struik, P.C. 2001. Physiological age index: A new, simple and reliable index to assess the physiological age of seed potato tubers based on haulm killing date and length of the incubation period. *Field Crops Research* **69**(1), 69–79.

Eremeev, V., Lõhmus, A., Lääniste, P., Jõudu, J. & Talgre, L., Lauringson, E. 2008a. The influence of thermal shock and pre-sprouting of seed potatoes on formation of some yield structure elements. *Acta Agriculturae Scandinavica, Section B-Soil and Plant Science* **58**(1), 35–42.

Eremeev, V., Jõudu, J., Lääniste, P., Mäeorg, E., Selge, A., Tsahkna, A. & Noormets, M. 2008b. Influence of thermal shock and pre-sprouting of seed potatoes on formation of tuber yield. *Spanish Journal of Agricultural Research* **6**(1), 105–113.

Eremeev, V., Jõudu, J., Lääniste, P., Mäeorg, E., Makke, A., Talgre, L., Lauringson, E., Raave, H. & Noormets, M. 2008c. Consequences of pre-planting treatments of potato seed tubers on leaf area index formation. *Acta Agriculturae Scandinavica, Section B - Soil and Plant Science* **58**(3), 236–244.

Essah, S.Y.C. & Honeycutt, C.V. 2004. Tillage and seed-sprouting strategies to improve potato yield and quality in short season climates. *American Journal of Potato Research* **81**, 177–186.

FAO, 2006. World Reference Base for Soil Resources 2006. *World Soil Resources Report 103*. Food and Agriculture Organization, Rome, 145 p.

Hagman, J. 2012a. Pre-sprouting as a tool for early harvest in organic potato (*Solanum tuberosum* L.) cultivation. *Potato Research* **55**, 185–195.

Hagman, J. 2012b. Different pre-sprouting methods for early tuber harvest in potato (*Solanum tuberosum* L.). *Acta Agriculturae Scandinavica, Section B - Soil and Plant Science* **62**(2), 125–131.

Hills, F.J. & Little, T.M. (eds.) 1972. *Statistical methods in agricultural research.* – Davis, CA: University of California, USA, 242 p.

Houba, V.J.G., van der Lee, J.J., Novozamsky, I. & Walinga, I. 1989. *Soil and Plant Analysis, Series of Syllabi, Part 5 Soil Analysis Procedures*. Wageningen Agricultural University, The Netherlands, 100 p.

Ierna, A. 2010. Tuber yield and quality characteristics of potatoes for off-season crops in a Mediterranean environment. *Journal of the Science of Food and Agriculture* **90**, 85–90.

Johansen, T.J. & Nilsen, J. 2004 Influence of low growth temperatures on physiological age of seed potatoes. Acta *Agriculturae Scandinavica Section B: Soil and Plant Science* **54**(3), 185–188.

Johansen, T.J., Møllerhagen, P. & Haugland, E. 2008. Yield potential of seed potatoes grown at different latitudes in Norway. *Acta Agriculturae Scandinavica Section B: Soil and Plant Science* **58**(2), 132–138.

Johansen, T.J. & Molteberg, E.L. 2012. Effect of storage and pre-sprouting regimes on seed potato performance in Norway. *Potato Research* **55**(3–4), 279–292.

Kulaeva, O.N. 1997. Heat shock proteins and plant stress resistance. *Soros Education Journal* **2**, 5–13 (in Russian).

Margus, K., Eremeev, V., Lääniste, P., Mäeorg, E., Tein, B., Laes, R. & Jõudu, J. 2014. The impact of using humic substance for growing potato on quality indicators of tubers. *Journal of Agricultural Science* **XXV**(2), 82–88 (in Estonian).

Möller, K. & Reents, H.J. 2007. Impact of agronomic strategies (seed tuber pre-sprouting, cultivar choice) to control late blight (*Phytophthora infestans*) on tuber growth and yield in organic potato (*Solanum tuberosum* L.) crops. *Potato Research* **50**, 15–29.

Reintam, E. & Köster, T. 2006. The role of chemical indicators to correlate some Estonian soils with WRB and Soil Taxonomy criteria. *Geoderma* **136**, 199–209.

Statistics Estonia database, 2013. http://www.stat.ee/en. [accessed 13 05 2014]

Struik, P.C., Haverkort, A.J., Vreugdenhil, D., Bus, C.B. & Dankert, R. 1990. Manipulation of tuber-size distribution of a potato crop. *Potato Research* **33**, 417–432.

Struik, P.C., Vreugdenhil, D., Haverkort, A.J., Bus, C.B. & Dankert, R. 1991. Possible mechanisms in size hierarchy among tubers on one stem of a potato (*Solanum tuberosum* L.) plant. *Potato Research* **34**, 187–203.

Struik, P.C. & Wiersema, S.G. 1999. *Seed potato technology*. Wageningen, The Netherlands. 350 p.

Struik, P.C. 2006. Trends in agricultural science with special reference to research and development in the potato sector. *Potato Research* **49**, 5–18.

Struik, P.C. 2007 The canon of potato science: 40. Physiological age of seed tubers. *Potato Research* **50**, 375–377.

Tein, B., Kauer, K., Eremeev, V., Luik, A., Selge, A. & Loit, E. 2014. Farming systems affect potato (*Solanum tuberosum* L.) tuber and soil quality. *Field Crops Research* **156**, 1–11.

Wurr, D.C.E. 1979. The effect of variation in the storage temperature of seed potatoes on sprout growth and subsequent yield. *Journal of Agricultural Science* **93**, 619–622.

Wurr, D.C.E., Fellows, J.R., Akehurst, J.M., Hambidge, A.J. & Lynn, J.R. 2001. The effect of cultural and environmental factors on potato seed tuber morphology and subsequent sprout and stem development. *Journal of Agricultural Science* **136**, 55–63.

Agronomy Research **13**(5), 1202–1214, 2015

Remobilization assay of dry matter from different shoot organs under drought stress in wheat (*Triticum aestivum* L.)

M. Golabadi[1,*], P. Golkar[2] and B. Bahari[1]

[1]Department of Agronomy and Plant Breeding, Collage of Agriculture, Khorasgan (Isfahan) Branch, Islamic Azad University, P.O. Box: 81595-158 Isfahan, Iran
[2]Institute of Biotechnology and Bioengineering, Isfahan University of Technology, P.O. Box: 84156-2781 Isfahan, Iran
[*]Correspondence: m.golabadi@khuisf.ac.ir

Abstract. Remobilization of dry matter during the grain filling period in wheat is capable of helping the plant recover its grain yield under drought stress. In this study, the genotypic variation of different traits related to dry matter remobilization were measured in seven genotypes of wheat under the three different environment conditions of well-watered, drought stress at heading stage with application of extra nitrogen fertilizer (30%), and drought stress in Isfahan, Iran. Analysis of variance showed that the genotypes were different not only in their dry matter remobilization from the spike, the stem, the peduncle, and the leaf sheath but also in their current photosynthesis. Different environmental conditions were found to affect dry matter remobilization from the leaves and sheath, current photosynthesis, grain yield, and the relative contributions by the stem and the spike to grain yield. The highest values of spike and stem contribution to grain yield were obtained under drought stress while current photosynthesis was found to be the sole supplier for grain filling in normal conditions. Application of extra nitrogen fertilizer under drought stress was found to reduce the loss of grain yield in some genotypes as a result of enhanced vegetative growth, reserve accumulation, and dry matter remobilization to the grain.

Key words: nitrogen, photosynthesis, stem, spike, water deficit.

INTRODUCTION

Receiving only an average annual precipitation of 240 mm, Iran is located in a semi-arid region (Kardavani, 1988), where drought stress is the most serious environmental factor affecting crop yield (Bradford 1994; Blum, 2011). Loss of yield is the main concern of plant breeders in such regions and they, hence, seek to maintain yield under drought stress conditions (Golabadi et al., 2006). Water deficit, particularly during the post-anthesis and seed filling stages, is one of the main limiting factors of wheat production in most parts of the Middle Asia and the Middle East including Iran (Kardavani, 1988). Although drought stress may occur in both early- and late-seasons, the highest drought-induced yield loss is caused by that during the post-anthesis stage (Blum, 2011). Current photosynthesis, as an important carbon source for grain filling, depends on the absorption of effective light by the green parts of plants such as the stem, spikes, and awns (Borras et al., 2004) after the pollination stage (Austin, 1989). Depending on environmental conditions, portions of these materials may be redistributed

to developing grains during post-pollination stages. The redistribution of the substances stored in transient sources to the sink organs is called remobilization (Gardner et al., 2003). Under drought stress, the photosynthesis loss is compensated for by the remobilization of material reserves to the grain (Yang & Zhang, 2006). Drought stress leads to reduced grain weight, grain yield, and photosynthetic rate as a result of reduced availability of assimilates for export to the sink organs (Kim et al., 2000; Blum, 2011). The amount of dry matter accumulation in the source organs varies from 58 to 48 percent in favorable and unfavorable conditions, respectively, while it also depends on the cultivar and environmental conditions (Ebadi et al., 2007). Studies have shown that reserve remobilization could contribute to 5–20% of the final grain yield under non-stress conditions, while it might rise to 40–60% under stressful growing conditions (Blum, 1998). On the whole, about 10% to 30% of the stem carbohydrates which are extant before and after anthesis are sent to the grain-bearing organ; this remobilization can be more than 70% in some grain crops (Wang et al., 1995; Setter et al., 1998).

Cereals, including wheat and barley, are of primary importance for the food security in the 21st century (Distelfeld et al., 2014). Globally, wheat is one of the most important crops providing over 20% of the calories consumed by the world's population and a similar proportion of protein by about 2.5 billion people (Braun et al., 2010). Different physiological processes are involved in grain development and wheat crop yield under water stress conditions (Austin, 1989). Grain filling period in most regions of wheat cultivation is diminished by high temperature and low moisture (Schnyder, 1993). Drought stress decreases grain yield of wheat due to reduced sink strength and source capacity (Yang et al., 2001). Grain filling rate in wheat depends on the current photo-assimilate supply and the capacity of remobilizing carbohydrate reserves from the vegetative organs to the grains under drought stress (Wang et al., 1995). Ehdaie and Waines (1996) found that about 50% of the grain yield in some of the wheat genotypes was dependent on pre-anthesis reservoirs under drought stress and detected genetic differences in the photo assimilate contents of the vegetative organs and their remobilization to the grain for yield recovery in wheat.

Wheat genotypes that are able to recover from post-anthesis stresses require improved understanding of source–sink relationship and physiological process that determine the magnitude of multiple stresses on grain growth (Spiertz et al., 2006).

This study was conducted to evaluate: 1) the role of stem, spike, peduncle, and internode organs as material reserves on dry matter remobilization to grain in different wheat genotypes under 'normal', 'drought', and ' drought + extra nitrogen fertilizer' treatments; 2) the genotype diversity with regard to remobilization from different organs.

MATERIALS AND METHODS

Field experiment

This experiment was carried out at Research farm of Department of Agriculture, Islamic Azad University in Khurasgan region of Isfahan (1,517 m above sea level with 51°36′ longitude and 32°63 latitude) at central geographical region of Iran during November 2014 to June 2015. This region had arid and hot climates. The means of annual precipitation and daily temperature were 120 (mm) and 16°C, respectively.

The soil was loam-silt (30% clay, 53% silt and 17% sand) with 1.1% organic matter,0.11% N, 45 mg kg^{-1} phosphorous, 415 mg kg^{-1} potassium, EC 3.9 dSm^{-1} and

pH 7.8. This study was conducted as a split plot based in a completely randomized block design with three replications. Three various regimes of drought stress and different genotypes of wheat were considered as main and sub plots, respectively. The genotypes including: Kavir, Ghods, Pishtaz, Rowshan, Sepahan, Line No. 9 and Line No. 11. Different irrigation treatments were normal irrigation (no stress), stop irrigation at 50% of heading stage (Zadoks 55) and stop irrigation at 50% of heading stage (Zadoks 55) plus application of 30% of extra nitrogen (N) fertilizer. Based on soil analysis, required fertilizers were used as follows: 50 kg ha^{-1} phosphorus as triple super phosphate ($Ca(H_2PO_4)_2 \cdot H_2O$), 50 kg ha^{-1} potassium as potassium chloride [KCl] and 250 kg ha^{-1} nitrogen as urea. Phosphorus, potassium and half of nitrogen fertilizers were added before sowing and the rest of nitrogen divided to two equal sections including at tillering and before heading stages. Each experimental sub- plots consisted of five rows with length of 5 m and inter rows distance of 25 cm. The sowing was done in mid -November. The sowing rate was 400 seeds per square meter. The three meter distance was considered between main plots to avoid water exchange. The final harvest was done at a square meter and using its was as obtained grain yield. The plots were treated periodically, pre- and post-emergence, with herbicides, to promote weed- development.

Measurement of studied traits

Remobilization traits were measured ten days after anthesis on 30 randomly selected stems from each plot at the stages of anthesis and physiological maturity. At anthesis stage, selected plants transported to the laboratory. In the lab, spike, peduncle, other internodes and the leaves and sheath were separated from stems and then placed inside a paper bag. These samples were dried for 72 hours at 70–72°C, after drying, the leaf sheath was separated from the stems and then each part was weighed. The same procedure was repeated at maturity stage (Zadoks 92). Then using the relations 1, 2, 3 and 4 the attributes associated with remobilization from vegetative organs to grain was calculated.

Dry matter remobilization (mg per plant) were calculated by difference of total dry matter (TDM) at different parts of plant (stem, spike, peduncle, other internodes, leaves and sheath) at anthesis by total dry matter at maturity in the same organ (Papakosta & Gagianas, 1991; Ehdaie & Waines, 1996), according to following formulae:

Dry matter remobilization (DMR) = $(TDM_{anthesis} - TDM_{maturity}) \times 100$.

Current photosynthesis (CP) = Grain yield $_{30\ spike} - DMR_{30\ spike}$ (Rawson and Evans, 1971).

Relative portion of spike reserves on grain yield (RPSP) %= DRM_{spike} / grain yield.

Relative portion of stem reserves on grain yield (RPST) %= DRM_{stem} / grain yield.

Analysis of variance carried out by SAS (9.1) and MSTATC soft wares. The mean comparisons were done by using least significant difference (LSD) test at 5% of probability.

RESULTS

Water deficit stress treatments were found to have significant effects on current photosynthesis (CP), proportion ratio of spike on stem (PRST), proportion ratio of stem on spike (PRSP), grain yield and remobilization of dry matter from the leaves and sheath (RDLS) (Table 1). Different genotypes of wheat showed significant differences in CP, grain yield and remobilization from different organs except for the internodes (Table 1). The effect of genotype × environment interaction was significant for the contribution of remobilization from spike, peduncle, leaves and sheath to grain yield, current photosynthesis and proportion ratio of spike on grain yield (Table 1). The highest (28.8) and the lowest (3.6) coefficients of variation (CV) % among the evaluated genotypes belonged to remobilization of dry matter from stem (RDST) and remobilization of dry matter from peduncle (RDP), respectively (Table 1).

Table 1. The analysis of variance for current photosynthesis, proportion ratio of spike and stem on grain yield and remobilization from different organs to grain in wheat under drought stress

S.O.V	df	CP¥	PRSP	PRST	GY	RDI	RDLS	RDP	RDST	RDSP
Rep.	2	24.7*	0.08	0.04	0.04	0.06	0.02	0.01	0.07	0.02
Environ.	2	964.5**	0.44*	0.26*	0.95**	0.06	0.2**	0.06	0.08	0.01
E_a¥	4	12.1	0.08	0.09	0.05	0.1	0.1	0.1	0.1	0.07
Genotype	6	18.5*	0.09	0.08	0.17*	0.03	0.1**	0.02*	0.05*	0.05*
G× E	12	18.6*	0.21*	0.06	0.1	0.04	0.1**	0. 1**	0.04	0.1**
E_b	36	6.9	0.08	0.07	0.07	0.05	0.03	0.07	0.04	0.04
CV%		15.5	23.1	28.7	19.5	8.4	6.7	3.6	8.1	7.6
R^2		0.91	0.61	0.49	0.62	0.55	0.78	0.58	0.54	0.65

¥: E_a: Rep.×Environ; Eb: Residuals; C.V: Coefficient of variation; R^2: Coefficient of determination; CP: Current photosynthesis; PRSP: Proportion ratio of spike on grain yield; PRST: Proportion ratio of stem on grain yield; RDSP: Remobilization of dry matter from spike; RDST: Remobilization of dry matter from stem; GY: Grain yield; RDP: Remobilization of dry matter from peduncle; RDI: Remobilization of dry matter from other internodes; RDLS: Remobilization of dry matter from leaves and sheath.

Current photosynthesis, proportion of stem and spike on grain yield and remobilization of dry matter in different environments

Current photosynthesis and the relative contributions of stem and spike to grain yield revealed significant differences among the different test environments (Table 2). The mean value of current photosynthesis was higher in the normal treatment, but the contribution stem remobilization to grain yield was greater in the treatments of drought/N fertilizer and drought than normal (Table 2). The contribution stem remobilization to grain yield was greater in drought and drought/ N fertilizer than normal condition (Table 2). No significant differences were observed among the means for remobilization from different organs under different water deficits, except for that from the leaves and sheath (Table 2). The highest (0.39) and the least (0.17) of remobilization of dry matter from leaves and sheath (RDLS) were denoted to normal and drought/N fertilizer treatments, respectively (Table 2).

Table 2. Effect of water deficit treatments on current photosynthesis, proportion ratio of spike and stem on grain yield and remobilization (mg plant^{-1}) of dry matter from several shoot organs

	CP¥	PRSP	PRST	GY	RDSP	RDST	RDP	RDI	RDLS
Environment									
Normal	9.9^{a}	16.8^{b}	23.5^{b}	638.1^{a}	0.21^{a}	0.3^{a}	0.07^{a}	0.23^{a}	0.39^{a}
Drought/ N Fertilizer	3.1^{b}	26.3^{a}	35.2^{a}	185.9^{b}	0.22^{a}	0.28^{a}	0.06^{a}	0.22^{a}	0.17^{b}
Drought	3.3^{b}	24.9^{ab}	31.1^{a}	162.5^{b}	0.18^{a}	0.23^{a}	0.05^{a}	0.17^{a}	0.21^{b}

Means followed by the same letter was not significantly different at 0.05 level using LSD test.
*, **: significant at P<0.05 and P<0.01, respectively; ns: not significant.
¥: CP: current photosynthesis; PRST: proportion ratio of stem on grain yield; PRSP: proportion ratio of spike on grain yield; GY: Grain yield; RDSP: Remobilization of dry matter from spike; RDST: Remobilization of dry matter from stem; RDP: Remobilization of dry matter from peduncle; RDI: Remobilization of dry matter from other internodes; RDLS: Remobilization of dry matter from leaves and sheath.

Table 3. The mean comparison of current photosynthesis, proportion ratio of spike and stem on grain yield and remobilization (mg plant^{-1}) of dry matter from several shoot organs in different genotypes of wheat

Genotype	CP¥	PRSP	PRST	GY (gm^{-2})	RDSP	RDST	RDP	RDI	RDLS
Kavir	6.9^{a}	13.2^{a}	24.3^{a}	329.2^{abc}	0.15^{b}	0.25^{b}	0.04^{b}	0.21^{a}	0.17^{b}
Ghods	4.8^{ab}	28.1^{a}	31.1^{a}	293^{bc}	0.25^{b}	0.27^{b}	0.05^{b}	0.21^{a}	0.23^{ab}
Pishtaz	3.2^{b}	26.3^{a}	41.1^{a}	386.9^{a}	0.2^{b}	0.32^{a}	0.06^{b}	0.26^{a}	0.32^{a}
Rowshan	3.4^{b}	23.5^{a}	29.9^{a}	231.9^{c}	0.17^{b}	0.22^{b}	0.07^{b}	0.15^{a}	0.29^{a}
Sepahan	7.7^{a}	23.6^{a}	23.9^{a}	372.7^{a}	0.26^{a}	0.28^{b}	0.05^{b}	0.23^{a}	0.29^{a}
Line - 9	6.6^{a}	18.7^{a}	25.6^{a}	382.2^{a}	0.18^{b}	0.23^{b}	0.03^{bc}	0.19^{a}	0.18^{b}
Line - 11	5.3^{ab}	25.2^{a}	33.3^{a}	298.9^{abc}	0.22^{b}	0.31^{a}	0.11^{a}	0.21^{a}	0.31^{a}

Means followed by the same letter was not significantly different at 0.05 level using LSD test.
*, **: significant at P<0.05 and P<0.01, respectively; ns: not significant.
¥: CP: current photosynthesis; PRST: proportion ratio of stem on grain yield, PRSP: proportion ratio of spike on grain yield, GY: Grain yield; RDSP: Remobilization of dry matter from spike, RDST: Remobilization of dry matter from stem, RDP: Remobilization of dry matter from peduncle, RDI: Remobilization of dry matter from other internodes, RDLS: Remobilization of dry matter from leaves and sheath.

Current photosynthesis, proportion of stem and spike on grain yield and remobilization of dry matter in different genotypes

Mean comparisons of dry matter remobilization from different organs of the shoot to the grain along with CP, PRSP and PRST and grain yield values in different genotypes are presented in Table 3. Among the studied genotypes, the highest current photosynthesis was obtained with Sepahan (7.7) whereas Pishtaz recorded the lowest (3.2) (Table 3). The highest grain yield (386.9 gm^{-2}) was observed at Pishtaz that showed significant difference with Rowshan and Ghods genotypes (Table 3). The highest remobilization of dry matter from spike (RDSP) and peduncle (RDP) were observed at Sepahan (0.26) and Line-11 (0.11), respectively (Table 3). Clearly, the Pishtaz genotype showed superiority among the genotypes evaluated with respect to its remobilization of dry matter from stem (0.32), but showed no significant difference with Line-11 (Table 3). The remobilization of dry matter from other internodes (RDI) showed

no significant difference among evaluated genotypes (Table 3). Also, the highest remobilization of dry matter from leaves and sheath was denoted to Pishtaz genotype (0.32), and it was significant with the genotypes of Kavir and Line-9 (Table 3).

Genotype × environment interaction of studied traits

The genotype × environment interaction revealed that the value of dry matter remobilization from the peduncle had different reactions to stress treatments in different genotypes (Fig. 1). The RDP in drought/ N fertilizer was significantly more than drought in Line-11 (Fig. 1), *vise vera* the RDP was more in normal than drought treatments in Rowshan genotype (Fig. 1). Dry matter remobilization from the peduncle recorded its highest value with line –11 (0.16) under the drought/N fertilizer application treatment as compared to other treatments (Fig. 1). It was concluded that these genotypes were capable of exploiting their peduncle reserves in a drought-stressed environment, especially when extra N fertilizer was applied.

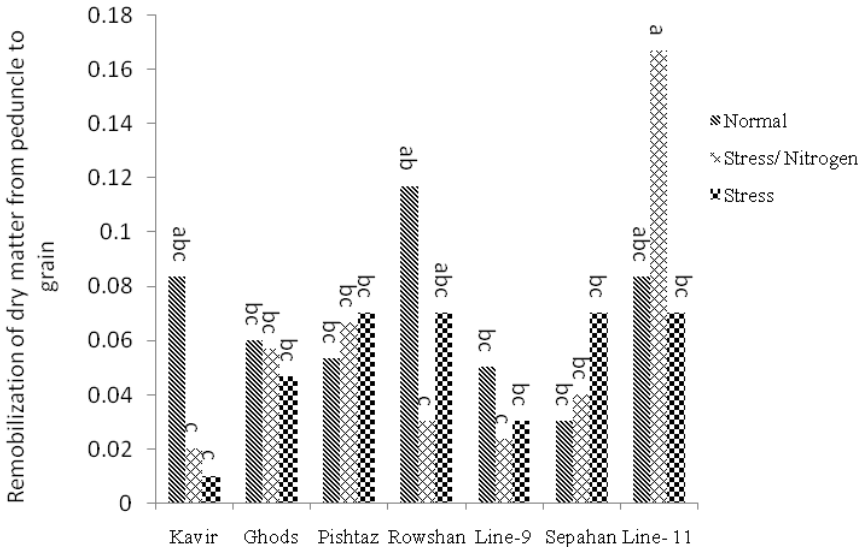

Figure 1. Genotype × environment interaction for remobilization from peduncle to grain.

The effects of genotype × environment interaction on dry matter remobilization from the spike to the grain are presented in Fig. 2. Clearly, the highest rate of RDSP was observed in Sepahan (0.51) under the drought/N fertilizer treatment that was significantly different with other genotypes, except for Line-11 (Fig. 2).

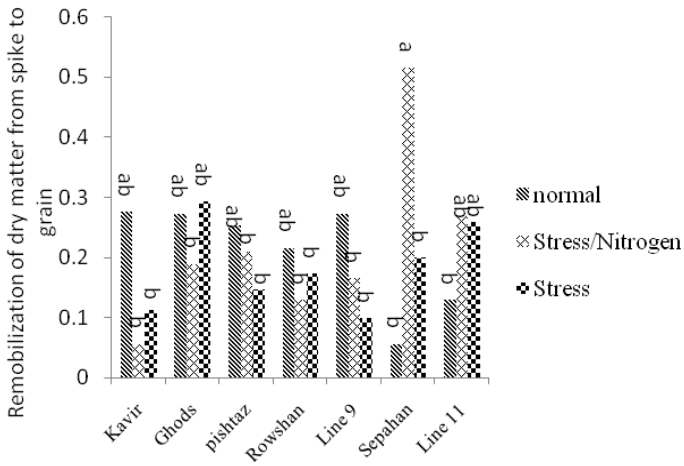

Figure 2. Genotype × environments interaction for remobilization from spike to grain.

The effects of genotype × environment interaction on dry matter remobilization from leaves and sheath are presented in Fig. 3. The genotypes of Ghods, Kavir, Rowshan, Line-9 and Line-11 showed higher rates of remobilization from leaves and sheath in normal condition, rather than drought/N fertilizer treatment (Fig. 3).

Remobilization from leaves and sheath in the Pishtaz and Sepahan genotypes under the drought/N fertilizer treatment were higher than those under drought stress (Fig. 3), which explains the benefits of using extra nitrogen in these genotypes under drought stress conditions. The Rowshan genotype, however, recorded the highest rate (0.41) for RDLS and RDST under drought stress treatment, that showed significant different from Kavir and Line-9 genotypes (Fig. 3). Also, this genotype had more RDLS at drought stress rather than drought/ N fertilizer.

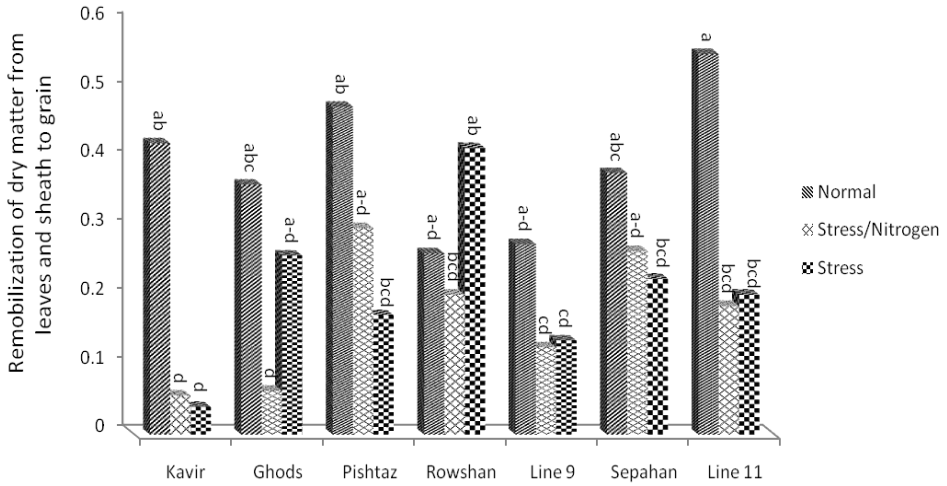

Figure 3. Genotype × environments interaction for remobilization from leaves and sheath to grain.

The genotype× environment interaction showed different relative ration of spike on grain yield for genotypes under normal condition, but they showed no significant difference under drought stress (Fig. 4). According to Fig. 4, the spike had the highest contribution to grain yield at the genotypes of Sepahan, Line 11 and Ghods under the stress/extra N fertilizer treatment (Fig. 4) rather than normal treatment.

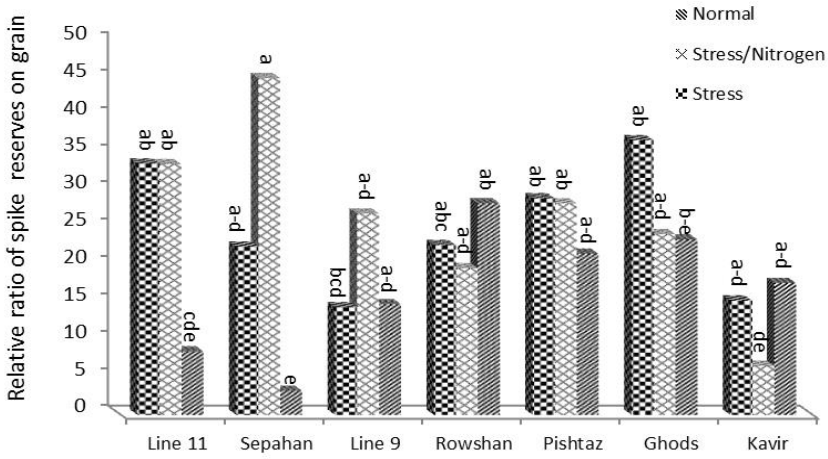

Figure 4. Genotype × environments interaction for relative ratio of spike on grain yield.

DISCUSSION

Before the anthesis stage, the amount of photosynthetic assimilates exceeds the plant's demand; therefore, the extra photo-assimilates accumulate in the shoot to be eventually stored in such secondary sources as stem, peduncle, and leaf sheath (Ebadi et al., 2007). Environmental stresses such as drought, especially during grain filling, lead to declining photosynthesis when the importance of secondary sources in grain filling becomes more pronounced. The highest dry matter remobilization values from the stem, the peduncle, the internodes, and the leaf sheath observed under normal irrigation implied the greater vegetative growth of various plant organs including the leaf sheath in the non-stress environment, which naturally explained the decreasing effect of water deficit on the dry matter translocation to sink (grain) organs (Blum, 2011). The relative contributions of dry matter remobilization from the spike and the stem to final grain yield depending on the genotype and environmental conditions (Blum, 1998; Ebadi et al., 2007). Similar to our findings, Ehdaei et al. (2006) reported higher values of the peduncle's mobile reserves under normal conditions than under stress conditions. Contrary to the present results, however, increased values of remobilization by the next internode (11%) and for other internodes (5%) have been reported under drought-stressed conditions (Yang et al., 2001; Ehdaei et al., 2006). The superiority of the Sepahan genotype for dry matter remobilization from the spike under drought/N fertilizer conditions explains the good adaptability of this genotype to drought stress as a result of consuming the spike assimilate reserves for grain filling. The Kavir, Ghods, and Rowshan cultivars were not capable of using the extra nitrogen present to increase

ear reserves and to redistribute them to the grain. These genotypes showed higher remobilization rates under drought stress conditions than in the drought/ N fertilizer treatment. The higher rate of remobilization from the spike observed in the drought/N fertilizer treatment compared to the non-stress treatment is in good agreement with the findings of Ehdaei et al. (2006). The contribution of spike to grain yield was found to be significantly influenced by the drought stress conditions; Ahmadi et al. (2004) reported different results in their study. It may be concluded that the quantity of spike assimilate reserve and its remobilization efficiency are related to the sensitivity or the tolerance of genotypes to drought stresses, a finding that is different from those reported previously (Ahmadi et al., 2004).

The highest yields by the genotypes under normal conditions may be attributed to the longer grain filling period and the enhanced grain filling ratio under no-stress conditions (Ebadi et al., 2007). Several studies have indicated that grain yield in wheat primarily originates as a result of translocation from the vegetative parts after anthesis (Haberle et al., 2008). Fathi (1997) found that increased nitrogen fertilizer had no considerable effect on yield increase under drought stress, which is confirmed by our results in this study. It had been previously reported that extra nitrogen would give rise to only a slight influence on the reaction by the plant under drought stress and that nitrogen consumption efficiency would increase if sufficient water was present (Palta et al., 1994). However, average ranges of yield components have also been reported in the Pishtaz genotype (Golabadi & Golkar, 2013). This finding indicates that the stress tolerating mechanism had been really active in this cultivar so that yield reduction was prevented and grain yield increased under drought stress. The highest value of grain yield observed in Pishtaz genotype also confirms the influence of the assimilate reserves on preventing yield reduction under drought stress. Similar to our results, Pheloung and Siddique (1991) found that, compared to the potentially lower yielding cultivars, the high yielding ones with lower reserve storage suffered greater reductions in grain yield under drought stress during the grain filling period. It is noteworthy that the superior grain yield of Kavir to that of Rowshan could be compromised by its better reaction to some yield components such as spike number per plant and some of its physiological traits (Golabadi & Golkar, 2013). Blum (1998) also maintained that it would be possible to recover grain yield under stress by remobilization from the stem to the seed. No significant differences were observed in dry matter remobilization from the stem in the different drought treatments. Palta et al. (1994), however, reported that stem reserve remobilization is affected by water stress during grain filling and that the intensity of water stress may affect shoot reserve remobilization. During the grain filling period, stem weight begins to decrease, which indicates the consumption of the stored materials in the following growth stages (Rawson & Evans, 1971; Evans & Wardlow, 1996). The higher contribution of the stem to grain yield observed in the drought stress treatment as compared to the normal conditions is in agreement with the findings of previous studies (Sabry et al., 1995; Niu et al., 1998). Stem reserve is an important source of carbon for grain filling (Blum, 2011). Lopez-Castaneda and Richards (1994) reported an obvious relationship between grain yield and weight reduction of stem after anthesis in wheat, barley, triticale, and oat. Ehdaie et al. (2006) reported that wheat growth depends more on its stem reserves for grain filling than on current photosynthesis. Considering the fact that endosperm cells start to be filled two weeks after anthesis, the extra photo-assimilates must then accumulate in the stem (Schnyder, 1993). In other words, cultivars

with a higher stem dry matter content exhibit a higher potential for storing photo-assimilates under favorite conditions in the early growth stage (before the onset of the dry season). This may be an advantage when the stored materials are transferred to the grain at a higher efficiency. The reaction of Rowshan genotype, with its relative semi-dwarf trait, was similar to that observed by Borrell et al. (1993) who reported that wheat dwarfness genes (Rht_1 and Rht_2) reduced the reserves in the stem (35%) and in the internodes (39%), which amount to a reduction of 21% in stem height. Ehdaei et al. (2006), in contrast, reported that there was no relationship between remobilization from the stem and stem height. The genotypes of Pishtaz, Sepahan, and Line-11 exhibited greater heights in the drought/N fertilizer treatment than in the drought stress condition (data not shown), indicating the complementary effect of nitrogen application on plant height. The significant differences observed among the genotypes in their rates of dry matter remobilization from the peduncle imply their physiological and morphological differences in terms of dry matter accumulation and remobilization of these assimilates to the grain (Ebadi et al., 2007). In the source–sink relationship for dry matter allocation, it is mainly the closest source that plays the more important role (Ebadi et al., 2007). Peduncle serves as a carbon source close to the grain; its dry matter could, therefore, be easily translocated to the grain when an environmental stress arises. Previous studies reported that the peduncle before the internode and the leaf sheath are the major places for dry matter accumulation and redistribution to the grain (Daniels & Alcock, 1982). The reducing current photosynthesis during grain filling observed in the water deficit treatments in this study has also been reported previously (Schnyder, 1993; Palta at al., 1994; Ahmadi et al., 2004). Under these conditions, the enhanced stem reserves and their remobilization serve as an important supporting process that can largely compensate for the reducing grain yield (Budakli et al., 2007). Ehdaie et al. (2006) noted that wheat crops grown in dry land areas would depend more on their stem reserves for grain filling than on current photosynthesis and the efficiency of dry matter transfer depends on the stem dry weight at anthesis and that higher dry matter contents give rise to great material transfers. Rowshan exhibited a similar mechanism for grain filling; however, it failed to achieve a high grain yield under drought stress conditions because this genotype does not have the genetic potential for high yield in all environments.

CONCLUSIONS

The results of the present study suggest that grain yield in wheat cultivars under water deficit conditions and photosynthetic inhibition of sources at the beginning of the grain filling period are controlled more by the source than by the sink limitation. Stem and spike were found to play important roles in supplying assimilate reserves for the grain filling process under stress conditions. This is while in normal conditions it is solely the current photosynthesis that supplies the materials required for grain filling without any need to the vegetative growth reserves. It seems that tolerant cultivars have a relatively higher capability for storing photo-assimilates while they are also more efficient in transferring their reserves under stress conditions.

In our study, leaf sheath dried quickly under drought stress and showed no considerable increase in remobilization. Other organs such as stem, spike, peduncle, and other internodes, however, exhibited increased rates of remobilization in the drought/N fertilizer treatment compared to the drought-stressed conditions. This indicates the

higher photosynthetic assimilate reserves in these organs due to their higher vegetative growths as a result of the greater amounts of nitrogen present. Also, the increased remobilization by the peduncle in the drought/N fertilizer treatment compared to the drought stress one implies the supplementary effects of nitrogen as a result of enhanced peduncle assimilate reserves and their fast remobilization to the grain under stress conditions. The highest value of remobilization from the leaf sheath in the Rowshan genotype under drought stress might have been due to the plant's strife to remain green under drought stress and also to the genetic properties of this genotype which produced small amounts of reserves in the leaf sheath for complete use under stress conditions. This genotype can, therefore, be exploited in future breeding programs aimed at identifying the mechanisms involved in remobilization improvement. At this study, Among the different assimilate sources, the spike and the stem were found to have more important contributions to grain filling, a potential that can be exploited in the production of wheat cultivars with higher grain yields. Based on our findings, the evaluated genotypes showed significant difference for remobilization of dry matter from spike, stem, peduncle, leaves and sheath. The Pishtaz genotype in this study was found to have the highest grain yield but the lowest current photosynthesis, which confirms the idea that more efficient and greater use was made of the available reserves for grain filling in the absence of high current photosynthesis. So, the Pishtaz genotype may be recommended as the candid genotype for cultivation in drought regions because of its higher spike contribution to grain yield; its efficient material remobilization from the stem, the internodes, and the leaf sheath; and finally its grain yield.

REFERENCES

Ahmadi, A., Si-o-Semardeh, A. & Zali, A.A. 2004. A comparison between the capacity of photoassimilate storage and remobilization, and their contribution to yield in four wheat cultivars under different moisture regimes. *Iran J. Agric. Sci*. **35**(4), 921–931.

Austin, R.B. 1989. Maximizing crop production in water-limited environments. In: Baker FWG (Ed). Drought Resistance in Cereals. CAB International, pp. 13–25.

Blum, A. 1998. Improving wheat grain filling under stress by stem reserve mobilization. *Euphytica* **100**, 77–83.

Blum, A. 2011. Plant breeding for water- limited environments. Springer. 255 pp. (In English)

Borras, L., Slafer, G.A. & Otegui, M.E. 2004. Seed dry weight response to source-sink manipulation in wheat, maize and soybean: a quantitative reappraisal. *Field Crops Res*. **86**, 131–146.

Borrell, A.K., Incoll, L.D. & Dalling, M.J. 1993. The influence of the *rht1* and *rht2* alleles on the deposition and use of stem reserves in wheat. *Ann. Bot.* **71**, 317–326.

Bradford, K.J. 1994. Water stress and the water relations of seed development: A critical review. *Crop. Sci*. **34**, 1–11.

Braun, H.J., Atlin, G. & Payne, T. 2010. Multi-location testing as a unit to identify plant response to global climate change. In: Reynolds MP, ed. Climate change and crop production. Surrey, UK: CABI Climate Change Series, 115–138.

Budakli, E., Celik, N., Turk M., Bayram, G. & Tas, B. 2007. Effects of post anthesis drought stress on the stem reserve mobilization supporting grain filling of two rowed barley cultivars at different levels of nitrogen. *J. Biol. Sci*. **7**, 949–953.

Daniels, R.W. & Alcock, M.B. 1982. A reappraisal of stem reserve contribution to grain yield in spring barley (*Hordeum vulgare* L.). *J. Agric. Sci*. **98**, 347–355.

Distelfeld, A, Avni, R. & Fischer, A.M. 2014. Senescence, nutrient remobilization, and yield in wheat and barley. *J. Exp. Bot*. **65**(14), 3783–3798.
Ebadi, A., Sajed, K. & Asgari, R. 2007. Effects of water deficit on dry matter remobilization and grain filling trend in three spring barley genotypes. *J. Food Agric. Environ.* **5**(2), 359–362.
Ehdaie, B. & Waines, J.G. 1996. Genetic variation for contribution of pre anthesis assimilates to grain yield in spring wheat. *J. Genet. Breed*. **50**, 47–56.
Ehdaie, B., Alloush, G.A., Madore, M.A. & Waines, G. 2006. Genotypic variation for stem reserves and mobilization in wheat: I. Postanthesis changes in internode dry matter. *Crop Sci.* **46**, 735–746.
Evans, L.T. & Wardlow, I.F. 1996. Photoassimilate distribution in plants and crops source-sink relationship. In: wheat. Eds. E. Zanneki, A.A. Sehalten. NewYork. PP: 501–518.
Fathi, G., McDonald, G.K. & Lance, R.C.M. 1997. Effects of post anthesis water stress on the yield and grain protein concentration of barley grown at two levels of nitrogen. *Aust. J. Agric. Res*. **48**, 67–80.
Gardner, F.P., Pearce, B. & Mitchell, R.L. 2003. Physiology of Crop Plants. Jodhpur Scientific, 328 p.
Golabadi, M., Arzani, A. & Maibody, S.A.M. 2006. Assessment of drought tolerance in segregating populations in durum wheat. *Afr. J. Agric. Res.* **1**(5), 162–171.
Golabadi, M. & Golkar, P. 2013. Compensation of grain yield reduction under drought stress by extra N fertilizer in bread wheat. *Int. J. Agric. Res. Rev*. **3**(3), 629–634.
Haberle, J., Svoboda, P. & Raimanová, I. 2008. The effect of post-anthesis water supply on grain nitrogen concentration and grain nitrogen yield of winter wheat. *Plant Soil Environ.* **54**, 304–312.
Kardavani, P. 1988. The Arid Lands. Tehran University Press, 376 p. (In Persian).
Kim, J.Y., Mahé, A., Brangeon, J. & Prioul, J.L. 2000. A maize vacuolar invertase, IVR2, is induced by water stress. Organ/tissue specificity and diurnal modulation of expression. *Plant Physiol*. **124**, 71–84.
Lopez-Castaneda, C. & Richards R. A. 1994. Variation in temperate cereals in rainfed environments I. Grain yield, biomass and agronomic characteristics. *Field Crops Res*. **37**, 51–62.
Niu, J.Y., Gan, Y.T., Zhang, J.W. & Yang, Q.F. 1998. Post-anthesis dry matter accumulation and redistribution in spring wheat mulched with plastic film. *Crop Sci.* **38**,1562–1568.
Palta, J.A., Turner, C. & Filery, I.R. 1994. Remobilization of carbon and N in wheat as influenced by post-anthesis water deficits. *Crop Sci.* **34**,118–124.
Papakosta, D.K. & Gagianas, A.A. 1991. Nitrogen and dry matter accumulation, remobilization and losses for Mediterranean wheat during grain filling. *Agron. J.* **83**, 864–870.
Pheloung, P.C. & Siddiqe, H.M. 1991. Contribution of Stem Dry Matter to Grain Yields in Wheat Cultivars. *Aust. J. Plant Physiol*. **18**, 53–64.
Rawson, H.M. & Evans, L.T. 1971. The contribution of stem reserves to grain development in a range of cultivars of different height. *Aust. J. Agric. Res.* **22**, 851–863.
Sabry, S.R.S., Smith, L.T & Smith, G.M. 1995. Osmoregulation in spring wheat under drought and salinity stress. *J. Genet. Breed*. **49**, 55–60.
SAS Institute. 2003. SAS/STAT User's Guide, Version 9**.** 1. SAS Institute, Cary. NC.
Schnyder, H. 1993. The role of carbohydrate storage and redistribution in the source-sink relation of wheat and barley during grain filling-a review. *New phytol.* **123**, 233–245.
Setter, T.L., Anderson W.K., Asseng, S., & Barclay, S. 1998. Review of the impact of high shoot carbohydrate concentration on maintenance of high yields in cereals exposed to environmental stress during grain filling. CAB Abstract. **51**, 23.
Spiertz, J.H.J., Hamer, R.J., Xu, H.Y., Primomartin, C., Don, C. & Van De Putten, P. E. L. 2006. Heat stress in wheat; effects on grain weight and quality within genotypes. *J. Eur. Agron*. **25**(1), 89–95.

Wang, Z.M., Wang, S.A. & Su, B.A. 1995. Accumulation and remobilization of stem reserves in wheat. CAB Abstract. **25**, 10.

Yang, J. & Zhang, J. 2006. Grain filling of cereals under soil drying. *New Phytologist* **169**, 223–236.

Yang, J., Zhang, J., Wang, Z., Zhu, Q. & Liu, L. 2001. Water deficit-induced senescence and its relationship to remobilization of pre-stored carbon in wheat during grain filling. *Agron. J.* **3**, 196–206.

Zadoks, J.C., Chang, T.T. & Konzak, C.F. 1974. A Decimal Code for the Growth Stages of Cereals, *Weed Res.* **14**, 415–421.

Agronomy Research **13**(5), 1215–1226, 2015

Evaluation of factors affecting crystallization of disparate set of multi-flower honey samples

A. Grégrová*, V. Kružík, E. Vrácovská, A. Rajchl and H. Čížková

University of Chemistry and Technology, Prague, Faculty of Food and Biochemical Technology, Department of Food Preservation, Technická 5, 16628 Prague 6 – Dejvice, Czech Republic; *Correspondence: Adela.Gregrova@vscht.cz

Abstract. Honey crystallization is considered to be a natural process during its maturing and an indicator of natural honey composition. However, consumer evaluation of honey crystallization is usually negative. Crystallization depends on honey composition and it is influenced by methods and conditions of honey processing and storage (mechanical and thermal treatment). The aim of this work was to identify and evaluate general factors which can affect crystallization of blend multi-flower honeys (a disparate set of samples). The following qualitative parameters were determined: a content of 5-hydroxymethylfurfural, furfural, glucose and fructose, water and diastase activity, moisture and an absolute pollen count. A degree of honey sample crystallization was assessed by a sensory analysis. Effects of the various qualitative parameters on the crystallization degree were statistically evaluated. The honey crystallization degree was found to be a qualitative parameter positively correlated with the absolute pollen count. Using a multi-regression method (a cluster analysis) it was proven that the 5-hydroxymethylfurfural and moisture parameters were suitable characters with certain explanatory power to classify blend honey samples according to their crystallization degrees.

Key words: honey crystallization, multi-flower honey, qualitative parameter.

INTRODUCTION

Honey crystallization is a natural occurrence in honey maturing and in some respects it can be taken as an indicator of natural honey composition (Venir et al., 2010). Unfortunately partial or entire crystallization of commercial honeys is often considered a defect (by consumers), because liquid and transparent honeys are wrongly regarded as better quality honeys. Besides causing obvious changes in sensory, mainly visual, properties, honey crystallization can have another unsatisfactory effects, such as technological and processing problems (e.g. pouring), a loss of honey homogeneity, higher water activity related to honey fermentation due to microorganisms' development (Tosi et al., 2002).

Tendency to crystallization of honeys depends mainly on the following factors: chemical composition, a degree of supersaturation, viscosity, a fructose/glucose (F/G) ratio, moisture (M) and a dextrine content, water activity (a_w), micro-crystals and nucleation seeds (e.g. pollen grains) presence, age, storage temperature and thermal history (Bogdanov, 1993; Tosi et al., 2002; Tosi et al., 2004; Juszczak & Fortuna, 2006; Sudzina et al., 2009; Venir et al., 2010). Duration of an entire crystallization process

varies considerably for different honey types. In most honeys, crystallization begins within weeks or months at room temperature (Townsend, 1975; Assil et al., 1991).

Generally, blossom honeys crystallise faster due to a higher content of less soluble glucose (a content of approx. 40–50 g 100 g^{-1} in dry matter Gleiter et al., 2006; Laos et al., 2011) and pollen grains. On the contrary, crystallization proceeds more slowly in honeydew honeys, which contain less glucose (a content of approx. 30–35 g 100 g^{-1} in dry matter Gleiter et al., 2006) and more fructose, but could under some circumstances have a significantly higher content of crystal-forming melezitose and trehalose (Dobre et al., 2012).

Honey maturing may be impaired by exposure to high temperatures or by filtration (removal of pollen grains). Crystallization occurs more easily when honeys are disturbed (e.g. stirring, shaking and agitating) (Rybak-Chmielewska, 2004).

Crystallization can be controlled mainly by heating and proper temperature storage conditions. If honey is held at 40–71°C during processing (bottling), a crystallization degree is reduced. Crystals can be dissolved by mild heating of honey and quick heating at 60–71°C tends to dissolve crystals and expel incorporated air (which can also stimulate honey crystallization) (Townsend, 1975; Assil et al., 1991).

Diastase activity and a 5-HMF (5-hydroxymethylfurfural) content are used as quality indicators of freshness or indicator of extensive heating of honey during its processing with limits given by the EU Honey Directive (Subramanian et al., 2007).

Tosi et al. (2004) determined the effect of high-temperature short time heating of honey on the following qualitative parameters related to honey quality and crystallization process: a 5-HMF content, diastase activity and crystallization starting time. Crystallization onset was proved to be delayed by 4 to 9 weeks for honeys treated by high-temperature short-time treatment at 80°C for 60 s in the transient stage and 30 s in the isothermal stage. 5-HMF and DN modifications recorded after the heat treatment were for example: a) the 5-HMF content increased to 7.9 mg kg^{-1} and the DN decreased to 14.4 in case of honey with a higher initial content of 5-HMF (7.5 mg kg^{-1}) and DN (14.6); b) both values stayed the same in case of honey with a lower initial content of 5-HMF (5.0 mg kg^{-1}) and DN (9.0) (Tosi et al., 2004).

Crystallization is also affected by presence and a number of crystallization centres, mainly pollen grains. Therefore, qualitative and quantitative melissopalynological analyses (Holdaway, 2004) of honeys mainly used to determine botanical and geographical origin of honeys can be employed (Louveaux et al., 1978; Song et al., 2012). Pollen grains but also plant and animal admixtures, e.g. spores and hyphae of fungi, algae, yeasts, chitin fragments, hairs, insects etc., can be removed by filtration (Přidal, 2003). Filtered honey has a significantly lower tendency to crystallise. Filtration also removes small crystals of glucose and contaminants that trigger crystallization process.

As was already mentioned, honey crystallization can be influenced by many factors and changes can be predicted to a certain extent only in the case of monoflower honeys. Since in the Czech Republic mainly blend honeys are processed, the aim of our study is to verify whether it is possible to identify general factors affecting a disparate set of multi-flower honey samples. The effects of various parameters on honey crystallization have been statistically processed.

MATERIALS AND METHODS

Honey samples

The total of 16 samples of different honeys were analysed including blend multi-flower honeys (European (EU) and Czech honeys; 2012) (Table 1). Samples no. 1–10 were sampled at different degrees of crystallization; they came from different batches with known thermal history (preheating at about 35°C and pasteurisation (75°C, 5 min) was the same for all the samples and varied only with time delays in a tank at 40°C), and were supplied directly by manufacturers. A set of samples no. 11–16 of different origin and with unknown thermal history was purchased in the Czech market.

Table 1. Analysed samples

Sample Number	Heating Period in a Tank	Manufacturer/Vendor	Origin
1	0 min	Medokomerc, CZ	EU
2	0 min	Medokomerc, CZ	EU
3	0 min	Medokomerc, CZ	EU
4	0 min	Medokomerc, CZ	EU
5	0 min	Medokomerc, CZ	EU
6	360 min	Medokomerc, CZ	EU
7	360 min	Medokomerc, CZ	EU
8	180 min	Medokomerc, CZ	EU
9	240 min	Medokomerc, CZ	EU
10	420 min	Medokomerc, CZ	EU
11	unknown	JSG med, CZ	EU
12	unknown	Kaufland, CZ	EU
13	unknown	Local Czech Beekeeper	CZ
14	unknown	Medokomerc, CZ	EU
15	unknown	Product Bohemia, CZ	CZ
16	unknown	IS import-export, SK	EU

Determination of qualitative parameters

The following physico-chemical, qualitative parameters were determined: a content of 5-hydroxymethylfurfural, furfural, glucose and fructose, diastase activity, water activity, moisture, presence and a number of crystallization centres (an absolute pollen count).

With the exception of water activity (Chirife et al., 2006) all the other analytical parameters were determined according to the harmonized methods for the analysis of honey (Bogdanov, 2009).

A content of 5-HMF and furfural was determined in a filtered, aqueous honey solution using HPLC equipped with UV detection (Thermostated Column Compartment TCC-100: Dionex, Germany; HPLC Pump Dionex P680; HPLC Dionex Summit ASI-100 Automated Sample Injector; UltiMate 3000, Photodiode Array Detector: Dionex, Germany).

A content of sugars (glucose and fructose) was analysed (after filtration of the solution) by HPLC with RI detection (Thermostated Column Compartment TCC-100: Dionex, Germany; HPLC Pump Dionex P680; HPLC Dionex Summit ASI-100 Automated Sample Injector; UltiMate 3000, RI Detector: Shodex RI – 101, Japan).

Diastase activity expressed as a diastase number (DN) was analysed using Phadebas tablets by a photometric method (Phadebas Amylase Test: Magle AB, Sweden) using Spectrofotometer Genesys 20 (Thermo Spectronic, USA) and water activity was determined using an electronic dew-point water activity meter, Aqua Lab Series 3 (Decagon Devices, USA).

Moisture was analysed by automatic digital refractometry, Refractometer RFM 340 (Bellingham + Stanley, United Kingdom). The water content was determined from the refractic index of the honey.

A quantitative melissopalynological analysis was performed using the modified procedure described in Přidal (2003). Pollen grains were determined microscopically and expressed as an absolute pollen count (APC, i.e. a number of pollen grains per 10 g of honey). Honey (10 g) were dissolved and diluted in distilled water; solution was centrifuged in a cuvette at 3 000 rpm (3 times for 5 min). The sediment was filtered through a microbiological filter and after drying it was illuminated by cedar oil. Pollen grains were counted in 60 view fields (at 1,000x magnification). A Digital Laboratory Microscope was used, Model DMBA-310 (Motic Deutschland GmbH, Germany).

Sensory evaluation

Samples were also sensorially assessed. Sensory evaluation was performed by 10 panellists from the Department of Food Preservation (University of Chemistry and Technology, Prague) according to Piana et al. (2004). To evaluate crystallization, a 10-point scale was used (1 = liquid; 10 = entirely crystallised).

Statistical analysis

The results were presented as mean values of three repetitions for each analysed qualitative parameter. A degree of linear relationship between the parameters was studied using the Pearson correlation matrix. A cluster analysis was performed to group the samples according to the studied variables. All statistical analyses were carried out using STATISTICA 10.0 (StatSoft, USA) software.

RESULTS AND DISCUSSION

The set of honey samples at different levels of crystallization (all samples were analysed approx. 18 month after production) and with different thermal history were analysed. The results for all determined qualitative parameters are given in Table 2.

Table 2. Comparison of the measured data

Sample number	Moisture (M; %)	Water Activity (a_w)	5-HMF (mg kg^{-1})	Furfural (mg kg^{-1})	Glucose (g 100 g^{-1})	Fructose (g 100 g^{-1})	Diastase Activity (DN)	F/G	G/M	Absolute Pollen Count (APC × 10^4)	Crystallization Degree
1	17.51	0.596	25.06	0.00	28.80	38.30	11.64	1.33	1.64	11.56	9
2	17.44	0.594	31.70	2.72	33.20	41.60	10.79	1.25	1.90	10.50	9
3	17.52	0.605	29.90	2.65	29.60	40.40	10.93	1.36	1.69	10.18	9
4	17.75	0.571	20.10	2.66	32.40	45.40	10.80	1.40	1.83	8.43	2
5	17.71	0.574	45.40	2.40	31.10	43.80	10.55	1.41	1.75	6.96	1
6	17.10	0.576	26.96	2.71	28.60	38.70	12.20	1.35	1.67	10.10	3
7	17.88	0.577	36.18	2.54	31.00	39.70	10.56	1.28	1.78	8.10	2
8	17.82	0.579	22.70	2.87	31.50	39.30	9.75	1.25	1.77	9.67	5
9	17.64	0.576	34.48	2.70	29.30	42.20	11.66	1.44	1.66	9.90	5
10	17.81	0.574	43.70	2.48	30.00	42.60	10.57	1.42	1.68	7.43	2
11	16.55	0.597	46.96	4.00	29.56	38.58	10.57	1.31	1.79	10.57	8
12	17.90	0.639	45.00	2.60	22.20	40.03	9.50	1.43	1.15	7.40	2
13	17.18	0.577	19.90	0.00	23.59	24.09	10.80	1.02	1.69	5.97	3
14	17.62	0.639	32.93	3.18	31.51	39.03	12.20	1.24	1.79	10.97	10
15	16.14	0.594	32.60	3.39	24.38	36.96	9.70	1.52	1.51	9.13	5
16	17.69	0.617	36.35	2.75	28.66	42.25	10.50	1.47	1.62	10.39	s5

DN = diastase activity expressed as diastase number; APC = number of pollen grains per 10 g of honey; crystallization degree: 10 point sensory scale from 1 = liquid to 10 = entirely crystallised; all samples were analysed approx. 18 month after production.

Crystallization degree varied considerably and ranged from 1 (liquid) to 10 (entirely crystallised) points (Fig. 1). Given the nature of our study qualitative assessment of the crystallization process was based on sensory evaluation. Because of obvious differences between samples sensory analysis was chosen as an appropriate and sufficient method and there was no need to apply strict quantitative methods for this purpose, e.g. microscopy and calorimetry (Mazzobre et al., 2003; Venir et al., 2010).

a) 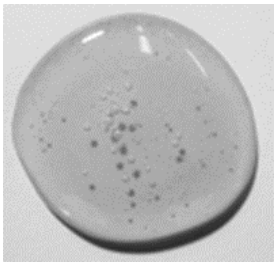 b) 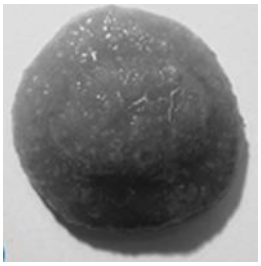 c) 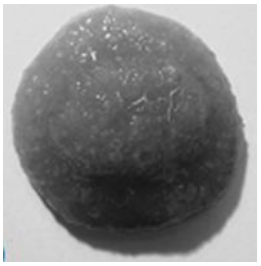

Figure 1. Honeys in different stages of crystallization (Panasonix Lumix DMC-FZ38; at 4x magnification; 5 g of blend multi-flower honeys on white anti-reflective surface) (a) natural liquid honey – crystallization degree 1, sample no. 5; b) partially crystallized honey – crystallization degree 5, sample no. 8; c) entirely crystallized honey – crystallization degree 10, sample no. 14).

For all samples, the moisture content, water activity, diastase activity, ratios of F/G and G/M were very balanced.

The content of 5-HMF (from 19.9 mg kg^{-1} to 47.0 mg kg^{-1}) and furfural (from not detected levels to 4.0 mg kg^{-1}) could point to heating or improper long-term storage of a sample. The diastase activity (indicating heating and/or improper storage) expressed as a DN ranged from 9.5 to 12.2. Quality of samples no. 1–10 heated in a tank at 40°C for varying periods of time was not negatively influenced by these temperature and storage conditions. Only in 2 samples, i.e. sample no. 5 and 10, the content of 5-HMF was slightly higher than the 40 mg kg^{-1} requirement (European Parliament and Council Directive, 2001), which could be caused by the raw material.

The glucose content was determined to range from 22.2 g 100 g^{-1} to 33.2 g 100 g^{-1} and the fructose content ranged from 24.1 g 100 g^{-1} to 45.4 g 100 g^{-1}. Botanical origin of multi-flower honey samples and the associated sugar composition influence honey crystallization (Escuredo et al., 2014). Honeys with a high glucose content and a low F/G ratio crystallised more rapidly (rape and sunflower based honeys). Honeys with a higher F/G ratio (more than 1.4) crystallised generally more slowly, e.g. bramble, chestnut, eucalyptus, heather, acacia and honeydew honeys (Escuredo et al., 2014); from the analyzed samples it was fulfilled by no. 5, 9, 10, 12, 15 and 16 with crystallization degree ranged from 1 to 5 points.

Moisture, and hence a crystallization degree, should be closely linked to water activity (a_w) (Tosi et al., 2004). In accordance with literature (Tosi et al., 2004) the water activity was determined in the range from 0.571 to 0.639 (a_w). Water activity increases with a moisture increase (Tosi et al., 2004). Moisture was determined in the range from 16.1% to 17.9% (M).

Most of the samples met the legislative requirements (European Parliament and Council Directive, 2001) for followed physico-chemical parameters except for samples no. 5 (5-HMF: 45.4 mg $kg^{-1;}$, limit max. 40), 10 (5-HMF: 43.7 mg kg^{-1}), 11 (5-HMF: 47.0 mg kg^{-1}), 12 (5-HMF: 45.0 mg kg^{-1}) and 13 (G+F: 47.7 weight %, limit min. 60).In accordance with the literature (Oddo & Piro, 2004; Song et al., 2012), the results of the quantitative melissopalynological analysis, i.e. the absolute pollen count (the number of pollen grains per 10 g of honey sample), varied significantly from $6.0 \cdot 10^4$ to $11.6 \cdot 10^4$. In the study by Song et al. (2012) 4 out of the 19 analysed samples (Chinese monoflower honeys) contained from $2.0 \cdot 10^4$ to $10.0 \cdot 10^4$ of pollen grains and 2 samples contained $> 10.0 \cdot 10^4$ of pollen grains (an absolute pollen count). Pollen grains from, for example, rape, black locust, sunflower and dandelion were identified in the samples; these plants are typical for Central and Eastern European countries (Oddo & Piro, 2004) (Fig. 2). Oddo & Piro (2004) determined mean absolute pollen counts for rape ($7.6 \cdot 10^4$), black locust ($0.9 \cdot 10^4$), sunflower ($1.9 \cdot 10^4$) and dandelion ($3.4 \cdot 10^4$) honeys.

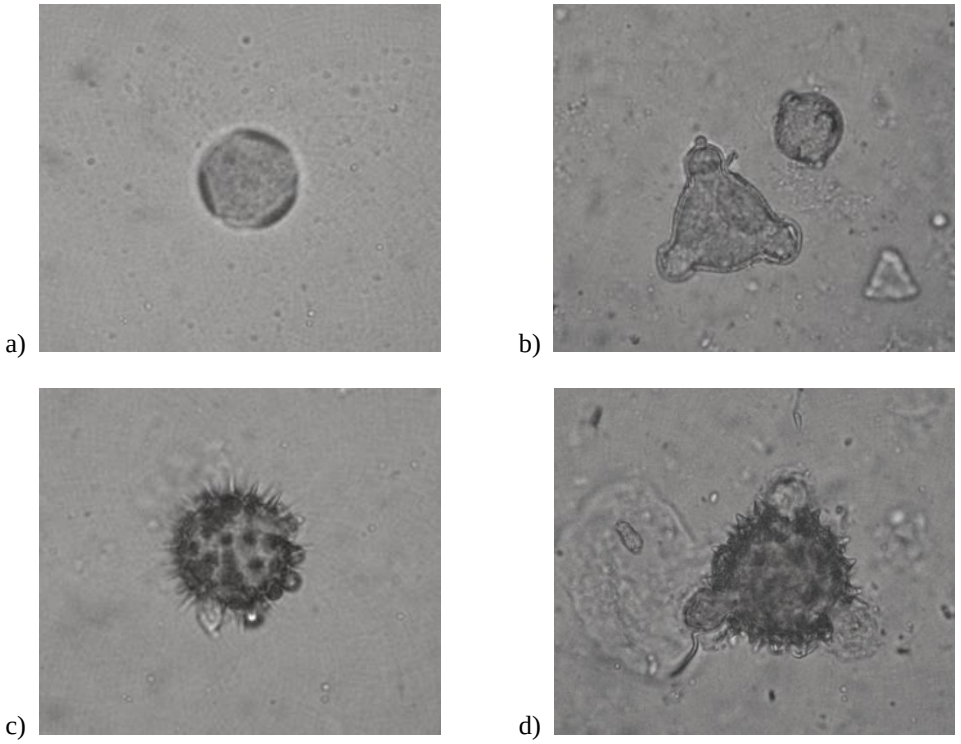

Figure 2. Examples of the found pollen grains (microscopy; at 1,000x magnification) (a) rape; b) black locust; c) sunflower; d) dandelion).

The effects of various parameters on honey crystallization were statistically evaluated. A correlation matrix and a cluster analysis were applied to evaluate relationships between the qualitative parameters and the properties of honey samples (Table 3; Figs 3, 4).

Table 3. Correlation matrix

	Moisture	a_w	5-HMF	Furfural	Glucose	Fructose	DN	Fructose/ Glucose	Glucose/ Moisture	APC	Crystallization
Moisture	**1.00**										
a_w	0.04	**1.00**									
5-HMF	0.00	0.28	**1.00**								
Furfural	– 0.21	0.20	0.48	**1.00**							
Glucose	0.35	– 0.29	– 0.08	0.28	**1.00**						
Fructose	0.40	0.01	0.37	0.54	0.59	**1.00**					
DN	0.05	– 0.04	– 0.27	– 0.20	0.35	– 0.01	**1.00**				
Fructose/Glucose	– 0.05	0.10	0.45	0.47	– 0.05	0.71	– 0.22	**1.00**			
Glucose/Moisture	0.02	– 0.48	– 0.30	0.07	0.83	0.11	0.40	– 0.41	**1.00**		
APC	–0.18	0.33	– 0.13	0.26	0.39	0.28	0.45	0.15	0.25	**1.00**	
Crystallization	– 0.25	0.47	– 0.14	0.07	0.25	– 0.05	0.37	– 0.20	0.28	**0.82***	**1.00**

DN = diastase activity expressed as diastase number; APC = number of pollen grains per 10 g of honey; * the critical limit for correlation coefficient r in the case of the 16 samples (confidence level $\alpha = 0.05$) = 0.497.

The results of the crystallization degree evaluation were correlated with the other determined qualitative parameters (Table 3). In accordance with the literature (Escuredo et al., 2014), a statistically significant correlation (α = 0.05) was demonstrated only in the case of the absolute pollen count (r = 0.82; critical value for correlation coefficient: 0.497) for the total disparate set of honey samples (no. 1–16). On the contrary, in the case of the samples with known thermal history and from the same producer (no. 1–10), a statistically significant correlation (α = 0.05) was also demonstrated between the crystallization degree and the water activity (r = 0.92; critical value for correlation coefficient: 0.632). In accordance with the literature (Gleiter et al., 2006; Zamora and Chirife, 2006), it was proven that a_w of crystallised honeys was higher than a_w of liquid (re-dissolved) honeys, because a_w increase during crystallization process is mainly related to glucose crystallization.

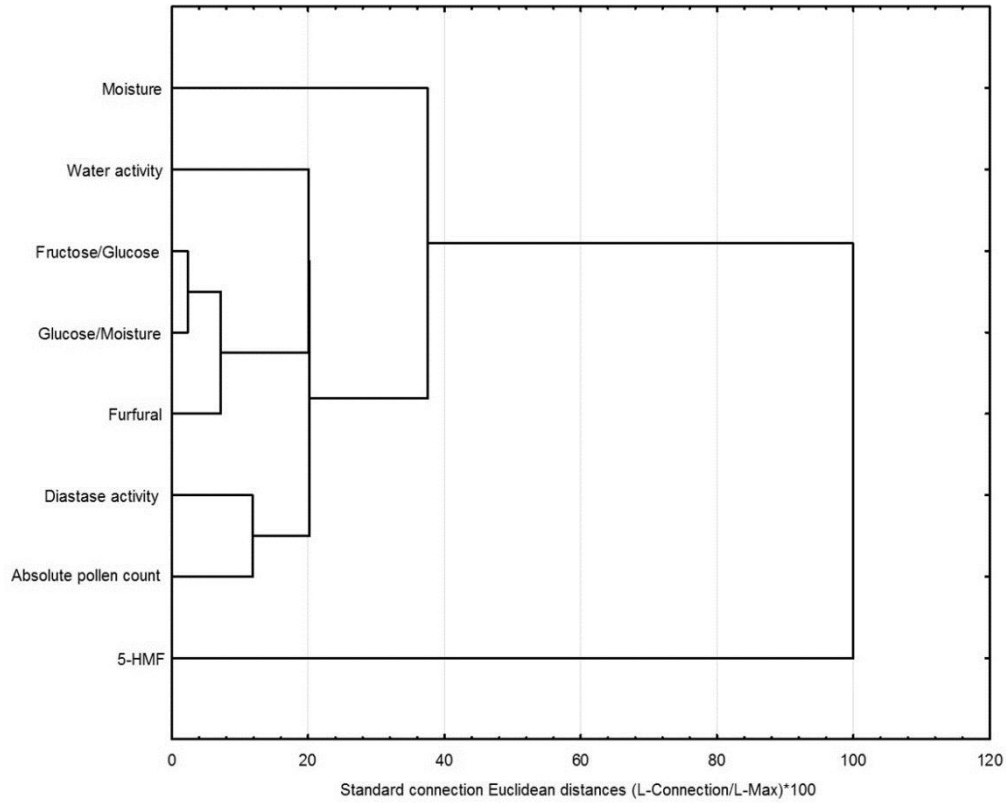

Figure 3. Dendrogram of 8 qualitative parameters for honey samples characterisation.

Since the direct linear correlation (the correlation matrix) was not very demonstrative due to the complexity of the honey crystallization process, a multivariate statistical technique (a cluster analysis) was applied to reveal deeper structures in the data set. This method assesses similarity of the objects based on a combination of all measured characters.

The cluster analysis was applied to prove the ability to distinguish between honeys of a different crystallization degree. For statistical evaluation, a data matrix of the 16 honey samples including the following qualitative parameters was used: moisture, water activity, ratios of G/F and G/M, a content of 5-HMF and furfural, diastase activity and an absolute pollen count (Tosi et al., 2004; Escuredo et al., 2014).

Fig. 3 shows a dendrogram of the characters (for the 8 qualitative parameters), which expresses their reciprocal similarity. Six similar characters (a sub-cluster for the F/G and G/M, furfural and water activity characters and a sub-cluster for the diastase activity and the absolute pollen count) create a large combined cluster (reading from the right to the left), to which a less similar moisture character is connected. The 5-HMF character is completely dissimilar to the others and it has been indicated as an outlying character.

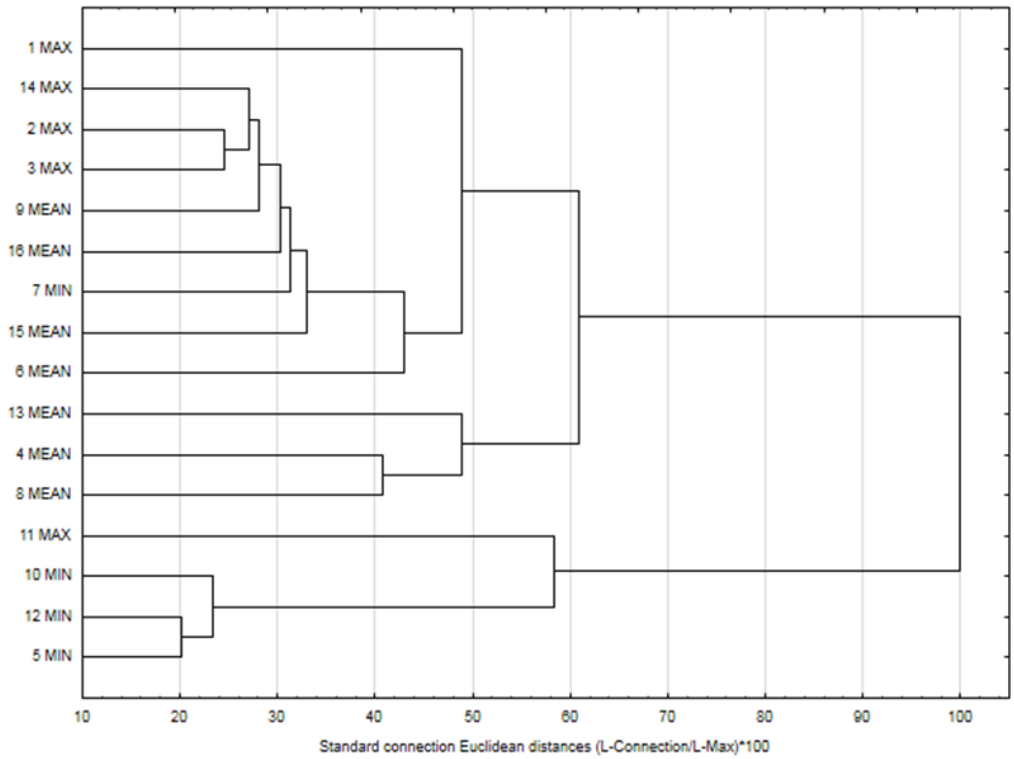

Figure 4. Dendrogram of the 16 honey samples classification (samples indication: maximal, mean and minimal crystallization degree).

A dendrogram of the objects (Fig. 4) allowed classifying the 16 honeys into several expectable clusters. Fig. 4 also shows the samples that were significantly different from the others. It is obvious (reading from the right to the left) that the samples are divided into 3 dominant clusters. The first cluster contains samples no. 1, 14, 2, 3, 9, 16, 7, 15 and 6. The second one contains honeys no. 13, 4 and 8; and the third one includes honeys no. 11, 10, 12 and 5. The first cluster contains maximally and mean crystallised honeys. This group of honeys is characterised by high water and diastase activity and a low

content of 5-HMF. This largest cluster includes both maximally and some mean crystallised honeys due to the similarity of the parameters analysed for these groups of samples. The second cluster of mean crystallised honeys is characterised by the lowest content of 5-HMF in its category. The third cluster is made up of minimally crystallised honeys that have the highest values for moisture and 5-HMF content; the values of absolute pollen count and diastase activity are the lowest. Because of high content of 5-HMF as a result of strong heating it should be emphasized that strongly heated honey crystallizes differently than fresh ones. Two atypical samples, i.e. no. 7 and 11, differ from the other samples in the group due to the following parameters (Fig. 4): F/G and absolute pollen count for sample no. 7; moisture and diastase activity for sample no. 11. Moisture and 5-HMF parameters could be considered as the characters with certain explanatory power to classify samples due to their different crystallization degree.

CONCLUSIONS

Due to complexity of honey crystallization, this process is influenced by a number of factors and conditions of processing and storage of honey. Contrary to the literature, only the absolute pollen count was demonstrated as a qualitative parameter positively correlated with the honey crystallization degree. Using a cluster analysis we found 2 more qualitative parameters, i.e. 5-HMF and moisture content, which influence crystallization degree of blend multi-flower honeys. It was found that most of the analysed multi-flower honey samples with the values of 5-HMF content around or higher than 40.0 mg kg^{-1}, moisture content > 17.7% and absolute pollen count < $9.0 \cdot 10^4$ stayed in a liquid state for approx. 18 months after production.

ACKNOWLEDGEMENTS: This project was supported by the Ministry of Education and Sports, project no. A1_FPBT_2015_002. The authors express their thanks to Dr. Havlík, MSc and to the company Medokomerc (Čestín, Czech Republic) for the provided samples, and to Dr. Horsáková, MSc for creating the pollen grains photos.

REFERENCES

Assil, H.I., Sterling, R. & Sporns, P. 1991. Crystal control in processed liquid honey. *J. Food Sci.* **56**, 1034–1037.

Bogdanov, S. 1993. Liquefaction of honey. *Apiacta.* **28**, 4–10.

Bogdanov, S. 2009. Harmonised methods of the International Honey Commission. *International Honey Commission*. 1–63.

Dobre, I., Georgescu, L.A., Alexe, P., Escuredo, O. & Seijo, M.C. 2012. Rheological behavior of different honey types from Romania. *Food Res. Int.* **49**, 126–132.

Escuredo, O., Dobre, I., Fernandez-González, M. & Seijo, M.C. 2014. Contribution of botanical origin and sugar composition of honeys on the crystallization phenomenon. *Food Chem.* **149**, 84–90.

European Parliament and Council, 2001: Directive 2001/110/EC of 20 December 2001 Relating to Honey. *Official Journal of the European Communities*, L 10, 12. 01. 2002, pp. 6.

Gleiter, R.A., Horn, H. & Isengard, H.D. 2006. Influence of type and state of crystallisation on the water activity of honey. *Food Chem.* **96**, 441–445.

Holdaway, C.A. 2004. *Automation of pollen analysis using a computer microscope*. Master Thesis. Massey University, Turitea. 124 pp.

Chirife, J., Zamora, M.C. & Mott, A. 2006. The correlation between water activity and % moisture in honey: Fundamental aspects and application to Argentine honeys. *J. Food Eng.* **72**, 287–292.

Juszczak, L. & Fortuna, T. 2006. Rheology of selected Polish honeys. *J. Food Eng.* **75**, 43–49.

Laos, K., Kirs, E., Pall, R. & Martverk, K. 2011. The Crystallization Behaviour of Estonian Honeys. *Agron. Res.* **9**, 427–432.

Louveaux, J., Maurizio, A. & Vorwohl, G. 1978. Methods of Melissopalynology. *Bee World* **59**, 139–157.

Mazzobre, M.F., Aguilera, J.M. & Buera, M.P. 2003. Microscopy and calorimetry as complementary techniques to analyze sugar crystallization from amorphous systems. *Carbohyd. Res.* **338**, 541–548.

Oddo, L.P. & Piro, R. 2004. Main European unifloral honeys: descriptive sheets. *Apidologie* **35**, 38–81.

Piana, M., Oddo, L., Bentabol, A., Bruneau, E., Bogdanov, S. & Declerck, Ch. 2004. Sensory analysis applied to honey: state of the art. *Apidologie* **35**, 26–37.

Přidal, A. 2003. *Včelí produkty - cvičení.* Mendelova zemědělská a lesnická univerzita, Brno, 61 pp.

Rybak-Chmielewska, H. 2004. Honey. In Tomasik, P. (ed): *Chemical and functional properties of food saccharides*. CRC Press LLC, Boca Raton, pp. 72–78.

Song, X.Y., Yao, Y.F. & Yang, W.D. 2012. Pollen Analysis of Natural Honeys from the Central Region of Shanxi, North China. *PLOS ONE* **7**, 1–11.

Subramanian, R., Hebbar, H.U & Rastogi, N.K. 2007. Processing of honey: A review. *Int. J. Food Prop.* **10**, 127–143.

Sudzina, M., Melich, M. & Kňazovická, V. 2009. Physicochemical characterization of natural honeys from different regions in Slovakia. *Acta U. Agr. Silvi. Mend. Brun.* **57**, 125–134.

Tosi, E., Caippini, M. & Lucero, E.R.H. 2002. Honey thermal treatment effects on hydroxymethylfurfural content. *Food Chem.* **77**, 71–74.

Tosi, E., Lucero, E.R.H. & Bulacio, L. 2004. Effect of honey high-temperature short-time heating on parameters related to quality, crystallisation phenomena and fungal inhibition. *LWT-Food Sci. Technol.* **37**, 669–678.

Townsend, G.F. 1975. Processing and storing liquid honey. In Crane, E. (ed): *Honey, a comprehensive survey*. Heinemann, London, pp. 269–292.

Venir, E., Spaziani, M. & Maltini, E. 2010. Crystallization in 'Tarassaco' Italian honey studied by DSC. *Food Chem.* **122**, 410–415.

Zamora, M.C. & Chirife, J. 2006. Determination of water activity change due to crystallization in honeys from Argentina. *Food Control* **17**, 59–64.

Agronomy Research **13**(5), 1227–1233, 2015

Adding biobutanol to diesel fuel and impact on fuel blend parametres

V. Hönig[1,*], L. Smrčka[2], R. Ilves[3] and A. Küüt[3]

[1]Czech University of Life Sciences Prague, Faculty of Agrobiology, Food and Natural Resources, Department of Chemistry, Kamýcka 129, 16521 Prague 6, Czech Republic
[2]University of Economics, Faculty of Business Administration, Department of Strategy, W. Churchill Sq., 13067 Prague 3, Czech Republic
[3]Estonian University of Life Sciences, Institute of Technology, Kreutzwaldi 56, EE51014 Tartu, Estonia
[*]Correspondence: honig@af.czu.cz

Abstract. One of the main arguments for the use of biofuels is environmental reason. Biofuels release significantly lower quantities of greenhouse gases (GHG) during the combustion opposed to conventional fossil fuels. Fatty acid methyl esters are commercially blended with diesel and bioethanol with gasoline. Biobutanol and bioethanol are using the same sources. Biobutanol can be used as a biofuel in internal combustion engines in the same manner as bioethanol. Application of biobutanol in diesel is rather marginal, but is definitely preferable in diesel engines in comparison with bioethanol. There are plenty of options to use biobutanol in diesel engines. The simplest are blends with diesel. Number of parameters can used to compare biobutanol with standard diesel. Fuel parameters are changing with the amount of butanol added. Maximum amount of butanol in diesel in order to prevent negative effects was assessed.

Key words: biofuel, cetane number, density, viscosity, cold filter plugging point.

INTRODUCTION

The issue of biofuels is still at an early stage in terms of their technological development. As ‘first generation’ biofuel is most often declared bioethanol produced from starch or sugar, biodiesel produced from vegetable oils (rapeseed, soy etc.) and animal fats without chemical modification or by a process of transesterification on fatty acid methyl esters (FAME, from rapeseed oil RME). Technologies are sophisticated and above all commercially available.

Among ‘second-generation’ biofuels are classified ethanol produced from lignocellulosic biomass part, BTL fuels produced by thermo–chemical processing of biomass into liquid synthetic fuels and also hydrogen produced from renewable energy sources.

It is an extremely complex and highly capital–intensive technology. Currently it is not possible to make a final assessment of the related processes in terms of energy and environmental balance and economics of production (De Wit & Faai, 2010; Carriquiry et al., 2011; Demirbas, 2011; Kumbar & Dostál, 2014).

Biobutanol (n–butanol, butan–1–ol) is an alternative to bioethanol, which is currently commercially produced and used as a component of motor gasoline or as E85 (Hönig et al., 2014).

Both bioethanol and biobutanol are produced from the same raw materials by ethanol fermentation of simple sugars, which is called ABE (Aceton–Butanol–Ethanol) process under the action of *Clostridium Acetobutylicum* (Campos et al., 2002; Gnansounou, 2010).

Raw materials for ABE fermentation are distinguished:

Starchy (potatoes, corn, wheat, rice).

Sugary (sugar beet molasses, whey).

Lignocellulosic (straw, wood).

The second generation biofuels produce currently both positive and negative emotions (especially ethanol but also butanol). Different materials containing saccharidic cellulose, e.g. straw or waste paper waste and energy crops are main source of raw materials for manufacturing of biofuels. Cellulose must be released from lignocellulosic matrix and its subsequent cleavage to glucose units is done either chemically or enzymatically being more costly opposed to conventional saccharidic sources (Groot et al., 1992; Melzoch et al., 2010; Sims et al., 2010; Nigam & Singh, 2011).

Biobutanol has up to 31% higher energy content and contributes to nearly 95% of the energy of biofuels oppose to bioethanol with 75%. Biobutanol as fuel is safer due to lower vapour pressure than bioethanol. Biobutanol unlike bioethanol not absorbs water and freezes at -89°C. The transport of biobutanol by pipeline systems, oppose to bioethanol, has no risk of corrosion and water separation. Biobutanol is well biodegradable and poses no threat to the environment being substance of natural origin.

Biobutanol advantage is that can be added in higher concentrations in gasoline and hypothetically can be added in higher amounts to diesel unlike bioethanol (Hazar & Aydin, 2010; Hönig et al., 2014).

Blends of hydrocarbon fuel and biobutanol are caused by the different chemical nature (Table 1). The main problem is the low reactivity (cetane number), which must be increased by special additives (Costagliola et al., 2013; Mařík et al., 2014).

Table 1. Comparison of the basic parameters of diesel, gasoline, bioethanol and biobutanol (Mužíková et al., 2010; Pospíšil et al., 2014)

Parameter	Diesel	Gasoline	Bioethanol	Biobutanol
Density at 15°C (kg m^{-3})	820–845	720–775	789	813
Cetane number	> 51	–	7	17
Octane number (research metod)	–	91 – 100	108	94
Calorific value (MJ dm^{-3})	36	31	21	27
Calorific value of mass (MJ kg^{-1})	42.6	43.6	28.9	33.1
Oxygen content (% wt.)	–	< 2.7	34.7	21.6
Boiling point (°C)	163–357	30 – 215	78	118
Melting point (°C)	–	–	-114.4	-88.6

There is a number of options to use alcohols in fuels (Pirs & Gailis, 2013). For example, E95 fuel consisting of 95% bioethanol and 5% of additives promotes lubricity and reactivity. It is also possible to use a bi–fuel system with separate tanks. It consists

in injecting alcohol into the combustion chamber simultaneously with the separate injector for diesel.

Application of alcohol in diesel fuel in Europe is increasingly considered and experimentally tested (Aydogan, 2015; Zhu et al., 2014). Biobutanol in diesel engine was tested but not in terms of the properties of fuel (Lebedavas et al., 2010; Kumar et al., 2013). Research suggests, that butanol is a preferable alternative to bioethanol also in diesel engines.

Ethanol also meets the fuel standard marked E–diesel (containing about 7–15% vol. of ethanol) and O2Diesel™ (consisting of 7.7% vol. of ethanol). The simplest solution, however, seems to add directly biobutanol into diesel. Technical adjustments are not only expensive, but do not allow return back to pure diesel combustion in diesel engines. This paper is aimed at assessing the impact of diesel parameters of biobutanol according to standard EN 590. The resulting blended fuels must comply with this standard for unmodified diesel engines.

MATERIALS AND METHODS

For laboratory tests was used diesel compliant to EN 590 without fatty acid methyl esters. Tested n–butanol had p.a. quality (LachNer, Ltd).

Model blends of diesel fuel were tested by methods compliant to standard EN 590.

Distillation test by EN 3405,

Density at 15°C by EN ISO 3675.

Kinematic viscosity at 40°C by EN ISO 3104.

CFPP – Cold filter plugging point by EN 116.

Cetane number by EN ISO 5165.

Cetane index by EN ISO 4264.

Flash point by EN 22719.

Value of viscosity and flash point was assessed by three analyses. Final value was calculated as the average of the three measurements. Three measurements of separate samples for assessment of distillation curve, where difference of temperature was below 1°C. The value of second sample was taken for further processing. Other values were measured directly without any statistical processing according to standard EN 590.

RESULTS AND DISCUSSION

Determination of distillation curve is the dominant test, which is always necessary to assess the quality of the fuel. Figs 1 and 2 show, that butanol significantly affects the start of a distillation curve. Admixture of butanol in diesel fuel will cause the fine spray of fuel injection. The resulting droplets have a greater total surface area and a higher evaporation rate. In blends up to 30% vol. are also ensured heavier components contained in diesel, which vaporize gradually during the compression stroke, wherein the walls of the combustion chamber are cooled. After distilling off the butanol distillation curve continues the course of a typical diesel.

Distillation curve has a typical course for diesel fuel after distilling off the butanol (Fig. 1 and 2).

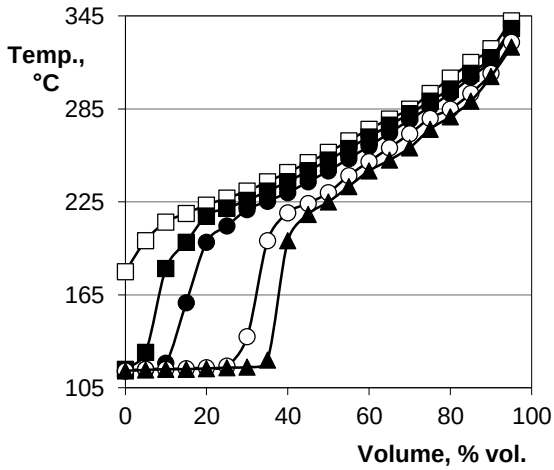

Figure 1. The distillation curve of diesel fuel containing n–butanol.
Distilled volume in % vol. is on horizontal axis, distillation temperature in ° C is on vertical axis y. Content of butanol is: □ 0% vol.; ■ 7.5%vol.; ● 15% vol.; ○ 30% vol.; ▲ 40% vol.

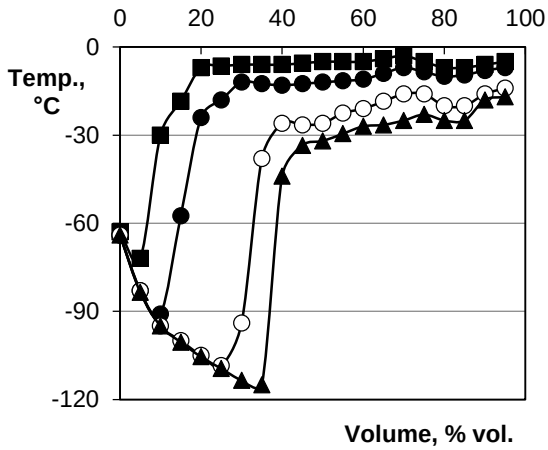

Figure 2. Changes in temperature distillation of diesel fuel containing n–butanol compared to diesel fuel base.
Distilled volume in % vol. is on horizontal axis and represents pure diesel fuel, change in distillation temperature in °C is on vertical axis y. Content of butanol is: ■ 7.5%vol.; ● 15% vol.; ○ 30% vol.; ▲ 40% vol.

Cetane number is ignition characteristic of diesel fuel and characterises the fuel's suitability for the engine. When the cetane number is too low, the fuel ignites in the cylinder too late, if at all. When the cetane number is too high, the burning starts too early. The consequences of this are power decrease, high fuel consumption and high possibility to break the engine.

Cetane number of butanol is very low compared to diesel fuel. EN ISO 5165 allows to measure up to 19.3 cetane units. Therefore, extrapolated data for 70% vol. and 80% vol. in Fig. 3 are calculated as it was not possible to verify them experimentally.

Test of cetane number is quite difficult. Therefore, the cetane index was introduced as characteristic of ignition. Cetane index was calculated from the density and points of distillation curve according to EN ISO 4264.

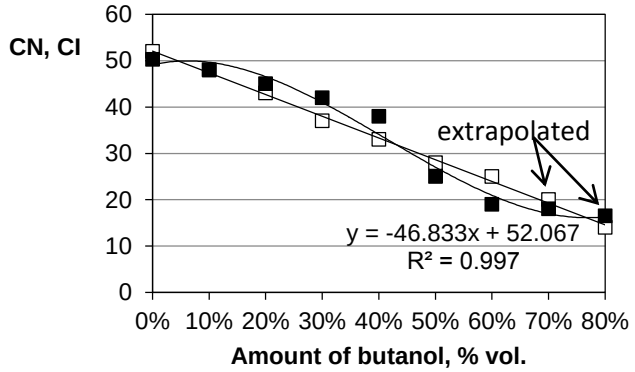

Figure 3. Effect of n–butanol in diesel fuel blend on the cetane number and cetane index: cetane number □; cetane index ■.

As seen in Fig. 4, the presence of butanol in the fuel does not decrease density significantly. Decrease of density corresponds with differences of densities of diesel and butanol. In the case of kinematic viscosity at 40°C a different course of decline has appeared. It is assumed that the more pronounced curvature of viscosity is caused by hydrocarbon chain. Viscosity also limits maximum of butanol in diesel fuel. Low viscosity may cause damages of moving parts of the fuel system.

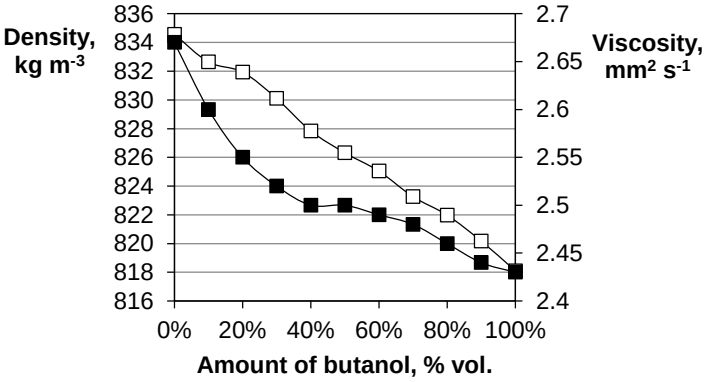

Figure 4. Effect of n–butanol in diesel fuel blend on the density at 15°C and kinematic viscosity at 40°C: density □; kinematic viscosity ■.

Fig. 5 shows the positive parameters of cold properties of diesel fuel. Even a small amount of butanol significantly reduces CFPP value. It is also important that at very low

temperatures the fuel blend doesn't split to two layers, which is typical for ethanol blends.

Also the flashpoint significantly changes with increased butanol content in fuel blend. Fig. 5 shows that from about 5% of butanol in diesel fuel is already second class combustible. This value is not changing to 100% of n–butanol.

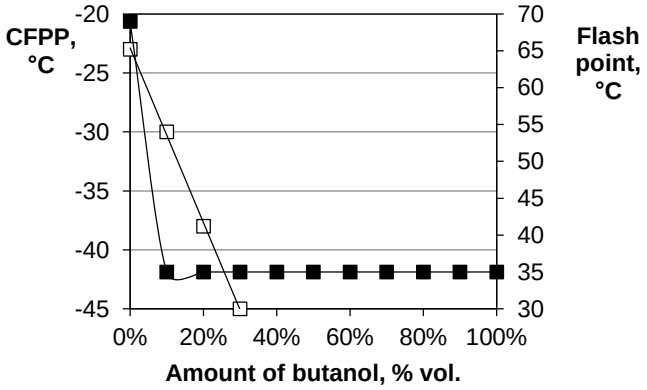

Figure 5. Effect of n–butanol in diesel fuel blend on the CFPP and flash point: CFPP □; flash point ■.

It is not recommended to add over 30% vol. of butanol to diesel fuel blend according to standard requirements (EN 590) and analysed values. Higher content of butanol would decrease power of diesel blend, increase consumption and cause irregular engine operation. Also, the density and kinematic viscosity would be below the standard, which could cause problems with the lubricity of the fuel. The wear would damage moving parts and ability to use the machine.

CONCLUSIONS

The paper evaluates impact of butanol in diesel blend for engines, which are not adjusted to non–standard fuels. The analyses suggest that blends of butanol with diesel fuel are in accordance with requirements of standard EN 590. Quantity of butanol in diesel blend is limited according to criteria observed. Absence of significant deterioration of the fuel is apparent, except for reducing the flash point of about 35°C if butanol is blend with diesel fuel. The decreased cetane number is necessary to compensate by commercial additives. Observed non–linear reduction in the density and kinematic viscosity of the reduced lubricity requires standardisation. When using n–butanol (biobutanol) as component of diesel fuel there were not observed problems with the stability of mixed fuels even at very low temperatures. These problems are characteristic for blends containing bioethanol. Adding butanol into diesel fuel has a positive effect on the low temperature characteristics and CFPP of fuel.

ACKNOWLEDGMENTS. The paper was created with the grant support project CIGA CULS Prague 20153001 – Utilization of butanol in internal combustion engines of generators.

REREFRENCES

Aydogan, H. 2015. Prediction of diesel engine performance, emissions and cylinder pressure obtained using Bioethanol-biodiesel-diesel fuel blends through an artificial neural network. *Journal of Energy in Southern Africa* **26**(2), 74–84.

Campos, E.J., Qureshi, N. & Blashek, H.P. 2002. Production of acetone Butanol ethanol from degermed corn using Clostridium beijerinckii BA 101. *Applied Biochemistry and Microbiology*, 553–556.

Carriquiry, M.A., Du, X. & Timilsina, G.R. 2011. Second generation biofuels: Economics and policies. *Energy Policy* **39**, 4222–4234.

Costagliola, M.A., De Simio, L., Iannaccone, S., Prati, M.V. 2013. Combustion efficiency and engine out emissions of a S.I. engine fueled with alcohol/gasoline blends. *Applied Energy* **111**, 1162–1171.

De Wit, M. & Faai, A. 2010. European biomass resource potential and costs. *Biomass Bioenergy* **34**, 188–202.

Demirbas, A. 2011. Competitive liquid biofuels from biomass. *Applied Energy* **88**, 17–28.

Gnansounou, E. 2010. Production and use of lignocellulosic bioethanol in Europe: Current situation and perspectives. *Bioresource Technology* **101**, 4842–4850.

Groot, W.J., Lans, R.G.J.M. & Luyben, K.Ch.A.M. 1992. Technologies for Butanol Recovery Integrated with Fermentations, *Process Biochemistry* **27**, 61–75.

Hazar, H., & Aydin, H. 2010. Performance and emission evaluation of a CI engine fueled with preheated raw rapeseed oil (RRO)-diesel blends. *Applied Energy* **87**, 786–790.

Hönig, V., Kotek, M. & Mařík, J. 2014. Use of butanol as a fuel for internal combustion engines. *Agronomy Research* **12**(2), 333–340.

Kumar, S., Cho, J.H., Park, J. & Moon, I. 2013. Advances in diesel–alcohol blends and their effects on the performance and emissions of diesel engines. *Renewable and Sustainable Energy Reviews* **22**, 46–72.

Kumbar, V. & Dostál, P. 2014. Temperature dependence density and kinematic viscosity of petrol, bioethanol and their blends. *Pakistan Journal of Agricultural Sciences* **51**(1), 175–179.

Lebedavas, S., Lebedava, G., Sendzikiene, E. & Makareviciene, V. 2010. Investigation of the Performance and Emission Characteristics of Biodiesel Fuel Containing Butanol under the Conditions of Diesel Engine Operation, *Energy & Fuels* **24**, 4503–4509.

Mařík, J., Pexa, M., Kotek, M., Hönig, V. 2014. Comparison of the effect of gasoline - ethanol E85 - butanol on the performance and emission characteristics of the engine Saab 9-5 2.3 l turbo. *Agronomy Research* **12**(2), 359–366.

Melzoch, K., Patáková, P., Lipovský, J., Fořtová, J., Rychtera, M. & Čížková, H. 2010. Exploitation of food feedstock and waste for production of biobutanol, *Czech Journal of Food Science* **27**(4), 276–283.

Mužíková, Z., Pospíšil, M. & Šebor, G. 2010. The use of bioethanol as a fuel in the form of E85 fuel. *Chemické listy* **104**(7), 678–683 (in Czech).

Nigam, P.S. & Singh, A. 2011. Production of liquid biofuels from renewable resources. *Progress in Energy and Combustion Science* **37**, 52–68.

Pirs, V. & Gailis, M. 2013. Research in use of fuel conversion adapters in automobiles running on bioethanol and gasoline mixtures, *Agronomy Research* **11**(1), 205–214.

Pospíšil, M., Šiška, J. & Šebor, G.: BioButanol as fuel in transport, Biom [online]. [cit. 2014-17-01]. Available at www: biom.cz.

Sims, R.E.H., Mabee, W., Saddler, J.N. & Taylor, M. 2010. An overview of second generation biofuel technologies. *Bioresource Technology* **101**(6), 1570–1580.

Zhu, Y.C., Chen, Z. & Liu, J.P. 2014. Emission, efficiency, and influence in a diesel n-butanol dual-injection engine. *Energy Conversion and Management* **87**, 385–391.

Agronomy Research **13**(5), 1234–1240, 2015

Using gas chromatography to determine the amount of alcohols in diesel fuels

V. Hönig[1,*], J. Táborský[1], M. Orsák[1] and R. Ilves[2]

[1]Czech University of Life Sciences Prague, Faculty of Agrobiology, Food and Natural Resources, Department of Chemistry, Kamýcká 129, 16521 Prague 6, Czech Republic
[2]Estonian University of Life Sciences, Institute of Technology, Kreutzwaldi 56, EE51014 Tartu, Estonia.
[*]Correspondence: honig@af.czu.cz

Abstract. The European Union tries to reduce carbon dioxide production and reduce fossil fuel consumption. One way to achieve this goal is adding biofuels to regular motor fuels. Biofuels also decrease the production of other harmful substances. This paper evaluates the identification of n-butanol and isobutanol in diesel fuel. The application of n-butanol to diesel fuel is currently being considered. Alcohols blended into diesel fuel have been shown to have a positive impact on solid particle production, smoke emission, etc. Bioethanol and biobutanol can be easily produced from waste products as second-generation biofuels. The experimental part of the paper focuses on the identification of n-butanol and isobutanol in diesel fuel, as it has been previously used for detecting bioethanol additions in diesel fuel. Test samples with the following composition were prepared: 10% of ethanol in diesel fuel; 5%, 10%, 20% of n-butanol in diesel fuel; 5% of n-butanol and 5% of isobutanol in diesel fuel; 10% of n-butanol and 10% of isobutanol in diesel fuel. This paper deals with the use of gas chromatography (GC) in the evaluation of motor fuels. GC analysis can provide a sort of a fuel 'fingerprint' that shows the approximate distillation profile and can reveal the presence of other foreign fractions. Regular evaluation procedures using gas chromatography for the determination of a diesel fuel's quality unfortunately do not exist at the moment. As it is shown, GC could provide very valuable information in fuel quality assessment, making it the method of choice for this procedure.

Key words: GC–FID, n-butanol, isobutanol, boiling point.

INTRODUCTION

The European Union is one of the main actors in the struggle for reducing the emission of greenhouse gases. The main producers of greenhouse gases in the European Union are the energy, transport and industry sectors (Nigam and Singh, 2011). The key to reducing greenhouse gas emissions is the introduction of renewable energy sources into the field of energy and industry. In the transport sector, the efficiency of combustion in engines must be improved and the use of biofuels must be significantly increased Dukulis et al., 2009; (Dukulis & Birkavs, 2013).

The growing transport load raises several fundamental problems that need to be solved in an optimal manner by the modern society. From the perspective of long-term sustainability in transport, we are presented with two major problems—fossil fuel consumption and carbon dioxide production. A possible solution to both these problems

is biofuel. Bioethanol and biobutanol are easy to manufacture compared to traditional fossil fuels (Demirbas, 2011; Da Costa Filho, 2014).

Diesel Flexi–Fuel vehicles with the respective marking are an equivalent of FFVs (Flexible–Fuel Vehicle) designed for burning high ethanol blends. There is also an alternative in the form of E–diesel, which is used mainly for heavy goods vehicles and agricultural machinery. Another option is O2 Diesel™ that can be used in unmodified engines within the existing infrastructure according to the manufacturer. This fuel is mainly available in the southern and south-eastern part of the United States.

Bioethanol has a low calorific value; however, in diesel fuel it causes a number of problems. Yet, it is also possible to use other alternative alcohols. Biobutanol can be produced from the same sources as bioethanol, and it has a more positive impact on the quality of the fuel (Hönig et al., 2014; Mařík et al., 2014). Cultures of *Clostridium acetobutylicum* are used to produce biobutanol in the form of n-butanol (butan-1-ol). Researchers also focus on the blue-green algae strain of *cyanobacteria* that produce biobutanol in the form of isobutanol (Mosier et al., 2005; Patáková et al., 2010; Pointner et al., 2014).

The contamination of diesel fuel in the tank due to residual gasoline is a common phenomenon. In the evaluation of diesel with the help of GC–FID it was found that there are also cases where diesel fuel contains other non-standard additives with different boiling points. The presence of undesirable admixtures in diesel fuel is explained by the fact that the fuels are not taxed and their import has not been checked (Lissitsyna et al., 2012; Hložek et al., 2014).

There are no standard procedures for using gas chromatography to determine the quality parameters of diesel fuels. However, GC procedures for simulated distillation could represent the standard of distillation. The results cannot be confused with the classic distillation test corresponding to EN ISO 3405. Nevertheless, gas chromatography provides very valuable information in the evaluation of diesel fuel.

This paper deals with the addition of bioethanol, n-butanol and isobutanol to diesel fuel and their identification through gas chromatography. This method may also identify impurities, such as gasoline; light fuel oil, etc. (Sarafraz–Yazdi et al., 2012).

Conventional gas chromatography is used to obtain the so-called fingerprint of the chromatogram. The device is comprised of a flame ionization detector (FID), simple linear temperature program, and chromatographic column with a nonpolar stationary phase (Mostafa & Górecki, 2013).

A commercially available fused-silica capillary column with the stationary phase of the polydimethylsiloxane (PDMS) type with a length of 5–30 m and an internal diameter of 0.2 to 0.53 mm may be used. For dispensing the sample, a standard heated injector with a divider (split/splitless injector) is generally used (Biedermann & Grob, 2012; Blasé et al., 2015; Caruso et al., 2011).

The quantities of individual substances (ethanol, isobutanol, n–butanol) are calculated according to the following formula (1):

$$c_i = \frac{P_i}{P_s} \cdot c_s \cdot k_i \qquad (1)$$

where: c_s – concentration of internal standard (μg ml^{-1}); c_i – concentration of analysed component (μg.ml^{-1}); P_i – area of respective peak (mm^2); P_s – peak area of internal

standard (nonane [mm^2]); k_i – the coefficient calculated from the respective calibration curve.

MATERIALS AND METHODS

Diesel fuel samples complying with EN 590 that do not contain fatty acid methyl esters were used for laboratory tests. Test n-butanol and isobutanol were p.a. (LachNer, Ltd.), isooctane p.a. (Lachema Brno) in quality. Ethanol corresponded to the standard prEN15379. Nonane (puriss grade, certified reference material, Slovak Institute of Metrology) was used according to an internal standard.

Test samples were prepared with the following composition (all figures in % vol.):

1. ethanol in diesel fuel: 10%;
2. n-butanol in diesel fuel: 5%, 10%, 20%;
3. isobutanol and n-butanol in diesel fuel: 5% and 10% (each component).

The volume percentage was calculated from the measured quantities of the individual substances before mixing. Samples were stored in dark brown glass bottles with the volume of 20 ml. For the purpose of GC measurement the test samples were dissolved in isooctane, and nonane was added to all samples according to an internal standard. Samples were mixed according to the following scheme: 1,000 µl of isooctane + 10 µl of diesel fuel + 10 µl of nonane. Diluting samples with a suitable solvent, in this case isooctane, has improved the separation efficiency in the chromatographic column.

The Varian 3300 gas chromatograph equipped with a fused silica capillary column DB–5 and a flame ionization detector was used for measurement. The device's parameters and measurement conditions are shown in Table 1. Evaluation was carried out pursuant to an internal standard. Hydrocarbon nonane was used as the internal standard.

Calibration curves for ethanol, n-butanol and isobutanol were measured using standard solutions of these substances in isooctane at three concentration levels (1,000 µl of isooctane + 2 µl or 5 µl or 10 µl of respective alcohol + 1 µl of nonane in each of the three vials).

All calculations were performed automatically using the chromatographic software, which is also specified in Table 1.

Table 1. Parameters of gas chromatograph with FID detector

Chromatograph	Varian 3300
Analytical column	DB–5, 30 m x 0.25 mm ID, film thickness 0.25 µm
Spray technique	manual; sample volume 1 µl, split ratio 1:20
Carrier gas	nitrogen 1 ml min^{-1}
Temperature program	50°C (3 min), gradient 8°C min^{-1}, 260°C (5 min)
FID detector	hydrogen 30 ml min^{-1}, air 300 ml min^{-1}
Software for data collection	Star Chromatography Workstation vs. 4.51

RESULTS AND DISCUSSION

It is important to know the area below the peak of the measured substance and the area of the internal-standard nonane to calculate the concentrations of n-butanol and isobutanol in diesel. The numbers above the peaks of the chromatogram are the values of retention time (in minutes) pertaining to the measured substances. The retention times of the measured substances are compared with the retention time of standards for ethanol, n-butanol and isobutanol. Quantity is identified from the area below the peaks.

Figs 1–6 are chromatograms of fuel samples,
where: R is detector response (V); t_R is retention time (min).

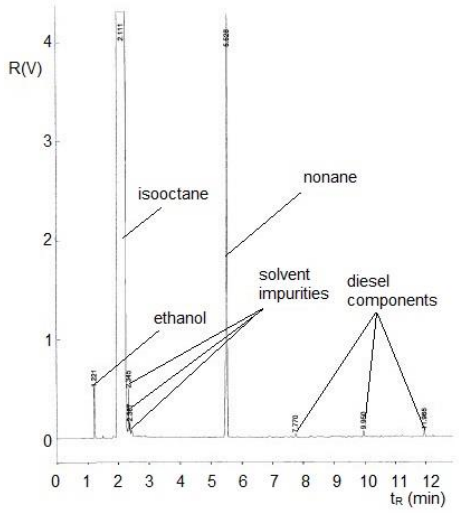

Figure 1. Diesel fuel with 10% vol. of ethanol.

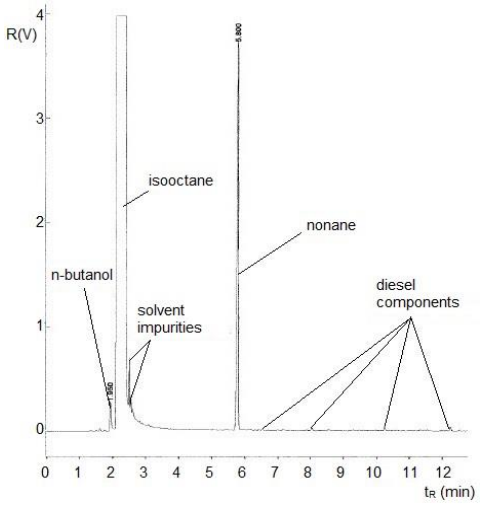

Figure 2. Diesel fuel with 5% vol. of n–butanol.

Chromatograms of normal commercial diesel fuel (without FAME) with the addition of ethanol and n-butanol (Figs 1, 2, 3, 4) have strong peaks of these substances with retention times in the interval of 1–2 min in the case of these measurement conditions.

Alcohols, nonane (internal standard) and isooctane (solvent) are observable in Figs 1–6. The chromatograms also indicate solvent impurities and diesel fuel components. All chromatograms were terminated after 12 min. Constituents of diesel fuel, a blend of hydrocarbons, have different boiling points. Therefore, some components were eluted even further for about 20 min.

Chromatographic records of clean diesel fuel may vary. Variability mainly depends on the refinery from which the fuel originates and also on the class of diesel fuel. Composition depends on seasons and the geographical conditions of the market to which the diesel fuel is distributed.

Therefore, a chromatographic 'fingerprint' also reflects the immediate limitations of a specific refinery. Despite the abovementioned differences, the chromatograms of commercial diesel fuels used in a moderate climate are rather similar.

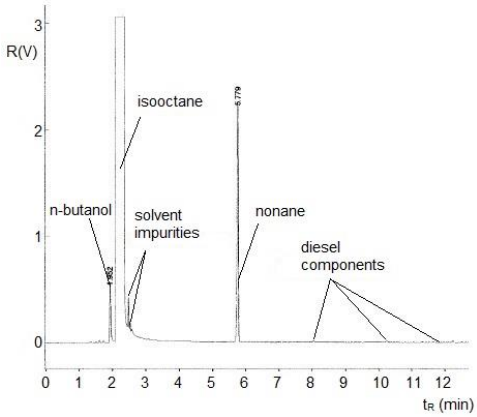

Figure 3. Diesel fuel with 10% vol. of n–butanol.

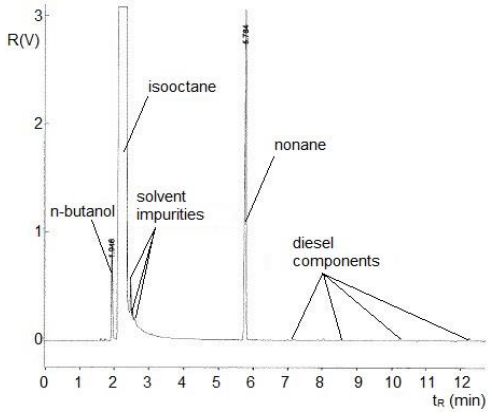

Figure 4. Diesel fuel with 20% vol. of n–butanol.

A nonpolar column is used in the GC–FID 'fingerprint' analysis (separated according to the boiling points of substances) so the arrangement of the gas-chromatographic system meets the basic requirement for simulated distillation. Classic simulated distillation requires special software for both analysing the calibration blend and evaluating the results to determine the relations between boiling points and retention time.

Gas chromatography allowed us to identify the simultaneous presence of n-butanol and isobutanol in diesel fuel (Figs 5 and 6); the peaks of both substances are well separated. The retention time of isobutanol is approximately 1.64 min under these measurement conditions.

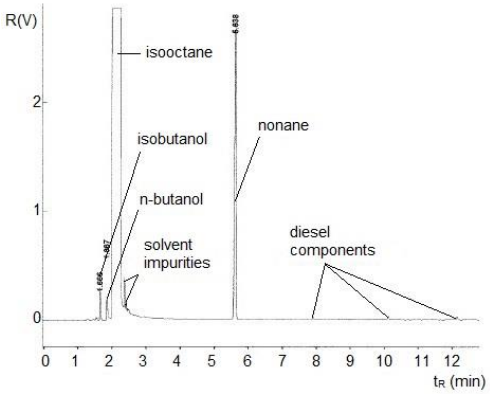

Figure 5. Diesel fuel with 5% vol. of n–butanol and 5% vol. of isobutanol.

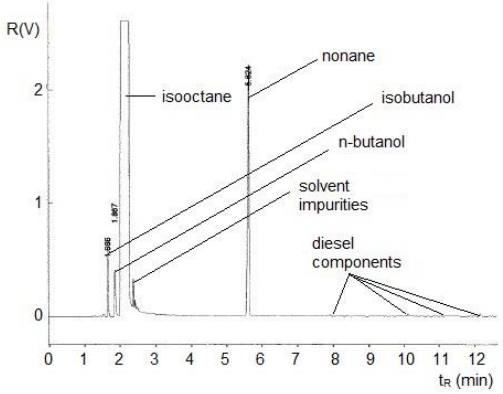

Figure 6. Diesel fuel with 10% vol. of n–butanol and 10% vol. of isobutanol.

Diesel fuel GC–FID allows estimating the flashpoint of the sample.

Gas chromatography identifies the presence of alcohol or gasoline in diesel fuel and quantifies the approximate alcohol concentration starting from about 0.1% vol. (Table 2) on the basis of peak areas (Figs 1–6).

Table 2. Measured concentrations of ethanol, n-butanol and isobutanol in diesel fuel

Fuel	Measured concentration of alcohol (% vol.)
Diesel fuel + ethanol 10% vol.	10.12
Diesel fuel + n-butanol 5% vol.	5.13
Diesel fuel + n-butanol 10% vol.	12.45
Diesel fuel + n-butanol 20% vol.	23.93
Diesel fuel + n-butanol 5% vol. + isobutanol 5% vol.	5.23 + 5.49
Diesel fuel + n-butanol 10% vol. + isobutanol 10% vol.	11.69 + 11.57

All values were calculated from three GC measurements as the arithmetic mean. Deviations of the measured values from the reference values may have occurred due to variations in detector response or the sorption of some components of the sample in the injection chamber. The variability of measured values can be improved by using the auto-sampler and devices with electronic gas flow control.

CONCLUSIONS

The regular evaluation of diesel fuel quality according to EN 590 does not allow gaining a thorough overview of the fuel's composition. On the other hand, GC–FID analysis is able to closely characterise the fuel's petroleum fractions and boiling ranges. It also allows detecting and quantifying the presence of other components in the diesel fuel and provides information about their approximate distillation profiles.

The regulatory adherence to dosing alcohols would require regular monitoring. A simple analytical method for the determination of bioethanol, isobutanol and n-butanol in diesel fuel using GC–FID was developed and verified.

Gas chromatography equipped with FID detection is a good method of choice for assessing the quality of diesel fuel and it can provide a wealth of useful information. This analytical technique shows the fuel's distillation profile and its fatty acid methyl esters content. In spite of using regular evaluation methods, GC–FID can also detect the presence of other compounds of interest like bioethanol, n-butanol and isobutanol that are already being considered as potential future additives to diesel fuel. The presented method has proven to have acceptable accuracy for the quantification of various alcohols. Therefore, gas chromatography analysis can provide a range of additional data to complement regular fuel evaluation and help to narrow selection parameters.

ACKNOWLEDGMENTS. This paper was created with the grant support project CIGA CULS Prague 20153001—Utilization of butanol in the internal combustion engines of generators.

REFERENCES

Biedermann, M. & Grob, K. 2012. On–line coupled high performance liquid chromatography–gas chromatography for the analysis of contamination by mineral oil. Part 1: Method of analysis, *Journal of Chromatography A* **1255**, 56–75.

Blasé, R.C., Patrick, E.L., Mitchell, J.N. & Libardoni, M. 2015. Analysis of cave atmospheres by comprehensive two–dimensional gas chromatography (GC×GC) with flame ionization detection (FID), *Analytical Chemistry Research* **3**, 54–62.

Caruso, R., Gambino, G.L., Scordino, M., Sabatino, L., Traulo, P. & Gagliano, G. 2011. Gas chromatographic quantitative analysis of methanol in wine: Operative conditions, optimization and calibration model choice, *Natural Product Communications* **6**, 1939– 1943.

Da Costa Filho, P.A. 2014. Developing a rapid and sensitive method for determination of trans–fatty acids in edible oils using middle–infrared spectroscopy, Food Chemistry 158, 1–7.

Demirbas, A. 2011. Competitive liquid biofuels from biomass. *Applied Energy* **88**, 17–28.

Dukulis, I. & Birkavs, A. 2013. Development of the Model for Running the Diesel Engine on Rapeseed Oil Fuel and Its Blends with Fossil Diesel Fuel. In: Engineering for Rural Development. Proceedings of the 12th International Scientific Conference, Latvia University of Agriculture, Jelgava, pp. 319–325.

Dukulis, I., Pirs, V., Jesko, Z., Birkavs, A. & Birzietis, G. 2009. Development of Methodics for Testing Automobiles Operating on Biofuels. In: Engineering for Rural Development. Proceedings of the 8th International Scientific Conference. Latvia University of Agriculture, Jelgava, pp. 148–155.

Hložek, T., Bursová, M. & Čabala, R. 2014. Fast determination of ethylene glycol, 1,2–propylene glycol and glycolic acid in blood serum and urine for emergency and clinical toxicology by GC–FID, *Talanta* **130**, 470–474.

Hönig, V., Kotek, M. & Mařík, J. 2014. Use of butanol as a fuel for internal combustion engines. *Agronomy Research* **12**(2), 333–340.

Lissitsyna, K., Huertas, S., Morales, R, Quintero, L.C. & Polo, L.M. 2012. Determination of trace levels of fatty acid methyl esters in aviation fuel by GC × GC–FID and comparison with the reference GC–MS method, *Chromatographia* **75**, 1319–1325.

Mařík, J., Pexa, M., Kotek, M. & Hönig, V. 2014. Comparison of the effect of gasoline – ethanol E85 – butanol on the performance and emission characteristics of the engine Saab 9–5 2.3 l turbo. *Agronomy Research* **12**(2), 359–366.

Mosier, N., Wyman, C., Dale, B., Elander, R., Lee, Y.Y., Holtzapple, M. & Ladisch, M. 2005. Features of promising technologies for pretreatment of lignocellulosic biomass. *Bioresource Technology* **96**(6), 673–686.

Mostafa, A. & Górecki, T. 2013. Sensitivity of comprehensive two–dimensional gas chromatography (GCXGC) versus one–dimensional gas chromatography (1D GC), LC GC Europe 26, pp. 672–679.

Nigam, P.S. & Singh, A. 2011. Production of liquid biofuels from renewable resources. Progress in Energy and Combustion Science 37, pp. 52–68.

Patáková, P., Pospíšil, J., Lipovský, J, Fribert, P., Linhová, M, Toure, S.S.M., Rychtera, M., Melzoch, K. & Šebor G. 2010. Prospects for biobutanol production and the use in the Czech republic, *Chemagazín* **20**(5), 13–15 (in Czech).

Pointner, M., Kuttner, P., Obrlik, T., Jager, A. & Kahr, H. 2014. Composition of corncobs as a substrate for fermentation of biofuels. *Agronomy Research* **12**(2), 391–396.

Sarafraz–Yazdi, A., Dizavandi, Z.R. & Amiri, A. 2012. Determination of phenolic compounds in water and urine samples using solid–phase microextraction based on sol–gel technique prior to GC–FID, *Analytical Methods* **4**, 4316–4325.

Agronomy Research **13**(5), 1241–1252, 2015

The impact of bioethanol on two-stroke engine work details and exhaust emission

A. Küüt[1,*], R. Ilves[1], V. Hönig[2], A. Vlasov[1] and J. Olt[1]

[1]Estonian University of Life Sciences, Institute of Technology, Kreutzwaldi 56, EE51014 Tartu, Estonia
[2]Czech University of Life Sciences Prague, Faculty of Agrobiology, Food and Natural Resources, Department of Chemistry, Kamycka 129, 16521 Prague 6, Czech Republic
[*]Correspondence: arne.kyyt@emu.ee

Abstract. This research is important for expanding the possibilities for using bioethanol as a fuel for internal combustion engines. Small displacement two-stroke engines are widely used as power sources for manual power units. By using bioethanol as a fuel for two-stroke engines, we significantly decrease the risk to human health. The main problems entailed with using bioethanol include achieving the required lubrication properties, more precisely, the poor mixing or immiscibility of ethanol and oil. In the course of the research, a breakthrough was achieved in solving the problem in order to produce a fuel mixture for two-stroke internal combustion engines.
Results covered include the effect of the fuel mixture on the functioning surfaces of an engine, but also the composition of the exhaust emissions. The aim of the investigation is to examine the effect of bioethanol fuel on the details and fuel system of a two-stroke engine. Test fuels are gasoline E 95 and bioethanol (96.3%), mixed by two-stroke engine oil. The mixture of bioethanol and oil shows the best results in the test of the friction force. That means wearing is not problematic but the problem is corrosion and CO emission.

Key words: two stroke engine, tribotechnology, bioethanol fuel blends, wearing.

INTRODUCTION

The use of bioethanol as an engine fuel is an increasing trend (IEA 2008), especially when it is manufactured based on lignocellulosic raw material. An advantage of bioethanol compared to engine fuel is the reduced concentration of hazardous components in the exhaust gases. This advantage makes it especially beneficial to use bioethanol in two-stroke engines, power saws, trimmers etc. In the case of the aforementioned equipment, the exhaust gases emitted from the engine often get into the respiratory tract of people working close to it. Such hazardous components as NO_X, CO and HC in the exhaust gases of an engine may cause headaches, irritate the mucous membranes of the eyes and throat, and cause cancer (Wargo et al., 2006). The use of bioethanol as fuel for a two-stroke engine is hampered by the fact that bioethanol does not dissolve in oils. As far as is known, a two-stroke engine requires fuel with good lubrication properties to ensure problem-free operation of the piston assembly of the engine. The reasons for that are the technical peculiarities of using bioethanol as a fuel

in piston engines (Pulkrabek & Willard, 1997; Demirbas, 2009; Schwarze et al., 2010; Vesela, 2014). The majority of tests have been carried out with four-stroke engines and engines with a bigger cubature (approx. 300 HP) (Hilbert, 2011) as well as tests with fuel apparatuses (Olt et al., 2011). Moreover, the impact on the sub-systems of a two-stroke engine resulting from bioethanol fuel not conforming to the standard is not known.

This research is a preliminary study to working out biofuel for two-stroke engines. The fuel which has been used in this experimental research is bioethanol with little water content (E100) and oil blend, which has not been widely studied in the world. The effects of different blends of gasoline and bioethanol on the exhaust gas emissions of a two-stroke engine have been studied worldwide (Tung & Gao, 2003; Ghazikhani et al., 2013). What is more, the effect of ethanol on the exhaust gas of an engine has been researched (Magnusson & Nilsson, 2011). However, the use of bioethanol and oil blends as the fuel in a two-stroke engine has not been widely studied.

The use of bioethanol as a two-stroke engine fuel generally decreases CO, HC and NOx emissions (Ghazikhani et al. (2013; 2014). Studies on the wearing of engine details have indicated that different engine details (valves, bearing shells) tend to break when E85 fuel is used in a two-stroke engine. In that particular study, lubrication component was not used in the fuel. (Hilbert, 2011)

The purpose of this paper is to conduct practical research and explore the tribotechnical system of a two-stroke engine using a bioethanol fuel mixture (ethanol 96.3% vol). The surface wear of the workpieces has been the main focus in researching tribotechnical systems. In addition, an overview of exhaust emissions has been added. A more thorough overview of exhaust emissions is published by Küüt et al. (2014).

MATERIALS AND METHODS

Aims of the preliminary study discussed in the article are to examine the effect of bioethanol fuel on the details and fuel system of a two-stroke internal combustion engine, in order to assess the reliability of the engine. In the field of using biofuels as motor fuel, the author is more specifically interested in the use of bioethanol, not biomethanol (Govindarajan, 2008). When using bioethanol as a fuel for a two-stroke engine, preparing the mixture is an issue. The problem in preparing the mixture is the bad solubility of ethanol and oil. The reason for non-solubility is the polarity of the substances. In addition to examining the effect of bioethanol, the behaviour of the fuel mixture produced by a novel production method was observed as well in the course of this research. The new method for producing the fuel mixture is full of potential, if we wish to use fuel mixtures produced of renewable and domestic raw material, such as a fuel mixture produced on the basis of bioethanol and oil.

The research method used to solve the set goal was test-based. Wear testing was performed to achieve the goal in order to find problematic assembles and details. Co-functioning of the components of the tribosystem was assessed in describing the results of testing. The nature of wear and corrosion on the surfaces of the engine elements were analysed (Baširov et al., 1978). The actual working condition (load and environmental conditions) of the equipment were imitated in performing the tests.

To carry out the tests, two Evolution NPEGG780-2 power generators equipped with two-stroke engines were chosen. The parameters of the engines are given in Table 1.

Table 1. Technical data of engine of NPEGG780-2 generator

Name	Manufacturer's data
Model	LTE145
Type	2-stroke, air-cooled, one-cylinder
Piston stroke	40 mm
Cylinder displacement	63 cm^3
Maximum engine power	2 hp (1.5 kW) 3,000 rpm
Fuel	Unleaded gasoline and oil blend
Fuel to oil ratio of the fuel	1/50
Ignition system	C.D.I
Spark plug type	F6RTC

In order to imitate the actual working situation and to ensure similar working conditions in performing the engine tests (Fig. 1), it was strictly ascertained that the tested generators worked only simultaneously. The generator carburettor working on bioethanol was adjusted so that the engine would work in a balanced way. To load the generators, consumers with the capacity of P = 200W for one test device were used (engine speed n_e = 3,000 rpm). The generator load was generated by electric light bulbs.

Figure 1. Test apparatus.

To determine the required oil content in ethanol, a device GUNT TM 260.03 (Table 2; Fig. 2) for ascertaining friction force was used. This device measures the friction force of a steel pin (1) rubbing against a rotating steel disc (2). The better the lubrication properties of the liquid between the steel rod and the plate, the smaller the friction force. The friction forces of gasoline E 95, 96.3% bioethanol, and gasoline and Addinol MZ 408 two-stroke engine oil mixture and a 96.3% bioethanol and MZ 408 oil mixture were compared. As the gasoline and MZ 408 oil mixture is meant to be used as fuel for a two-stroke engine, the friction force of the bioethanol and MZ 408 mixture must be similar to or smaller than the friction force of the gasoline and oil mixture. Oil was added to the gasoline and bioethanol at a ratio of 1:50. The chapter 'Results and discussion' include the measured static and kinetic friction forces with the abovementioned fuels (Table 3). Using static and kinetic friction force for describing tribotechnical processes is justified with the nature of the work between the cylinder and the piston ring. In carrying out the test, a load of 35 N was applied to the rod.

Table 2. Specification of the test stand GUNT TM 260.03 (GUNT Hamburg)

GUNT TM 260.03	Manufacturer's data
Friction disc	Stainless steel, hardened, ground
Operating speed	Adjustable 0...0.42 m s^{-1}
Friction pin diameter	4mm
Pin material	Steel, aluminium, brass
Load	0...80N
Friction force measuring range	0...50N

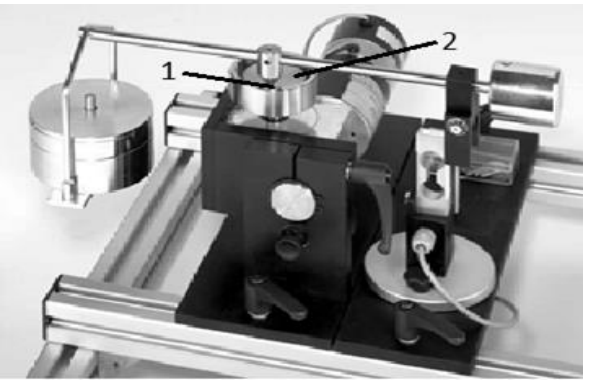

Figure 2. Pin of experimental Module TM 26003 on Disc (GUNT Hamburg).

The main issue explored in this paper is the effect of the tribotechnical processes on work surfaces. In order to describe friction and wear, elements were measured before and after an engine test. Measuring equipment MAHR MMQ-100 (Fig. 3) that enabled recording the graphic measurement results electronically was used for measuring.

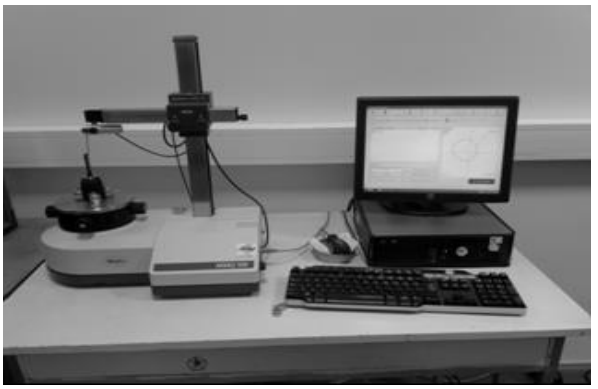

Figure 3. Measurement apparatus MAHR MMQ-100.

In order to estimate the rate of wear, the diameter of the cylinder was measured in three different positions (*I, II, II*). On the basis of the acquired results, the mean diameter was calculated. The roundness of the cylinder was also measured on two levels (*I, II)* (Fig. 4). The measurements were repeated three times for each element.

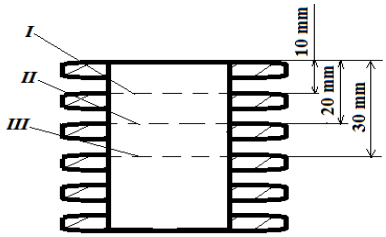

Figure 4. Measurement methods for cylinder.

The measurement points (a, b, c) for piston ring thickness are presented on Fig. 5. In order to estimate the rate of wear of the piston rings, three different measurement points were used. In determining the wear of the piston, diameter and roundness measurements were performed at two different heights (*I*, *II*).

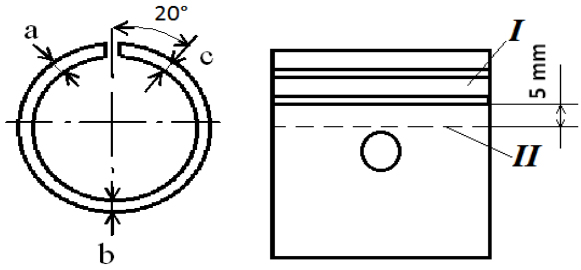

Figure 5. Measurement methods for piston rings and piston.

Roundness, diameter, and the diameter of the upper opening of the connecting rod were measured at the position of the gudgeon pin (Fig. 6).

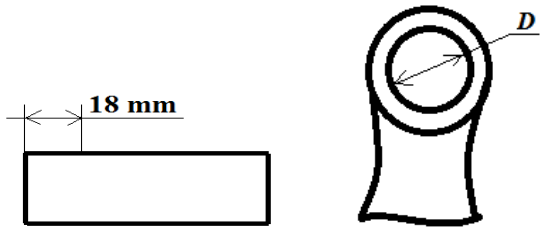

Figure 6. Measurement methods for piston pin and connection rod.

Exhaust gas emission was measured with Bosch BEA 350 exhaust gas analyser. Measured exhaust gases were CO, CO_2, HC, and NO_x. The test data was analysed in Excel 2010 program. The average results were calculated and analysed using Descriptive Statistics method.

RESULTS AND DISCUSSION

Table 3 and Figs 7, 8 show the tested fuels and the measured friction forces of the steel disc in various speed conditions. The data shows that the smallest friction force was measured about the bioethanol and oil blend. The oil content in bioethanol is 2%. The oil content was determined using test method (Standard EN ISO 3405). Comparing the kinetic friction force of bioethanol and oil mixture with the kinetic friction force of the gasoline and oil mixture, it is evident that the lubrication properties of the bioethanol and oil mixture are approx. 27% better (Fig. 8). The static friction force of the bioethanol and oil blend is 13% lower than the respective data of a gasoline blend (Fig. 7). This leads to the conclusion that the oil content in ethanol may also be less than 2%. But as it is a fuel not normally used in two-stroke engines, the oil content in the ethanol was not reduced in these tests. When comparing the friction forces of bioethanol with those of the bioethanol and oil mixtures, adding oil to the bioethanol at a ratio of 1:50 reduces the friction force by approximately 50%.

The values of the kinematic friction forces of bioethanol and gasoline are comparable (Table 3). At the same time, the static friction force of bioethanol is 20% higher than that of gasoline. As a result, it can be claimed that the quality of blending is extremely important when preparing a bioethanol fuel mixture since it directly influences the tribotechnical processes of the workpieces.

Table 3. Tested fuel properties and friction forces while verifying lubrication properties of fuel

Fuel	Density ($kg\ m^{-3}$)*	Viscosity (KV) ($mm^2\ s^{-1}$)**	Testing regime and performance data (N)			
			Start	*20 rpm*	*50 rpm*	*70 rpm*
BE ***	0.8096	1.653	25.1	20.9	19.6	19.4
BE + oil	0.8297	1.746	13.6	11.8	10.9	10.4
Gas. + oil	0.7672	0.660	16.3	15.8	14.8	14.4
Gas.	0.7593	0.584	20	20.7	21.3	19.8

* Measured at 15°C

** Testing method for kinematic viscosity (Standard ASTM D445)

*** BE – bioethanol.

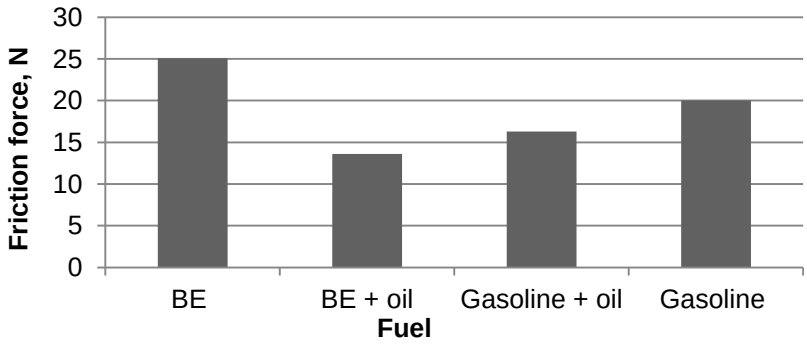

Figure 7. Static friction force of tested fuel.

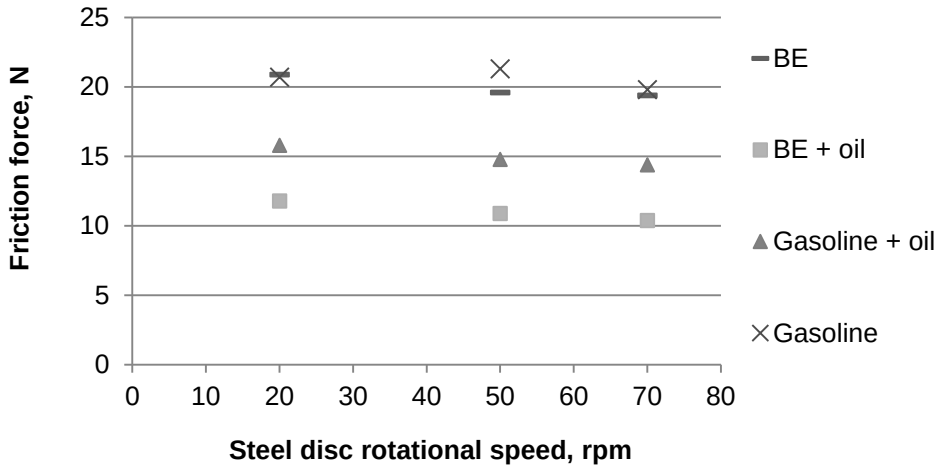

Figure 8. Kinetic friction force of tested fuel.

During the test, several problems arose in the engine of the generator working with the bioethanol and oil mixture. An overview of the problems and analysis of the measuring data is available below. The appendix includes measurement data recorded before testing and after 200 operation hours.

In the case of Generator 1 (working with the gasoline E95 and Addinol MZ 408 oil mixture) it was noted that the diameter of the cylinder had decreased. The average diameter of the cylinder had reduced by 6 μm. This was caused by thermal processes and residue accumulating between the structures of the workpieces due to the wear of the piston rings. In the case of Generator 2 (working with a 96.3% bioethanol and oil mixture) the average diameter of the cylinder had increased by 7 μm. This was caused by the running-in of the engine. The diameter of the cylinders can also be influenced by the repeated warming and cooling of the material, which is a constant process during the operation of the engine. (All engine details measurement data is presented in Table 5).

In this test the diameter of the engine piston in Generator 1 increased. In the case of Generator 2, the diameter of the piston decreased. This was influenced by the operation temperature of the engine and fuel combustion residue accumulating on the surfaces of the part. In the case of Generator 1, a lot of fuel combustion residue accumulated on the piston. In the case of Generator 2, there was less fuel combustion residue on the piston, which was also easier to clean.

Residue generated during fuel combustion (mainly soot) may get in between the piston rings and onto the sides of the piston when mixed with the fuel mixture. In the case of Generator 2, accumulation of this nature was observed to a lesser extent. Soot is a fine-fractioned by-product of incomplete combustion or the thermal decomposition of hydrocarbons. The exhaust gas analysis of the given engines (Appendix) shows that the content of unburned hydrocarbons (HC) in the exhaust gases is significantly lower (61%) for the engine working on the bioethanol and oil mixture (Fig. 9).

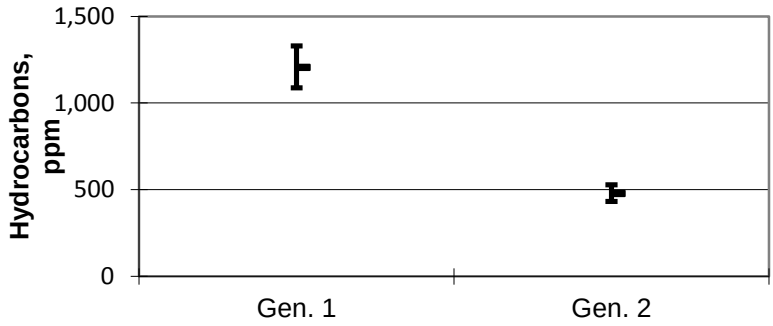

Figure 9. Comparison of the amounts of hydrocarbons.

This is caused by cleaner combustion of bioethanol due to the reduced content of substances causing the presence of hydrocarbons in fuel. As far as is known, hydrocarbons can irritate the mucous membranes of the eyes and throat, cause cancer, etc. Besides this, the quantity of soot is also greater in the combustion chamber of Generator 1. When the engines operated on a bioethanol and oil mixture, the CO emission level of the engines was 85% higher (Fig. 10) and CO_2 emission level 6% lower.

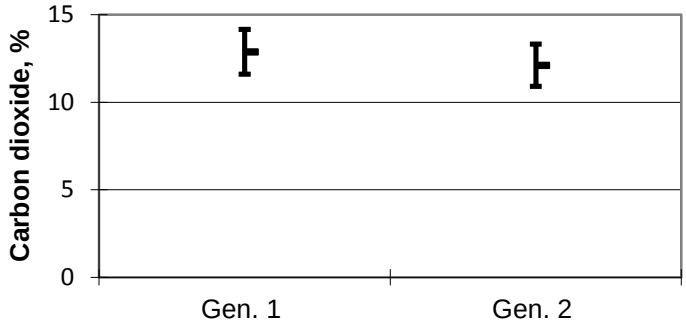

Figure 10. Comparison of the amounts of carbon dioxide.

In the case of the spark plugs, no increase in the content of combustion residue was detected. Such mixing of soot and fuel may cause the piston rings to stick or bring about engine failure when loads are bigger and temperatures higher. (All measurements of exhaust gases of the engine are presented in Table 6).

These engines were equipped with a needle roller bearing operating in the opening of the connecting rod neck. Thus the main wear surface is the area under the bearing. The diameter of the connecting rod neck of Generator 1 increased by 7 μm and the diameter of the piston pin increased by 7 μm. The reason for such an increase was the accumulation of fuel combustion residue and material from the bearing on the working surface of the piston pin. Also, thermal reactions may cause an increase in diameter. In the case of Generator 2, the diameter of the connection rod neck decreased by 5 μm and the diameter of the piston pin by 4 μm. This leads to the conclusion that these working surfaces had started wearing. When viewing the piston pin under a microscope, no

differences on the working surfaces were detected. The working surface of the piston pin of Generator 2 was corroded, which can also be seen in the photo in Table 4. Corrosion was present in the deeper parts of the structure of the material, which the surfaces of the working elements of the needle roller bearing did not reach. In addition, in both engines a pin had started moving in the piston opening. Such movement is not desired. As a result, the material of the piston had stuck to the piston pin (see Table 4).

Table 4. Working surfaces of piston pin

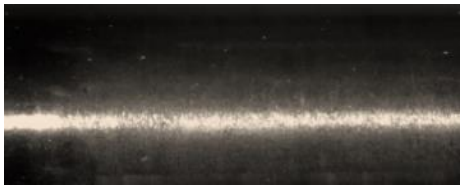	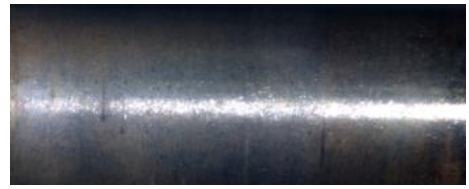
Gen. 1 piston pin, working surface below the bearing.	Gen. 2 piston pin, working surface below the bearing.
	
Gen. 1 piston pin, the end of the piston pin.	Gen. 2 piston pin, the end of the piston pin.

Based on observation and measuring data, it can be concluded that the piston pin is exposed to the greatest load and highest temperature. At the same time, supplying the piston pin and its needle roller bearing with the fuel mixture is insufficient. This may be caused by the design peculiarities of the engine.

One of the problems is the accumulation of oil at the bottom of the carburettor float chamber, which caused the fuel jet to clog (see Fig. 11).

Figure 11. Accumulated oil in carburettor float chamber.

This problem mostly occurs at low temperatures. This means that the method used for mixing does not guarantee that the oil and ethanol mixture is 100% homogenous. To improve this, fuel additives should be used to help to reduce the abovementioned problem. Another major problem is starting an engine at temperatures lower than 10°C. To achieve this easily, evaporating substances (e.g., ether) should be added to the fuel used. This would guarantee the engine starting even at lower temperatures. The emergence of these problems provides a great deal of information for the development of a bioethanol fuel for two-stroke engines.

CONCLUSIONS

Addinol MZ 408 two-stroke engine oil can be used with bioethanol in a two-stroke engine. The oil ensures that the fuel has sufficient lubrication properties and does not cause generating significant amount of soot in the engine. Based on the results of test, the recommended oil to bioethanol ratio is 1/50, the same as prescribed by the oil manufacturer when using gasoline. A major problem is the lubrication of the piston pin, although this also depends directly on the design peculiarities of the engine. In conclusion, it can be said that according to test results, it was not detected that using a bioethanol and oil mixture cause the more rapid wear of engines compared to the use of an gasoline and oil mixture. When measuring the parts of an engine working on gasoline, it was noted that some measurements had increased. The reason for this is the high temperature in the cylinder. It is well known that bioethanol absorbs more energy than regular fuel during evaporation, and, thus, the temperatures in the cylinder are lower. When the engines operated on a bioethanol and oil mixture, the CO emission level of the engines was approx. 80% higher, which means that it is important to adjust the ignition angle of the engine and to reconstruct the carburettor, which ensures the combustion of the higher quality fuel mixture in the cylinder. The abovementioned improvements also reduce fuel consumption. The concentration of other components of exhaust gases—HC and CO_2—was reduced.

The problem was the stratification of the oil in the float chamber of the carburettor, on account of which the jet opening was clogged with oil. To solve the given problem, it is necessary to lessen the amount of oil in the fuel mixture and change the construction of the carburettor in order to guarantee the effective work of the engine.

ACKNOWLEDGEMENTS. The authors would like to especially thank Addinol Lube Oil OÜ (Estonia) for collaboration in this study.

REFERENCES

Baširov, R., Kislov, V., Pavlov, V., Popov, V. 1978. Reliability of fuel injection equipment tractor and combine diesels. *Engineering*, 184 pp. (in Russian).

Demirbas, A. 2009. *Biohydrogen: For Future Engine Fuel Demands*. In Chapter 3. Biofuels, p. 61–84, Springer Verlag. 336 p.

Ghazikhani, M., Hatami, M., Safari, B., Ganji, D.D. 2013. Experimental investigation of performance improving and emissions reducing in a two stroke SI engine by using ethanol additives. *Propulsion and Power Research* **2**(4), 276–283.

Ghazikhania, M., Hatamib, M., Safaria, B., Ganji, D.D. 2014. Experimental investigation of exhaust temperature and delivery ratio effect on emissions and performance of a gasoline-ethanol two-stroke engine. In *'Case Studies in Thermal Engineering'* **2**. Iran, pp. 82–90.

Govindarajan, K. 2008. Alcohol as an Automotive Fuel.
http://www.cheresources.com/energy_future/ethanol_transportation_fuel.shtml Accessed 14.06.2014.

GUNT Hamburg. *http://www.mutiaranata.com/product/detail/tm-260-03-experimental-module-pin-on-disc* Accessed 08.12.2014.

Hilbert, D. 2011. *High Ethanol Fuel Endurance: A Study of the Effects of Running Gasoline with 15% Ethanol Concentration in Current Production Outboard Four-Stroke Engines and Conventional Two-Stroke Outboard Marine Engines*. National Renewable Energy Laboratory, Colorado.

IEA. 2008. *Energy technology perspectives to 2050*. Paris.

Küüt, A., Ilves, R., Vlasov, A., Soots, K., Olt, J. 2014. Imact of bioethanol fuel on output parameters of two-stroke reciprocating engine. International Scientific Conference *Engineering for Rural Development*, Latvia University of Agriculture, Jelgava, 288–295.

Magnusson, R., Nilsson, C. 2011. The influence of oxygenated fuels on emissions of aldehydes and ketones from a two-stroke spark ignition engine. *Fuel* **90**, (3), 1145–1154.

Olt, J., Mikita, V., Ilves, R., Küüt, A., Madissoo, M. 2011. Impact of ethanol on the fuel injection pump of diesel engine. 10th International Scientific Conference '*Engineering for Rural Development*', Latvia University of Agriculture, Jelgava 248–253.

Pulkrabek, Willard, W. 1997. *Engineering Fundamentals of the Internal Combustion Engine*. Upper Saddle River, NJ 07458, 411 pp.

Schwarze, H., Brouwer, L., Knoll, G., Longo, C., Kopnarski, M., Emrich, S. 2010. Effect of Ethanol Fuel E85 on Lubricant Degradation and Wear in Spark-ignition Engines, *MTZ worldwide Edition*: 2010-04.

Standard ASTM D445. *Test Method for Kinematic Viscosity of Transparent and Opaque Liquids*.

Standard EN ISO 3405. *Petroleum products - Determination of distillation characteristics at atmospheric pressure*.

Tung, S.C., Gao, H. 2003. Tribological characteristics and surface interaction between piston ring coatings and a blend of energy-conserving oils and ethanol fuels. *Wear*, Volume 255, Issues 7–12, 1276–1285.

Wargo, J., Wargo, L., Alderman, N. 2006. The Harmful Effects of Vehicle Exhaust. *Report. Environment & Human Health*, Inc. Yale University. 64 pp.

Vesela, K., Pexa, M., Marik, J. 2014. The effect of biofuels on the quality and purity of engine oil. International Scientific Conference. *Agronomy Research* **12(**2), 425–430.

APPENDIX

Table 5. Engine details measurement data

Name	Parameter	Before the test		After the test	
		Gen. 1	Gen. 2	Gen. 1	Gen. 2
Average cylinder diameter at the depth of 10, 20 and 30 mm from the upper surface of the cylinder	Diameter, mm	45.036	45.017	45.030	45.024
Average diameter of the piston	Dimension, mm	44.759	44.798	44.779	44.782
Piston pin diameter at 18 mm from the edge	Diameter, mm	9.988	10.001	9.995	9.997
Piston ring **1** (upper) measured points	Measurement a, mm	1.86	1.92	1.86	1.92
	Measurement b, mm	1.93	1.91	1.93	1.91
	Measurement c, mm	1.86	1.91	1.86	1.90
Piston ring **2** (lower) measured points	Measurement a, mm	1.90	1.93	1.90	1.90
	Measurement b, mm	1.92	1.91	1.91	1.89
	Measurement c, mm	1.90	1.91	1.89	1.89
Diameter of the upper opening of the connecting-rod	Diameter, mm	13.998	13.995	14.005	14.000
Engine compression	Compression, bar	7.00	6.75	8.0	7.75
Roundness of the working elements of the engine					
Cylinder roundness at the depths of 10 and 20 mm from the upper surface	Deviation at the depth of 10 mm, µm	6.469	5.676	6.205	5.103
	Deviation at the depth of 20 mm, µm	5.852	5.850	5.965	6.180
Piston pin roundness, 18 mm from the edge	Deviation, µm	2.616	1.091	2.5104	1.716
Piston, roundness between the rings and 5 mm below the groove of the second ring	Deviation, µm (between the rings)	12.368	15.679	38.026	19.868
	Deviation, µm (5 mm below the groove of the second ring)	48.966	39.641	47.807	58.177

Table 6. Measurements of exhaust gases of the engine

	Gen 1	Gen 2	Gen 1	Gen 2
Rotational speed of the crankshaft of the engine, rpm	3,000	3,000	3,000	3,000
	Before test		After test	
CO, %vol	0.111	0.157	0.104	0.176
HC, ppm	655	119	1172	487
Lambda	1.154	1.240	1.227	1.415
CO_2, %vol	9.17	9.31	12.96	11.64
O_2 %vol	7.80	7.24	3.18	3.88

Agronomy Research **13**(5), 1253–1259, 2015

Water and water clusters in biological systems

P. Laurson and U. Mäeorg*

Faculty of Science and Technology, Institute of Chemistry, University of Tartu, Ravila 14a, EE50411 Tartu, Estonia; *Correspondence: Uno.Maeorg@ut.ee

Abstract. Water is inherently a simple substance, but from Aristotle's time until today it raises a lot of questions. Living cells are about eighty per cent water. Organisms consist essentially of liquid water, which fulfils a lot of functions and should never be considered just an inert diluent. The unique properties of water are of fundamental relevance for human life and play a substantial role in many biochemical and biological systems. In the second half of the previous century, researchers came to an understanding about the differences between biological water and ordinary water. This article reviews previous studies on water function and its significance in biological systems. Present knowledge about water clusters, the understanding of water cluster role in biological systems and common methods used in the analysis of determining water clusters are examined in this paper.

Key words: biological water; water structure; water biology; clustered water; cell water; hydrogen bonding.

INTRODUCTION

About 600 BC, the Greek philosopher Thales asserted that water is the primal substance from which all things arose and of which they consist (Morra, 2001). Two hundred years later, the philosopher Aristotle deemed that water is one of the four fundamental elements, in addition to fire, air and earth (Sokolowski, 1970). Nowadays it is known that water is the most opulent molecule on earth. Almost 70% of the planet is covered by water (Robinson et al., 1996). The properties of liquid water are unique for a liquid: it has huge heat capacity and uncharacteristically high melting and boiling temperatures. Water also has one of the most highly dielectric constants amongst non-metallic liquids and many anomalies in its specific volume as e.g. ice floats on water (Cabane et al., 2005). At first sight, water looks like an ordinary molecule consisting of two hydrogen atoms connected to one oxygen atom, and only a few molecules are known to be smaller in size. Its size misleads the complexity of its characteristics, which seem to fit ideally into the conditions of carbon-based life (Chaplin, 2001). This substance is the most extraordinary and indispensable constituent in every living organism. Water makes up about 80% of the chemical compounds in a living cell; it is the matrix and medium for the origin and operation of life (Szent-Györgyi, 1971). However, water is not just a tasteless, neutral transporter system for biochemical processes, but also an active participator in biology, which simply could not act the way it does without the specific mediating properties of water. Moreover, it is widely believed that water is the first molecule to contact biomaterials in any clinical application (Vogler, 2004).

This paper gives an overview of the current knowledge on water function and its significance in biological systems. The present concept of water clusters, understanding water cluster role in biological systems and common methods used in the analysis of determining water clusters are studied in this paper.

Formation of understandings about water in a biological system

Cells, organs and all living organisms are in constant water demand. Without the presence of water, several chemical reactions would not take place. Also, biological systems would not function, and life, as we know it, might not even have come to be without water (Ellabaan et al., 2012). The task of water in chemical, biochemical and cellular occasions has been recognized as a universal solvent. The common belief was that biological water is not markedly different from normal liquid water. However, the relevance of biophysical and biochemical characteristics of water have been pointed out since the second half of the last century. These researches focused on the fundamental question: what are the differences between biological water and ordinary water (Lo et al., 2000). Water molecules that surround solute molecules form with them frozen patches or microscopic icebergs (Frank & Evans, 1945). The concept of cell as a membranous bag of solutions has been seriously challenged. For the first time, it was claimed that the partitioning of solutes between the cell and extracellular solution is not determined only by the throughput of the membrane, but that protoplasm itself preferentially accumulates some solutes and excludes others. The understanding that water in the protoplasmic gel is different from water in a simple aqueous solution was at the centre of this concept (Troschin, 1966). Many extensive studies on water in biological systems have been carried out. It has been concluded that the water density of *Artemia cyst* was smaller than of normal water at the same temperature (Clegg, 1984). Some authors claim there is both high and low-density water inside the cell. Others claim that the water inside the cell is different from free water in bulk (Wiggins, 1990). One of the main problems in biochemistry is to understand how the structure is built up and what are the functions of proteins at the molecular rate. Water molecules also act as catalysts for many enzymes in biochemical reactions. The particular inclusion of water is indispensable for detecting many problems in biochemistry. Thus, it could be implied that without principal and detailed knowledge of water, many phenomena in molecular biology would be impossible to understand (Robinson et al., 1996). Bulk water is only one of the many various ways that liquid water can be organized. ‘Dense’ water (low degree of hydrogen bonding) and ‘less dense’ (‘expanded’) water (high degree of hydrogen bonding—extreme in ice with straight hydrogen bonds) were proposed to exist under specific conditions (Wiggins, 2001). Water ionizes and permits simple proton exchange between molecules to facilitate the affluence of ionic synergies in biology. The structuring of water around molecules makes it possible to sense them and helps them sense each other from a distance. The unique hydration properties of water towards biological macromolecules (especially proteins and nucleic acids) designate their three-dimensional structures to a large range, and hence their functions in a solution (Chaplin, 2001). A surprising characteristic of water is its preferential orientation in the hydration cell of nonpolar solutes and nonpolar side groups appended to biopolymers. The structure obtained by liquid water that is in close proximity to nonpolar solutes is a primary characteristic of modern theories about hydrophobic hydration and effects, which are of high importance to our knowledge of many important chemical and

biological processes. Placing a solute molecule in liquid water brings about a rearrangement of the random H-bond network. Also, in order to create some space for the guest molecule, the water tries to strengthen its network around the non-polar solute. This can best be done by placing its tetrahedral bonding directions in a straddling mode (Ludwig, 2001). In a closed system, these kinds of water moieties are balanced: deviation of water density from that of bulk water in one partial volume of the system is presumably compensated by an inverse deviation of the density of the water moiety in some neighbouring partial volume to maintain a balance. There seem to be no strictly defined borderlines between the different water densities, and it should be kept in mind that the partitioning of cell water into water moieties of different density cannot be static, but rather a procession of transient states of high dynamic activity (Mayer et al., 2006). Self-association of water through hydrogen bonding is the essential mechanism behind water solvent properties and understanding self-association effects near surfaces is a key to understanding water properties in contact with biomaterials (Vogler, 2004). Specifically for proteins, the dynamics of water–protein interactions govern various activities, including facilitating protein folding, maintaining structural integrity, mediating molecular recognition and accelerating enzymatic catalysis. Thus, it is important to characterize the dynamic behaviour of biomolecule-associated water—biological water—at a molecular level. Every water molecule in the hydration shell is dynamic (not in an iceberg), and their ultrafast motion is established experimentally to be significantly slower than the one in bulk water. The reorientation motion of water in the shell occurs in a few picoseconds in the inner layers and becomes faster in the outer layers (Zhong et al., 2011). Water transport through biological membranes can occur in three ways: 1) over diffusion through the lipid matrix; 2) through transport proteins, such as channels, and some occlusion transport proteins, such as glucose transporters, and 3) through water channel proteins specifically expressed by cells for such purpose (Disalvo et al., 2015).

Water clusters

The simplest water system, the water cluster, is an accurate assembling of water molecules synergized together by hydrogen bonds. In the biological system, water molecules form an unlimited hydrogen-bonded net with structured clustering. It has been hypothesized that small clusters composed of four water molecules already have the ability to form comparatively stable water octamers. These clusters may further form much larger water clusters that can interlink and tessellate throughout space (Chaplin, 2001). The fundamental knowledge of water clusters can be investigated computationally or experimentally (Ludwig, 2001). Water clusters influence a large number of aspects of biological functions. The water-protein interaction has been accepted as a major decider of chain folding, internal dynamics, conformational stability, binding specificity and catalysis for a long time (Pocker, 2000). A different allocation of water clusters in natural water (rain and river) and in the biological matrix of fruits (apples, bananas) and vegetables (potatoes, carrots, tomatoes, onions, red beets) has been determined. It has been found that the structure of natural water clusters is different from the water of the biological matrix of fruits and vegetables and it is dependent on dryness and the biological matrix. It has been identified that water clusters in natural water are not as stable and reproducible as water clusters in plants (Zubov et al., 2006). Lo *et al*. advance the hypothesis that the water clusters are active partners in any biochemical

reactions occurring inside a living organism. These water clusters are created by the interaction of minute inorganic or organic substance with water (Lo et al., 2000). During plant growth, water clusters and their distribution (downfallen or expanded) play an important role. The behaviour of water clusters in plants can possibly be exploited in the future as the indicator for biological matrix development during the time of plant growth. Oscillation of water clusters inside plants makes communication between plants and surroundings possible through a resonance field. The right choice of natural water concerning the long-range order of water clusters could advance plant growth and decrease costs (Zubow et al., 2010). Wang *et al*. explored the effects of small water clusters in *Escherichia coli* bacterial culture and found that the *E. coli* grew faster in small water clusters than in normal water (Wang et al., 2013).

Calculated water clusters

There have been numerous semi-empirical and *ab initio* quantum mechanical studies on water clusters (Ludwig, 2001). Discussions have shown that water clusters, depending on their size and connectivity, can play an important part in experimental and theoretical investigations.

Small Cyclic Water Clusters (n = 3–6), including ring structures, are the optimal structures with harmonic vibrational frequencies (Xantheas et al., 1993).

Isoenergetic Water Hexamer Clusters (n = 6) or cyclic hexamers, as discussed above, are the building blocks of numerous ice forms and they appear to be relevant to liquid water as well (Kim et al., 1998).

A variation of Water Heptamers (n = 7), although, to date, only a few theoretical investigations on the water heptamer are available and knowledge is still scarce (Mir & Vittal, 2007).

Water Octamers (n = 8): Cubic or Cyclic. The cyclic topology has fewer H-bonds than the cubic octamers (8 versus 12) and is therefore energetically not favoured. Its powerful thermodynamic balance is induced by entropic factors (Weinhold, 1998).

Ice-Like and Clathrate-Like Structures (n = 12–26) are well known structural components of crystallographic ice forms (Ludwig & Weinhold, 1999).

Larger Clusters: Icosahedral Networks (n = 280), which are built in a way that each water molecule is connected with four H-bonds. Two of them act as acceptors and two as donors (Chaplin, 2001).

Experimental determination of water clusters

The physical characteristics of water clusters are principally investigated through size-dependent multitude researches in the mass spectra of protonated water clusters of $(H_2O)_nH^+$ and deprotonated water clusters $(H_2O)_nH^-$ in a size ranging up to a hundred molecules (Hansen et al., 2009), through infrared (IR) spectroscopy (Mizuse et al., 2010) and by using photoelectron spectroscopy (Ma et al., 2009). Electron diffraction tests were performed during the years 1975–2000 and it was the preferred method for experiments with crystalline water where the size range of clusters was n = 200–1,000 molecules (Torchet et al., 1989). Vibrational IR spectroscopy experiments validate these results in a study on pure water and Na-doped clusters (Mizuse et al., 2010). With IR excitation-modulated photoionization spectroscopy, the beginning of crystallization in a range of n = 275 water molecules was registered (Pradzynski et al., 2012). In the computer simulations it is assumed that the amorphous-crystalline transition takes place

at n = 200 water molecules (Kazimirski & Buch, 2003). Turning to amorphous structures is expected to occur between n = 21–275 molecules.

All up-to-date published studies which examine water in biological systems have reached the conclusion that water is not a passive spectator in the molecular biological processes. Research on water has given the result that water performs a variety of important roles in cells and tissues and in the functioning of the biological organisms overall (Lo et al., 2000). Almost all the activity of proteins and nucleic acids depends on the presence of water. Theories that describe the role of water in proteins and nucleic acids activity are under ongoing scientific debate. Long-standing 'iceberg' theory has replaced the theory of water molecules in the hydration shell being all dynamic (Frank & Evans, 1945; Zhong et al, 2011). Water in biological systems is surrounded by intervening cellular components and also affected by structural effect, as well as having different structure and characteristics than bulk water. The biological system generates stabilized clustered networks from water molecules (Wiggins, 1990). Researchers have shown that water clusters have internal and external influence on biological processes. Many studies describe the influence of biological processes in which water clusters help to complete biological systems, for example, in conformational stability, internal dynamics, catalysis, etc. The results which have been obtained by the external contact with clustered water and biological systems are also remarkable. However, the mechanisms of action in those processes need more investigation. There is still a lot of incomplete knowledge about water clusters or biological water and theories of cell biochemistry are not explicit. Some studies have shown that clustered water also has an effect on the yield of crops (Zubow et al., 2010). Until now there have been a lot of theoretical researches carried out on structures of water clusters in biological systems, which help to contribute to interpreting biological processes of nature. Different physical experimental methods are used for researching biological water and determining water clusters. However, there is no unique method for defining biological objects in water clusters—the existing methods need continuous development to be in an agreement with specific biological system characteristics.

CONCLUSIONS

Water clusters in biological systems have an active role in all biochemical reactions that exist inside living organisms. Understanding the mechanism of the self-association of water molecules through hydrogen bonding is essential for understanding water properties in contact with biomaterials. It can be derived that clustered water can have a similar essential effect in the human organism as clustered water has in plants. Considering that water clusters in plants may have an influence on the human organism, there is a need for further research of water clusters in plant cells. It is very likely that further research on water clusters in plant cells will reveal new insights into fresh herbal food and plant juice benefits for human health.

REFERENCES

Cabane, B., Vuilleumier, R. 2005. The physics of liquid water. *Comptes Rendus Geoscience* **337**, 159–171.

Chaplin, M.F. 2001. Water: its importance to life. *Biochem Mol Bio Edu.* **29**, 54–59.

Clegg, J.S. 1984. Interrelationships between water and cellular metabolism in *Artemia cysts.* XI. Density measurements. *Cell Biophys*. **6**, 153–169.

Disalvo, E.A., Pinto, O.A., Martini, M.F., Bouchet, A.M., Hollmann, A., Frías, M.A., 2015. Functional role of water in membranes updated: A tribute to Träuble. *Biochimica et Biophysica Acta* **1848**, 1552–1562.

Ellabaan, M.M.H., Ong, Y.S., Nguyen, Q.C., Kuo, J-L. 2012. Evolutionary discovery of transition states in water clusters. *J Theor Comp Chem*. **11**, 965–995.

Frank, H.S., Evans, M.W. 1945. Free volume and entropy in condensed systems III. Entropy in binary liquid mixtures; partial molal entropy in dilute solutions; structure and thermodynamics in aqueous electrolytes. *J Chem Phys.* **13**, 507–532.

Hansen, K., Andersson, P.U., Uggerud, E. 2009. Activation energies for evaporation from protonated and deprotonated water clusters from mass spectra. *J Chem Phys.* **131**, 124303/1-124303/7.

Kazimirski, J.K., Buch, V. 2003. Search for Low Energy Structures of Water Clusters $(H_2O)_n$, n=20-22, 48, 123, and 293. *J Phys Chem A.* **107**, 9762–9775.

Kim, J., Kim, K.S., 1998. Structures, binding energies, and spectra of isoenergetic water hexamer clusters: Extensive *ab initio* studies. *J Chem Phys*. **109**, 5886–5895.

Lo, S.Y., Li, W.C., Huang, S.H. 2000. Water clusters in life. *Med Hypotheses.* **54**, 948–953.

Ludwig, R. 2001. Water: From Clusters to the Bulk. *Angew Chem Int Ed.* **40**, 1808–1827.

Ludwig, R., Weinhold, F. 1999. Quantum cluster equilibrium theory of liquids: Freezing of QCE/3-21G water to tetrakaidecahedral 'Bucky-ice'. *J Chem Phys.* **110**, 508–515.

Ma, L., Majer, K., Chirot, F., von Issendorff, B. 2009. Low temperature photoelectron spectra of water cluster anions. *J Chem Phys.* **131**, 144303/1-144303/6.

Mayer, F., Wheatley, D., Hoppert, M. 2006. Some properties of interfacial water: Determinants for cell architecture and function. In: Pollack, G.H., Cameron, I.L., Wheatley, D.N. *Water and the Cell.* Springer, Dordrecht, 253 pp.

Mir, M.H., Vittal, J.J. 2007. Phase Transition Accompanied by Transformation of an Elusive Discrete Cyclic Water Heptamer to a Bicyclic $(H_2O)_7$ Cluster. *Angew Chem Int Ed Eng.* **46**, 5925–5928.

Mizuse, K., Mikami, N., Fujii, A. 2010. Infrared Spectra and Hydrogen-Bonded Network Structures of Large Protonated Water Clusters $H^+(H_2O)_n$ (n=20–200). *Angew Chem Int Ed Eng.* **49**, 10119–10122.

Morra, M. 2001. *Water in Biomaterials Surface Science.* John Wiley & Sons Ltd., England, 408 pp.

Pocker, Y. 2000. Water in enzyme reactions: biophysical aspects of hydration-dehydration processes. *Cell Molec Life Sci.* **57**, 1008–1017.

Pradzynski, C.C., Forck, R.M., Zeuch, T., Slavíček, P., Buck, U. 2012. A Fully Size-Resolved Perspective on the Crystallization of Water Clusters. *Science* **337**, 1529–1532.

Robinson, G.W., Singh, S., Shu, S-H., Evants, M.W. 1996. *Water in Biology, Chemistry, and Physics: Experimental Overviews and Computational Methodologies.* World Scientific Publishing Co.Pte. Ltd., Singapore, 528 pp.

Sokolowski, R. 1970. Matter, Elements and Substance in Aristotle. *J Hist Philo.* **8**, 263–288.

Szent-Györgyi, A. 1971. Biology and pathology of water. *Perspect Biol Med.* **14**, 239–249.

Torchet, G., Farges, J., de Feraudy, M. F., Raoult, B. 1989. Structural study of CH_4, CO_2 and H_2O clusters containing from several tens to several thousands of molecules. *Ann Phys Fr.* **14**, 245–260.

Troschin, A.S. 1966. *Problems of cell permeability.* Pergamon Press, Oxford, 564 pp.
Vogler, E.A. 2004. Role of water in biomaterials. *Biomaterials Science, 2nd ed.* 59–65.
Wang, J., Zhao, F., Chen, B., Li, Y., Na, P., Zhuo, J. 2013. Small water clusters stimulate microcystin biosynthesis in cyanobacterial *Microcystis aeruginosa*. *J Appl Phycology* **25**, 329–336.
Weinhold, F. 1998. Quantum cluster equilibrium theory of liquids: General theory and computer implementation. *J Chem Phys.* **109**, 367–372.
Wiggins, P.M. 1990. Role of water in some biological processes. *Microbiological Reviews* **54**, 432–449.
Wiggins, P.M. 2001. High and low density intracellular water. *Cell Mol Biol.* **47**, 735–744.
Xantheas, S.S., Dunning, T.H. 1993. *Ab initio* studies of cyclic water clusters $(H_2O)_n$, n=1-6. I. Optimal structures and vibrational spectra. *J Chem Phys*. **99**, 8774–8792.
Zhong, D., Pal, S. K., Zewail, A.H. 2011. Biological water: A critique. *Chemical Physics Letters.* **503**, 1–11.
Zubov, A.V., Zubov, K.V., Zubov, V.A. 2006. Investigation of the distribution of water clusters in vegetables, fruits, and natural waters by flicker noise spectroscopy. *Biofizika* **52**, 585–592.
Zubow, K., Zubow, A.V., Zubow, V.A. 2010. Water clusters in plants. Fast channel plant communications. Planet influence. *J Biophys Chem*. **1**, 1–11.

Agronomy Research **13**(5), 1260–1274, 2015

OHSAS 18001 contribution to real and formal safety elements in safety management system in manufacturing

Õ. Paas*, K. Reinhold and P. Tint

Tallinn University of Technology, Faculty of Economics, Institute of Business Administration, Chair of Work Environment and Safety, Ehitajate 5, EE19086 Tallinn, Estonia; *Correspondence: onnela.paas@gmail.com

Abstract. The current paper examines safety management systems in the Estonian manufacturing industry. The aim of this research is to assess via safety audit, to what extent OHSAS18001 contributes to real and formal safety elements of SMS in manufacturing companies. In 2014, eight OHSAS 18001-certified organisations and eight non-certified Estonian enterprises from different branches of manufacturing were interviewed and assessed using MISHA method. The results show via statistical analysis that OHSAS 18001 has a significant impact on formal safety, real safety and combined safety elements. It can be also concluded that the OHSAS 18001 certification facilitates companies' commitment to health and safety activities and leads to dealing with additional topics promoting workplace health and safety. Therefore, OHSAS 18001 can be seen as a strategic unit for improving safety performance. However, after examining three types of companies, we can conclude that a safety management system can be effectively implemented also without possessing the OHSAS 18001 certification, but in the Estonian economy market it usually requires affiliation with a larger corporation or concern. Based on the analysis, a conceptual model is created which helps the company reallocate the resources in a way that all possible safety elements will be covered.

Key words: MISHA method, OHSAS 18001, safety audit, safety management.

INTRODUCTION

The safety management system (SMS) can be considered as a systematic and comprehensive process for proactive managing of safety risks that integrates operations and technical services with financial and human resource management. In order to ensure a successful outcome, the SMS must: (1) be comprehensive and integrated into all of the organization's decisions and actions with respect to adopted control measures; (2) be documented, implemented and readily accessible and used as the primary means of ensuring safe operation; (3) comply with all the requirements stated in the occupational health and safety (OHS) regulation and (4) be continually reviewed and revised so that the SMS remains up-to-date and effective (Kamp & Blansch, 2000; Bottani et al., 2009; Fernandez-Muniz et al., 2009; Möldri et al., 2012; Rebelo et al., 2014; Mežinska et al., 2015; Yorio et al., 2015).

Frazier et al. (2013) suggest the following sub-factors in SMS: safety policy, procedures and rules, training, communication, incident reporting and analysis, safety

audits and inspections, rewards and recognitions, employee engagement, safety meetings / committees, suggestions / concerns and discipline.

After the SMS procedures have been developed, they need to be implemented by people with appropriate skills and knowledge. Training packages should be developed to explain the SMS and they should be delivered effectively to all workers. One possibility for establishing and ensuring effective SMS is to apply for an SMS certification (such as OHSAS 18001 (EVS, 2007)), which creates the basis for systematic work in the area of safety management, hazard identification and prevention, and promotes strong improvement process being put to use (Paas et al., 2015b). The benefits of OHSAS 18001 have been studied by several authors in recent years (Nielsen, 2000; Torp et al., 2000; Hale, 2009; Rocha, 2010; Granerud & Rocha, 2011; Fernandez-Muniz et al., 2012a; Fernandez-Muniz et al., 2012b; Koivupalo et al., 2015;). The aforementioned studies indicate that adopting OHSAS 18001 may improve the organisation's image, reputation and performance. Moreover, it integrates OHS into the company's management system, reduces the risk of accidents, improves the company's compliance with legal obligations, favours a learning process and helps to create a higher level of transparency. However, OHSAS 18001 certification has also been criticised, especially for having a tendency to increase the bureaucratisation of health and safety issues and therefore discourage genuine worker involvement. This may shift the focus from health and safety issues towards paperwork control, which may diminish the activities dealing with OHS problems (Kamp & Blansch, 2000; Nielsen, 2000; Granerud & Rocha, 2011).

The aforethought SMS contributes to a positive safety culture (Fernandez-Muniz et al., 2007a; Fernandez-Muniz et al., 2007b; Hale et al., 2010; Nordlöf et al., 2015; Yourio et al., 2015). A healthy and positive safety culture actively seeks improvements, is constantly aware of hazards and uses adequate units for continuous monitoring, analysis and investigation. Other elements of positive safety culture include the personnel and management being committed to safety responsibilities and the existence of a documented set of rules and policies. Several studies prove that management's strong commitment to safety ensures the establishment of and adherence to sound safety practices (Nielsen, 2014; Koivupalo et al., 2015; Nordlöf et al., 2015). It is important to note that a safety culture cannot be effective without devolving to organizational culture (Järvis, 2013; Yourio et al., 2015). Therefore, the SMS should not rely on a pure paperwork system—rather it should reflect the overall safety culture and be consistent with the mitigation of occupational hazards gained from the risk assessment.

Poor safety culture will encourage an atmosphere of non-compliance to safe operating practices. Violations are likely to be most common in organizations where the unspoken attitudes and beliefs are that production and commercial goals should get priority, rather than safety. Several studies illustrate the cultural expression where there is a constant competition between productivity and safety—e.g. taking shortcuts without using the appropriate units or ignoring safe procedures to increase productivity (Brown et al., 2000; Atak & Kingma, 2011; Nazaruk, 2011). Managers tend to perceive the resources for OHS as expenditures rather than investments. Therefore, it remains difficult to convince the management of the benefits of investing into safety activities—implementation costs are often overestimated and potential failure costs underestimated (Amador-Rodenzo, 2005). Effective SMS should promote the achievement of an acceptable level of safety while balancing the distribution of resources between

production and protection. In any manufacturing organization, production and safety risks are strongly linked (Fig. 1). According to James Reason (1997), when production increases, safety risks may also increase if the necessary resources or process enhancements are not available. A company should determine its key objectives of production and safety by balancing the output with acceptable safety risks. If the resources are excessively allocated for protection or risk controls, it may result in the product becoming unprofitable, thus jeopardizing the viability of the organization. On the other hand, favouring the allocation of resources for production at the expense of protection might have an impact on the safety performance and it might ultimately lead to an accident. Perhaps the most extensive effect of a poor safety culture will be evident in an unwillingness to be proactive with no deficiencies—safety shortcomings will be worked around and allowed to persist.

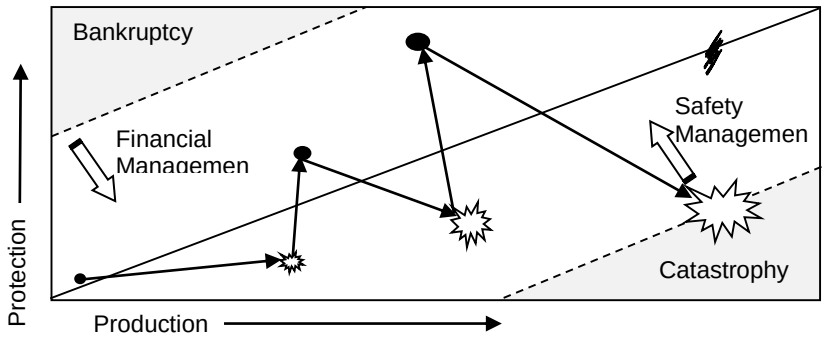

Figure 1. Relationship between safety and financial management to ensure positive safety practice (adopted from James Reason 1997).

Good safety culture should have favourable characteristics that contribute to a positive, desirable and primarily stable state of safety. According to Silva & Lima (2005), an implemented prescriptive safety culture involves not only the congruence between *Safety values exposed* and *Safety values in use*, but a complete real and positive safety response encompassing values, behaviours, organisation and engineering. Naturally, manufacturing companies with relatively high level of hazards should declare safety values and compose the safety policy as a part of formal safety. However, this does not ensure a prescriptive safety culture. According to some researchers (Granerud & Rocha, 2011; Meliá et al., 2012), a formal accent on safety can sometimes be used as an internal and external marketing procedure. It may thus hide some of the real safety weaknesses and lead to window coupling. Some of the flaws which may affect the safety response negatively are: 1) a formal but inefficient use of safety programmes; 2) the existence of general safety instructions not adopted to the company's real needs; 3) hazard analyses existing only on paper without any further action plans or activities being created; 4) lack of real safety communication including immediate intervention and 5) group specific descriptive safety cultures against safety procedures, which sometimes result in developing poor behaviours and attitudes towards safety practices.

The aim of this research was to assess via safety audit in what extent OHSAS 18001 contributes to the real and formal safety elements of SMS in manufacturing companies.

The main objectives were: (1) to examine the impact of OHSAS 18001 on real and formal safety elements, (2) to conduct a safety audit in 16 industrial companies (eight OHSAS 18001-certified companies (OHSAS), four non-certified locally established and owned companies (NOHSASL) and four organisations which belong to a larger corporation or concern but are not OHSAS 18001-certified (NOHSASC)) in order to find the relationships between company type and safety activities and (3) to perform a statistical analysis to find out the significant difference in formal, real and formal+real (combined) safety elements based on company type.

MATERIALS AND METHODS

In 2014, 16 safety audits were conducted in manufacturing companies in Estonia by means of the MISHA method (Method for Industrial Safety and Health Activity Assessment) (Kuusisto, 2000) in the form of quantitative assessment (scale 0–3 for each item) and qualitative interviews. OHSAS companies were selected using the database of Estonian Association for Quality (2014). In order to compare the results with non-certified organizations, eight companies with a similar background were selected—four represented organisations which belong to a larger corporation or concern but are not OHSAS 18001-certified and four that were non-certified, locally established and owned companies representing main manufacturing areas in Estonia such as printing, textile, metal, food, furniture, plastic, glass, heat and electronics industry.

In order to see whether there is difference in OHSAS 18001 impact for formal and real safety performance, the authors interviewed top and line managers and also safety specialists and workers' representatives in enterprises by the MISHA method. As a result, it was determined (using statistical methods) whether the safety element contributes to formal, real or combined safety. Some of the elements indicated possessed properties from both groups, which formed the third group—combined safety elements (Fig. 2b).

A total of 55 questions were asked from each of the person interviewed (MISHA method). Once data collection had ceased, the first author and the interviewer (ÕP) re-listened to the records, checked the coding strategy used for consistency and ensured that all questions had been answered. The second author (KR) then listened to the records and made notes about understanding the answers. After that, the first two authors discussed the answers of each company in order to come to a good level of agreement on the results. The enterprises' number of workers varied from 50 to 250 (Paas et al., 2015b).

Statistical analyses were prepared using the programme *IBM SPSS Statistics 22.0 and R 2.15.2*. The following statistical methods were used: correlation, *MANOVA* and *Factor Analysis Principal Component method* (Field, 2013).

RESULTS AND DISCUSSION

This section presents the empirical findings of the study. For determination of the impact of OHSAS 18001 on formal and real safety performance, a statistical analysis was conducted. As a result, a conceptual model was created based on whether the safety element contributes to formal, real or combined safety (Fig. 2a, 2b, 2c).

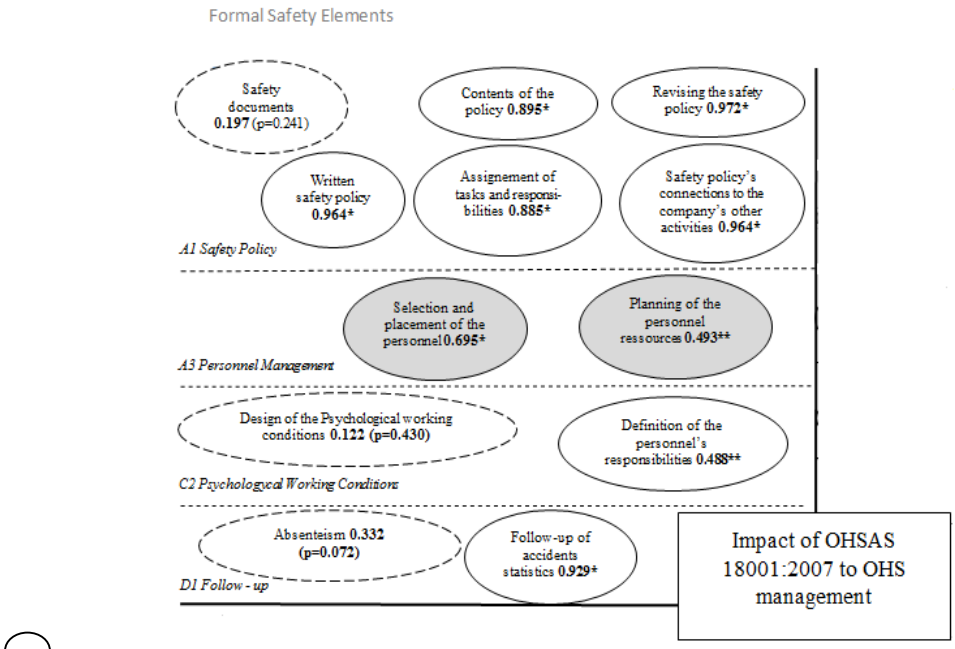

Safety elements covered in OHSAS 18001
Safety elements examined through audit but not covered with OHSAS 18001

Figure 2a. Formal safety elements.

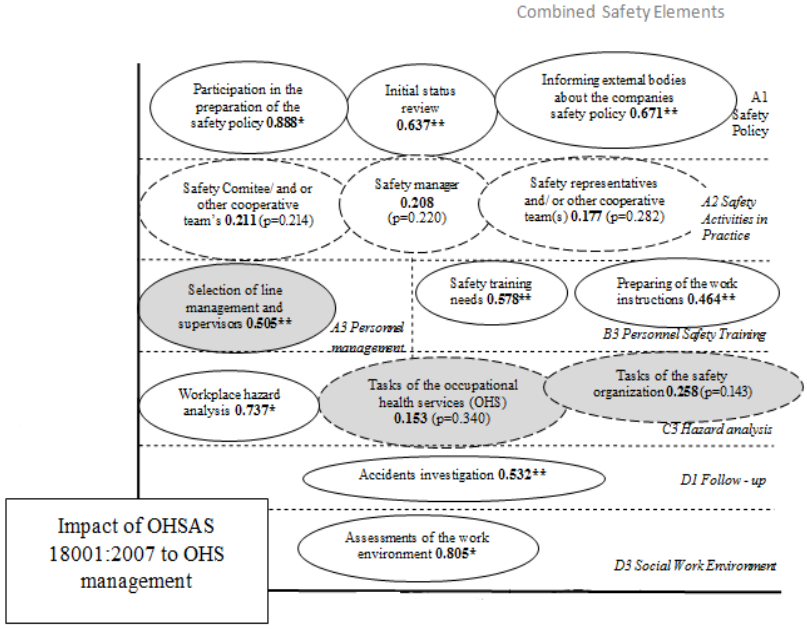

Safety elements covered in OHSAS 18001
Safety elements examined through audit but not covered with OHSAS 18001

Figure 2b. Combined safety elements.

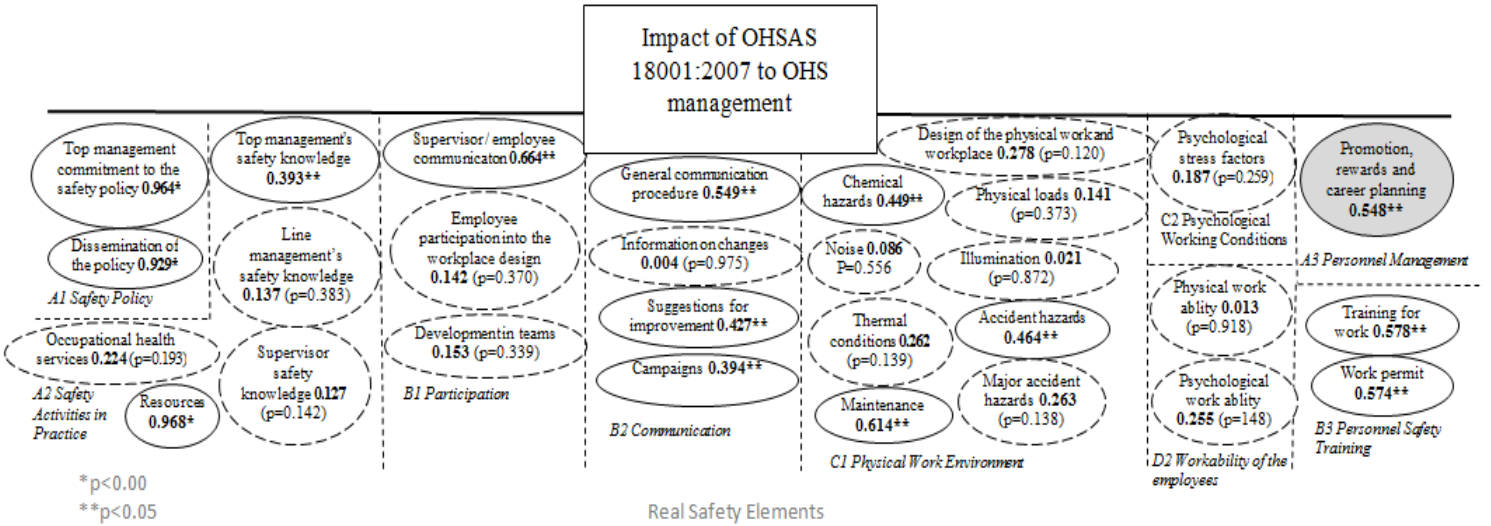

Safety elements covered in OHSAS 18001
Safety elements examined through audit but not covered with OHSAS 18001

Figure 2c. Real safety elements.

Testing the significant impact of company type (OHSAS NOHSASL, NOHSASC) on the abovementioned safety elements with Multivariate Analysis *MANOVA*, the results demonstrate that there was a significant multivariate main effect of company type on formal safety performance ($p < 0.05$). The results also showed that there was a significant difference in real safety performance as well as in combined safety performance between different company types *($p < 0.1$).*

A conceptual model (Fig. 2 SUM): OHSAS 18001 and the impact of the safety elements in the scope of formal, real or combined safety can be combined from Fig. 2a, 2b, 2c.

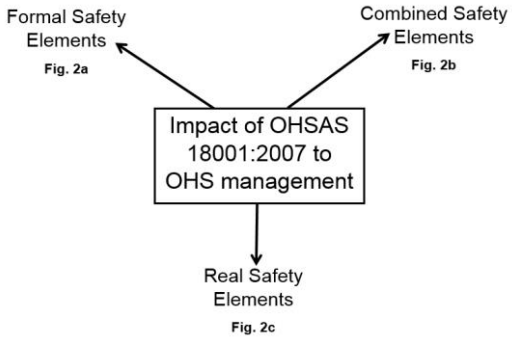

Figure 2 SUM. A conceptual model: OHSAS 18001 and the impact of the safety elements in the scope of formal, real or combined safety.

a) Formal Safety Elements

MANOVA analysis showed that there was a statistically significant difference in formal safety performance based on the company type (OHSAS, NOHSASL, NOHSASC), $F(22, 6) = 10.047$, $p < 0.05$; *Wilk's $\Lambda = 0.001$, partial $\eta 2 = 0.974$*. The power to detect the effect was *0.988*. Fig. 2a shows three formal safety elements—safety documents, absenteeism and design of the psychological working conditions—were not dependent on company type since they did not show any correlation. The majority of safety documents are required by OHS legislation and therefore OHSAS 18001 does not play a significant role in implementing basic safety documents. Absenteeism investigation is required by OHSAS 18001, however this is complicated to conduct in practice due to restrictions in Estonian Personal Data Protection Act (2007), and therefore our study showed that all types of companies have difficulties reaching absenteeism. The active approach to dealing with psychological working conditions is still low in all Estonian companies with no differences between three company types. This was also supported by the qualitative interviews conducted by the authors, in addition to the current research (Paas et al, 2015a).

All other formal safety elements were dependent on company type. The highest impact was shown on written safety policy (0.964, $p < 0.00$), revising the safety policy (0.972, $p < 0.00$), safety policy's connections to the company's other activities (0.964 $p < 0.00$) and follow-up of accidents statistics (0.929, $p < 0.00$).

Company type also showed significant impact on contents of the policy (0.895, $p < 0.00$), assignment of tasks and responsibilities (0.885, $p < 0.00$), selection and placement of the personnel (0.695, $p < 0.00$), planning of the personnel resources (0.493,

$p < 0.05$) and definition of the personnel responsibilities (0.488, $p < 0.05$). This means that implementing OHSAS 18001 contributes to a higher formal safety performance—safety activities are systematically planned and it guarantees higher preconditions for formal safety performance.

Fig. 3 presents the results of each formal safety element calculated by the MISHA method according to company type. From there we can conclude that for some elements OHSAS 18001 does not give the expected added value. For instance, organisations which belong to a larger corporation or concern but are not OHSAS 18001-certified (NOSHASC) show higher results in defining personnel's responsibilities and planning personnel resources. This shows that these elements are more strongly related to the company's general personnel management and the content of job descriptions. Some of the corporated companies have applied a strong content for safety policy which indicates that if the top management reports full engagement to safety, the content of safety policy may be more comprehensive and far-reaching than required by OHSAS 18001. Non-certified, locally established and owned companies (NOHSASL) show considerably lower results than OHSAS 18001 certified (OHSAS) and NOHSASC companies in formal safety elements which can be explained by more random attitudes and activities towards OHS management. Only a few of NOHSASL companies possess a written safety policy or deal with regular personnel resources and selection. Additionally, the follow-up of accidents statistics is very low among NOHSASL companies. Meliá et al. (2012) conducted an in-depth analysis of a NOHSASL company dealing in process industry in Southern Europe and identified several safety flaws such as formal use of preventive observations, formal but not useful safety programmes, lack of safety communication etc.

Safety audits revealed that NOHSASC companies gained slightly higher results preparing safety documents, such as work instruction, instructions for safety training, training of new employees, instruction for supervisors' safety duties etc. than OHSAS companies. The reason behind this might rather depend on the size of the company than its type as smaller firms tend to put less effort into the bureaucracy of safety documents.

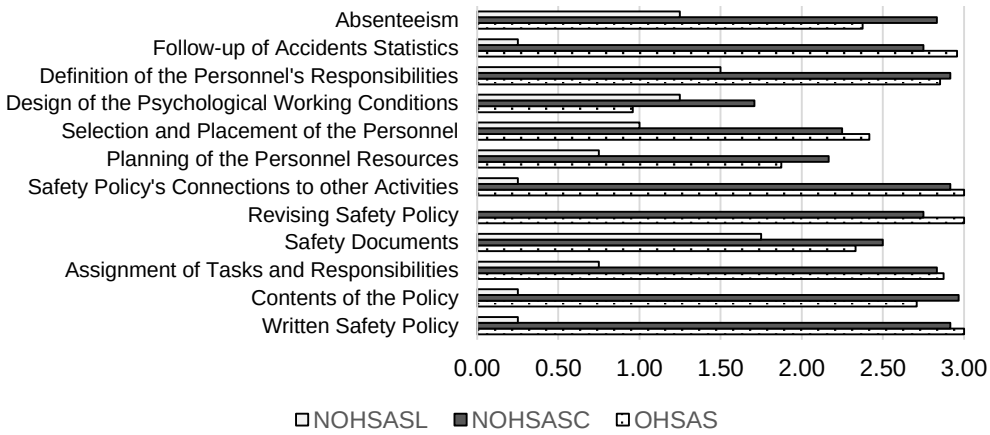

Figure 3. Descriptive statistics of formal safety elements providing mean (calculated using the MISHA method) for the dependent variables according to company type. Scale 0–3.

b) Real Safety Elements

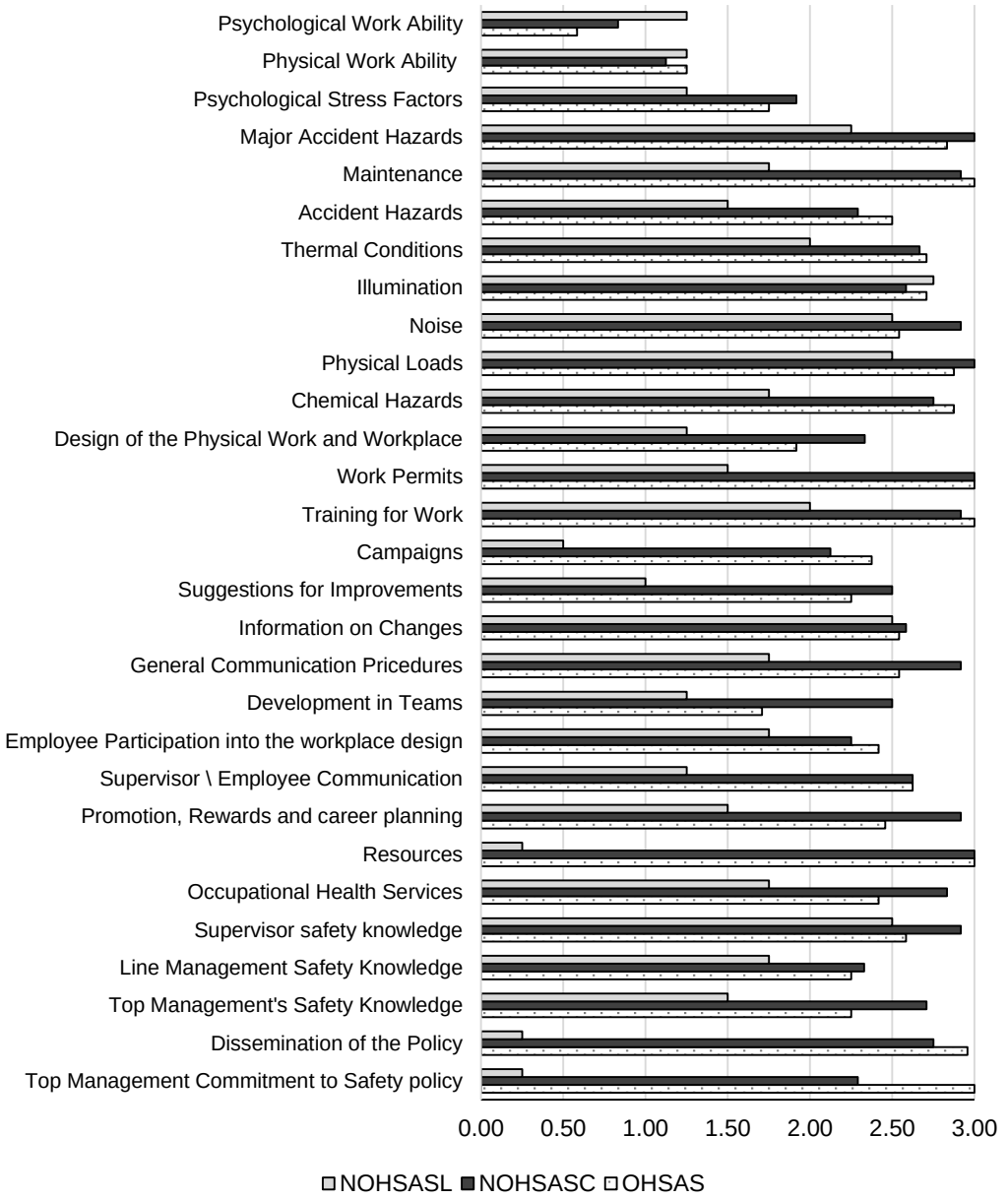

Figure 4. Descriptive statistics of real safety elements providing mean (calculated using the MISHA method) for the dependent variables according to company type. Scale 0–3.

Examining real safety elements, there was a statistically significant difference in real safety performance based on the company type (OHSAS, NOHSASL, NOHSASC), $F\ (26, 2) = 17.311$, $p < 0.1$; $Wilk's\ \Lambda = 0.000$, partial $\eta^2 = 0.996$. The power to detect the effect was 0.854. Among real safety elements, statistical analysis showed a lot more

safety factors which do not depend on company type (Fig. 2): in activity area A2 of occupational health services, supervisor safety knowledge, line management safety knowledge; in B1employee participation in workplace design, development in teams; in B2 information on changes; in C1 noise, thermal conditions, illumination, physical loads, major accident hazards and design of physical work and workplace; in C2 psychological stress factors; in D2 physical workability and psychological workability.

This indicates that OHSAS 18001 does not contribute to a great extent to many of the real safety activities. For example, dealing with physical work environment (C1) is a strict requirement derived from the OHS act and it is one of the main focuses of the annual visit of the labour inspector. Employee participation in workplace design is rarely used in all three types of companies due to the common belief that there is low OHS knowledge among employees. Therefore, companies prefer to rely on engineers rather than involving employees in the stage of design, with a few exceptions (Paas et al., 2015a). Development in teams is also seldom practiced among companies as it is not supported by Estonian OHS legislation.

Other real safety elements were dependent on company type: in activity area A1: top management commitment to the safety policy and dissemination of the policy; A2: resources, top management's safety knowledge, line management's safety knowledge and supervisor safety knowledge; A3: promotion, rewards and career planning; B1: supervisor\employee communication; B2: general communication procedure, suggestions for improvement and campaigns; B3: training for work and work permits; C1: chemical hazards, maintenance and accident hazards.

Very high influence emerged in top management's commitment to the safety policy (0.964, $p < 0.00$), dissemination of the policy (0.929, $p < 0.00$) and OHS resources (0.964, $p < 0.00$). There are several other real safety elements that significantly depend on company type: top management's safety knowledge, supervisor employee communication, promotion, rewards and career planning, training for work, work permits, and so on. From Fig. 4, all scores for real safety element according to company type can be seen. From these results we can conclude that implementing the OHSAS 18001 standard contributes only partly to real safety elements such as top management commitment to the safety policy, dissemination of safety policy and resources. For many real safety elements (Fig. 4), strong demands from corporations influence safety activities more than requirements derived from the OHSAS 18001 standard, for example suggestions for improvements; general communication procedures; promotion, rewards and career planning and safety knowledge among supervisors, line managers and top managers.

In 2011, Granerud and Rocha conducted in-depth analyses in five OHSAS manufacturing companies. One of the companies (plastic production) used several formal safety elements, but in practice it was difficult to find visible signs of safety activities—formal feedback channels and written procedures were not used, employees were not involved in suggesting or making improvements and several physical and chemical risks were inadequately mitigated. This example shows that the OHSAS 18001 certificate is used merely as a window dressing for the company's customers. In other four OHSAS companies, both formal and real safety elements were handled with top management's commitment, as safety is seen as a high priority, and workers were actively participating in the enhancement of health and safety.

There was a statistically significant difference in combined safety performance based on the company type (OHSAS, NOHSASL, NOHSASC), F *(26, 2) = 11.472*, p < *0.1; Wilk's Λ = 0.000, partial* η^2 *= 0.993*. The power to detect the effect was 0.730. Fig. 5 presents the results of each real and formal safety element calculated by the MISHA method according to company type.

c) Elements from Combined Safety

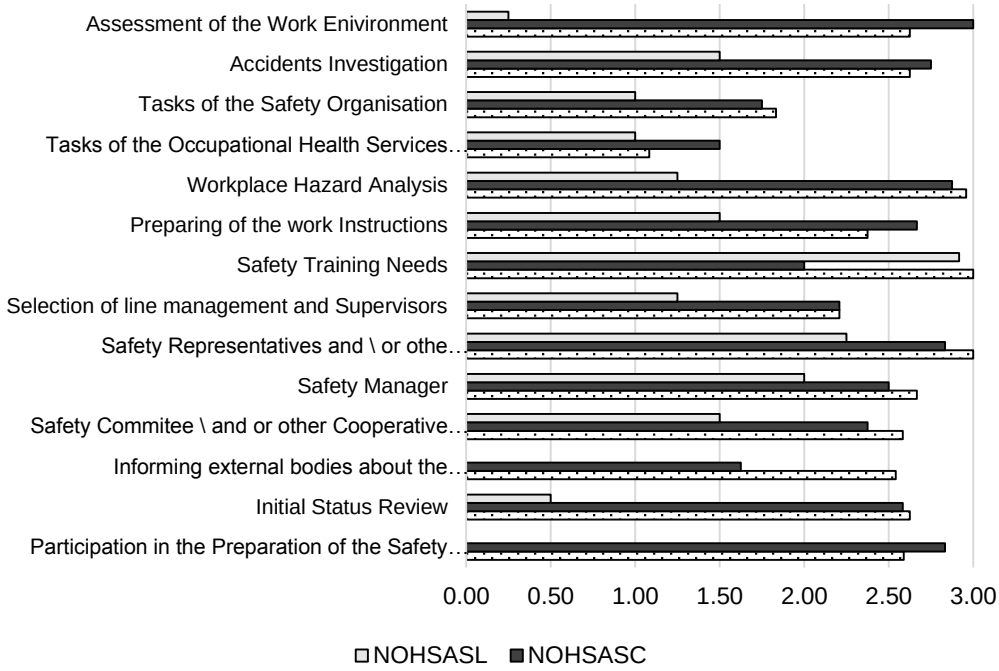

Figure 5. Descriptive statistics of real and formal safety elements providing mean (calculated using the MISHA method) for the dependent variables according to company type. Scale 0–3.

The results indicate that all elements of the safety policy (A1) depended on the company type while all elements from safety activities in practice (A2) had no significance for the company type. From hazard analysis procedures (C3), two elements—tasks of the occupational health services and tasks of the safety organization—did not correlate with company type, while workplace hazard analysis was dependent on company type. Additionally, elements from personnel safety training, accident investigation and assessment of the work environment showed significant difference. It is clear why the OHSAS 18001 standard contributes to participation in the preparation of the safety policy as it is reasonable to engage employees in the preparation stage in order to strengthen the relationship between employees' safety principles and employers' safety standards. The assessment of work environment was strongly dependent on the company type, although NOHSASC companies tend to carry out comprehensive risk assessment and occupational hazards measurements even more regularly than OHSAS companies, while NOHSASL companies hardly perform regular

activities in this field. Interestingly, accident investigation is performed more actively by NOHSASC companies. Obviously, the need to report and compare numeric results between subunits determines it. Clearly, elements from A2 (presence of a safety manager, safety committee and safety representatives) are required by the general OHS law which every company, irrespective of its type, has to follow.

d) OHSAS 18001 contribution to overall safety

Our conceptual model presented in Fig. 2 highlights (in grey colour) those important safety elements that should be covered in safety audits but fall out of the scope of OHSAS 18001. The statistical analysis showed that four out of six mentioned elements were dependent on company type and OHSAS 18001 certification. This indicates that OHSAS companies tend to have higher commitment to OHS and therefore readily solve additional OHS related topics not required by the OHSAS 18001. This result may increase the attractiveness of OHSAS 18001 certification for managers and companies may see it as a strategic unit for improving safety performance. Those results are in line with other similar studies. Abad et al. (2013) proved via various statistical assessments that the work accident rate was lower in OHSAS 18001 certified companies and the certification had positive impact on operational performance as well as productivity. Fernandez-Muniz et al. (2009) stated in their study among Spanish OHSAS companies that occupational safety depends on managerial decisions related to preventive activities, and confirm that effective safety management system is a factor of productivity and essential ingredient for improving the firms' position in the market. From this we can conclude that certified safety experience may have long-term benefits and OHSAS 18001 adds value not only to safety performance but also to overall business performance.

CONCLUSIONS

In conclusion, following statements can be presented:

1. Based on the research on 16 manufacturing companies in Estonia, a conceptual model of the contribution of OHSAS 18001 to companies' safety activities is created. We can say that OHSAS 18001 certification contributes significantly to formal safety elements such as the existence of safety policy, the follow-up procedures of accidents statistics, assigning safety tasks and responsibilities for employees. OHSAS 18001 contributes to some of the real safety elements as well, but most of them do not depend on whether the company possess the OHSAS 18001 certification or not. Concerning combined elements, many of them—such as workplace hazard analysis, working environment assessments, evaluation of safety training needs etc.—are dependent on the OHSAS 18001 certification.

2. Some of the elements examined by the safety audit that do not fall into the scope of OHSAS 18001 are still dependent on company type: selection and placement of the personnel, planning of the personnel resources, selection of line management, supervisors and promotion, rewards and career planning. This result shows that the OHSAS 18001 certification facilitates a company's commitment to health and safety activities and leads to dealing with additional topics promoting workplace health and safety. Therefore, OHSAS 18001 might be seen as a strategic unit for improving safety performance.

3. Conducting safety audits and determining the company's tendency to lean its focus either towards formal or real safety assists the company in reallocating the resources in a way that all possible safety elements are covered. It is essential to deal with real safety, as this is often most visible and forms the employee's safety attitudes and performance, but also with formal and combined safety as those elements often add value to the systematic health and safety work in a company.

REFERENCES

Abad, J., Lafuente, E. & Vilajosana, J. 2013. An assessment of the OHSAS 18001 process: Objective drivers and consequences on safety performance and labour productivity. *Safety Science* **60**, 47–56.

Amador-Rodenzo, R. 2005. An overview to CERSSO's self-evaluation of the cost-benefit on the investment in occupational safety and health in the textile factories: 'A step by step methodology'. *Journal of Safety Research* **36**(3), 215–229.

Atak, A. & Kingma, S. 2011. Safety culture in an aircraft maintenance organisation: A view from the inside. *Safety Science* **49**(2), 268–278.

Bottani, E., Monica, L. & Vignali, G. 2009. Safety management systems: performance differences between adopters and non-adopters. *Safety Science* **47**(2), 155–162.

Brown, K.A., Willis, P.G. & Prussia, G.E. 2000. Predicting safe employee behaviour in the steel industry: development and test of sociotechnical Model. *Journal of Operations Management* **18**, 445–465.

Estonian Association for Quality. 2014. Database of Certificates. http://eaq.ee/sisu/sertifikaatide-andmebaas. Accessed 05.01.2014 (in Estonian).

EVS 18001:2007 (OHSAS 18001). *SMSs*. Estonian Centre for Standardization (in Estonian).

Fernández-Muñiz, B., Montes-Peón, J.M. & Vázquez-Ordás, C.J. 2007a. Safety culture: analysis of the causal relationships between its key dimensions. *Journal of Safety Research* **38**, 627–641.

Fernández-Muñiz, B., Montes-Peón, J.M. & Vázquez-Ordás, C.J. 2007b. Safety management system: Development and validation of a multidimensional scale. *Journal of loss Prevention in the Process Industries* **20**, 52–68.

Fernández-Muñiz, B., Montes-Peón, J.M. & Vázquez-Ordás, C.J. 2009. Relation between occupational safety management and firm performance. *Safety Science* **47**(7), 980–991.

Fernández-Muñiz, B., Montes-Peón, J.M. & Vázquez-Ordás, C.J. 2012a. Occupational risk management under the OHSAS 18001 standard: analysis of perceptions and attitudes of certified firms. *Journal of Cleaner Production* **24**, 36–47.

Fernández-Muñiz, B., Montes-Peón, J.M. & Vázquez-Ordás, C.J. 2012b. Safety climate in OHSAS 18001-certified organisations: Antecedents and consequences of safety behaviour. *Accident Analysis and Prevention* **45**, 745–758.

Field, A. 2013. Discovering Statistics using IBM SPSS Statistics. Fourth Edition, SAGE Publications Ltd, London.

Frazier, B.F., Ludwig, T.D., Whitaker, B. & Roberts, D.S. 2013. A hierarchical factor analysis of a safety culture survey. *Journal of Safety Research* **45**, 15–28.

Granerud, L. & Rocha, R.S. 2011.Organisational learning and continuous improvement of health and safety in certified manufacturers. *Safety Science* **49**, 1030–1039.

Hale, A. 2009. Why safety performance indicators? *Safety Science* **47**, 479–480.

Hale, A.R., Guldenmund, F.W., H. van Loenhout, P.L.C. & Oh, J.I.H. 2010. Evaluating safety management and culture interventions to improve safety: Effective intervention strategies. *Safety Science* **48**(8), 1026–1035.

Järvis, M. 2013. Assessment of the Contribution of Safety Knowledge to Sustainable Safety Management Systems in Estonian SME-s. [dissertation] Tallinn (Estonia): Tallinn University of Technology.

Kamp, A. & Blansch, K.L. 2000. Integrating management of OHS and the environment: participation, prevention and control. In: Systematic Occupational Health and Safety Management. Perspectives on an International Development, Emerald Group Publishing Limited, Ed. Frick, K., Jensen, P.L., Quinlan, Wilthagen, M. T., Bingley, T.

Koivupalo, M., Sulasalmi, M., Rodrigo, P. & Väyrynen, S. 2015. Health and safety management in a changing organisation: Case study global steel company. *Safety Science* **74**, 128–139.

Kuusisto, A. 2000. Safety management systems: Audit units and reliability of auditing. [dissertation] Tampere (Finland): Tampere University of Technology.

Meliá, J.L., Silva, S.A. & Fugas, C.S. 2012. Formal safety versus real Safety: Quantitative and Qualitative Approaches to Safety Culture. Conference 72 proceedings: Insights into the sustainable growth of business. PSAM 11 / ESREL 2012, 25–29. June, Helsinki, Finland: (6 pp.). CD-Rom

Mežinska, I., Lapiņa, I. & Mazais, J. 2015. Integrated management systems towards sustainable and socially responsible organisation. *Total Quality Management & Business Excellence*, **26**(5–6), 469–481.

Möldri, M., Tammepuu, A., Tint, P., Paas, Õ. & Laaniste, P. 2012. Integration of the SMS to IMS in Estonian Seveso II establishments: selected case studies. Brebbia, C. A. (ed.). Risk Analysis VIII. ArhurstLodge, Arhurs, Southampton: Wessex Institute of Technology Press. 227–236.

Nazaruk, M. 2011. Developing Safety Culture Interventions in the Manufacturing Sector. [dissertation] UK, University of Bath.

Nielsen, K.J. 2000. Organizational theories implicit in various approaches to OHS management. In: Frick, K., Jensen, P.L., Quinlan, M., Wilthagen, T. (eds.), Systematic Occupational Health and Safety Management: Perspectives on an International Development, Emerald Group Publishing Limited, Bingley.

Nielsen, K.J. 2014. Improving safety culture through the health and safety organization: a case study. *Journal of Safety Research* **48**, 7–17.

Nordlöf, H., Wiitawaara, B., Winband, U., Wijk, K. & Westerling, R. 2015. Safety culture and reasons for risk-taking at a large steel-manufacturing company: Investigating the worker perspective. *Safety Science* **73**, 126–135.

Occupational Health and Safety Act. 1999. RT I 1999, 60, 616. https://www.riigiteataja.ee/akt/108102014007. Accessed 31.01.2015 (in Estonian).

OHSAS Project Group. 2007. OHSAS 18001:2007. SMSs – requirements.

Paas, Õ., Reinhold, K. & Tint, P.2015a. Estimation of safety performance by MISHA method and the benefits of OHSAS 18001 implementation in Estonian manufacturing industry. *Agronomy Research* **13**(3), 792–809.

Paas, Õ., Reinhold, K. & Tint, P. 2015b. Voluntary safety management system in manufacturing industry – to what extent does OHSAS 18001 certification help? *Scientific Journal of Riga Technical University*. Safety of Technogenic Environment, accepted.

Personal Data Protection Act. 2007. RT I 2007, 24, 127. https://www.riigiteataja.ee/akt/112072014051. Accessed 02.02.2015 (in Estonian).

Reason, J. 1997. Managing the Risks of Organizational Accidents, pp. 252.

Rebelo, M.F., Santos, G., & Silva, R. 2014. A generic model for integration of Quality, Environment and Safety Management Systems. *The TQM Journal* **26**(2), 143–159.

Rocha, R.S. 2010. Institutional effects on occupational health and safety management systems. *Human Factors in Ergonomics and Manufacturing* **20**, 211–225.

Silva, S. & Lima, M.L. 2005. Safety as an organizational value: improving safety practices and learning from accident. In K. Kolowrocki (Ed). Advances in Safety and Reliability **2**, 1818–1824, London: Taylor & Francis.

Torp, S., Riise, T. & Moen, B.E. 2000. Systematic health, environment and safety activities: do they influence occupational environment, behaviour and health? *Occupational Medicine* (Oxford) **50**, 326–333.

Yorio, P.L., Willmer, D.R. & Moore, S.M. 2015. Health and safety management systems through a multilevel and strategic management perspective: Theoretical and empirical considerations. *Safety Science* **72**(2), 221–228.

INSTRUCTIONS TO AUTHORS

Papers must be in English (British spelling). English will be revised by a proofreader, but authors are strongly urged to have their manuscripts reviewed linguistically prior to submission. Contributions should be sent electronically. Papers are considered by referees before acceptance. The manuscript should follow the instructions below.

Structure: Title, Authors (initials & surname; an asterisk indicates the corresponding author), Authors' affiliation with postal address (each on a separate line) and e-mail of the corresponding author, Abstract (up to 250 words), Key words (not repeating words in the title), Introduction, Materials and methods, Results and discussion, Conclusions, Acknowledgements (optional), References.

Layout, page size and font

- Use preferably the latest version of **Microsoft Word**, doc., docx. format.
- Set page size to **B5 Envelope or ISO B5 (17.6 x 25 cm)**, all margins at 2 cm.
- Use single line spacing and justify the text. Do not use page numbering. Use indent 0.8 cm (do not use tab or spaces instead).
- Use font Times New Roman, point size for the title of article **14 (Bold)**, author's names 12, core text 11; Abstract, Key words, Acknowledgements, References, tables and figure captions 10.
- Use *italics* for Latin biological names, mathematical variables and statistical terms.
- Use single ('…') instead of double quotation marks ("…").

Tables

- All tables must be referred to in the text (Table 1; Tables 1, 3; Tables 2–3).
- Use font Times New Roman, regular, 10 pt. Insert tables by Word's 'Insert' menu.
- Do not use vertical lines as dividers; only horizontal lines (1/2 pt) are allowed. Primary column and row headings should start with an initial capital.

Figures

- All figures must be referred to in the text (Fig. 1; Fig. 1 A; Figs 1, 3; Figs 1–3). Use only black and white or greyscale for figures. Avoid 3D charts, background shading, gridlines and excessive symbols. Use font **Arial** within the figures. Make sure that thickness of the lines is greater than 0.3 pt.
- Do not put caption in the frame of the figure.
- The preferred graphic format is EPS; for half-tones please use TIFF. MS Office files are also acceptable. Please include these files in your submission.
- Check and double-check spelling in figures and graphs. Proof-readers may not be able to change mistakes in a different program.

References

- **Within the text**

In case of two authors, use '&', if more than two authors, provide first author 'et al.':

Smith & Jones (1996); (Smith & Jones, 1996);
Brown et al. (1997); (Brown et al., 1997)

When referring to more than one publication, arrange them by following keys: 1. year of publication (ascending), 2. alphabetical order for the same year of publication:

(Smith & Jones, 1996; Brown et al., 1997; Adams, 1998; Smith, 1998)

- **For whole books**

Name(s) and initials of the author(s). Year of publication. *Title of the book* (*in italics*). Publisher, place of publication, number of pages.

Shiyatov, S.G. 1986. *Dendrochronology of the upper timberline in the Urals*. Nauka, Moscow, 350 pp. (in Russian).

- **For articles in a journal**

Name(s) and initials of the author(s). Year of publication. Title of the article. *Abbreviated journal title* (*in italic*) volume (in bold), page numbers.

Titles of papers published in languages other than English, German, French, Italian, Spanish, and Portuguese should be replaced by an English translation, with an explanatory note at the end, e.g., (in Russian, English abstr.).

Karube, I. & Tamiyra, M.Y. 1987. Biosensors for environmental control. *Pure Appl. Chem.* **59**, 545–554.

Frey, R. 1958. Zur Kenntnis der Diptera brachycera p.p. der Kapverdischen Inseln. *Commentat.Biol*. **18**(4), 1–61.

Danielyan, S.G. & Nabaldiyan, K.M. 1971. The causal agents of meloids in bees. *Veterinariya* **8**, 64–65 (in Russian).

- **For articles in collections:**

Name(s) and initials of the author(s). Year of publication. Title of the article. Name(s) and initials of the editor(s) (preceded by In:) *Title of the collection (in italics)*, publisher, place of publication, page numbers.

Yurtsev, B.A., Tolmachev, A.I. & Rebristaya, O.V. 1978. The floristic delimitation and subdivisions of the Arctic. In: Yurtsev, B. A. (ed.) *The Arctic Floristic Region*. Nauka, Leningrad, pp. 9–104 (in Russian).

- **For conference proceedings:**

Name(s) and initials of the author(s). Year of publication. Name(s) and initials of the editor(s) (preceded by In:) *Proceedings name (in italics)*, publisher, place of publishing, page numbers.

Ritchie, M.E. & Olff, H. 1999. Herbivore diversity and plant dynamics: compensatory and additive effects. In: Olff, H., Brown, V.K. & Drent R.H. (eds) *Herbivores between plants and predators. Proc. Int. Conf. The 38th Symposium of the British Ecological Society*, Blackwell Science, Oxford, UK, pp. 175–204.

.....……

Please note

- Use '.' (not ',') for decimal point: 0.6 ± 0.2; Use ',' for thousands – 1,230.4;
- Use '–' (not '-') and without space: pp. 27–36, 1998–2000, 4–6 min, 3–5 kg
- With spaces: 5 h, 5 kg, 5 m, 5°C, C : D = 0.6 ± 0.2; $p < 0.001$
- Without space: 55°, 5% (not 55 °, 5 %)
- Use 'kg ha^{-1}' (not 'kg/ha');
- Use degree sign ' ° ' : 5 °C (not 5 ^{O} C).